Elucidating the function of nuclear-encoded repair proteins in Plasmodium mitochondrial genome repair

A Thesis Submitted to the University of Hyderabad for the award of a Ph.D. Degree in Department of Biochemistry School of Life Sciences

By

Payal Jha

(15LBPH01)

Under the Supervision of

Prof. Mrinal Kanti Bhattacharyya





Department of Biochemistry
School of Life Sciences
University of Hyderabad
Hyderabad 500046
Telangana (India)



Hyderabad -500046, India

Certificate

This is to certify that this thesis entitled "Elucidating the function of nuclear-encoded repair proteins in *Plasmodium* mitochondrial genome repair" submitted by Payal Jha bearing registration number 15LBPH01 in partial fulfilment of the requirement for the award of Doctor of Philosophy in the Department of Biochemistry, School of Life Sciences, is a bonafide work carried out by her under my supervision and guidance.

This thesis is free from plagiarism and has not been submitted previously in part or in full to this University or any other University or Institution for the award of any degree or diploma.

Part of this thesis has been:

- A. Published in the following journal:
 - Payal Jha, Abhilasha Gahlawat, Sunanda Bhattacharyya, Sandeep Dey, Kota Arun Kumar, Mrinal Kanti Bhattacharyya. Bloom Helicase Along with Recombinase Rad51 Repairs the Mitochondrial Genome of the Malaria Parasite. mSphere. 2021;6(6):e0071821. doi:10.1128/mSphere.00718-21
- B. Presented in the following conferences:
 - Payal Jha, Shyamasree Laskar, Sunanda Bhattacharyya, Mrinal Kanti Bhattacharyya. "Plasmodium Export Element motif-containing Hsp40 proteins interact with human Hsp70". Presented poster in National Conference on Malaria Parasite Biology: Drug Designing and Vaccine Development held on September 9th and 10th, 2016 at Institute of Science, Nirma University, Ahmedabad, India. (National)
 - Payal Jha, Shyamasree Laskar, Sunanda Bhattacharyya, Mrinal Kanti Bhattacharyya. "Plasmodium Export Element motif-containing Hsp40 proteins forms combo-chaperone with human Hsp70". Presented poster in International workshop on Malaria Parasite Biology: Strategies for Drug and Vaccine Development held from November 29th to December 1st, 2017 at International Centre for Genetic Engineering and Biotechnology, Delhi, India. (International)
 - Payal Jha, Sunanda Bhattacharyya, Mrinal Kanti Bhattacharyya. "Plasmodium mitochondrial genome maintenance and repair is PfRad51 dependent". Presented poster in BioQuest 2019 "Cellular Homeostasis: From the Basic to Translation Research" held on March 11th, 2019 at School of Life Sciences, University of Hyderabad, Hyderabad, India. (National)
 - Payal Jha, Sunanda Bhattacharyya, Mrinal Kanti Bhattacharyya. "Novel function of Plasmodium recombinosome in maintenance and repair of the mitochondrial genome".
 Presented poster in National Seminar on Biomolecular Interactions in Development and

Diseases held from September 26th to 28th, 2019 at School of Life Sciences, University of Hyderabad, Hyderabad, India. (National)

Further the student has passed the following courses towards fulfilment of coursework requirement for Ph.D.

Course code	Name	Credits	Pass/Fail
BC-801	Analytical Techniques	4	Passed
BC 802	Research ethics, Data analysis and Biostatistics	3	Passed
BC 803	Lab seminar and Records	5	Passed

Supervisor

Dr. MRINAL KANTI BHATTACHARYYA PhD
PROFESSOR
DEPARTMENT OF BIOCHEMISTRY
SCHOOL OF LIFE SCIENCES
UNIVERSITY OF HYDERABAD

HYDERABAD-500046, INDIA.

Head, Dept. of Biochemistry

HEAD

Dept. of Biochemistry SCHOOL OF LIFE SCIENCES UNIVERSITY OF HYDERABAD HYDERABAD-500 046.

University of Hyderabad Hyderabad-500 046.

ii



University of Hyderabad

Hyderabad -500046, India

Declaration

I, PAYAL JHA, hereby declare that this thesis entitled "Elucidating the function of nuclearencoded repair proteins in *Plasmodium* mitochondrial genome repair" submitted by me under the guidance and supervision of Prof. Mrinal Kanti Bhattacharyya, is an original and independent research work. I also declare that it has not been submitted previously in part or in full to this University or any other University or Institution for the award of any degree or diploma.

Date: 23/02/2022

Signature of the Student

Signature of the Supervisor

(Prof. Mrinal Kanti Bhattacharyya)

Dr. MRINAL KANTI BHATTACHARYYA PhD DEPARTMENT OF BIOCHEMISTRY SCHOOL OF LIFE SCIENCES UNIVERSITY OF HYDERABAD HYDERABAD-500046, INDIA.

Dedicated to my beloved mother.

CONTENT

Content	vii
List Of Figures	χi
List Of Table	xiii
Abbreviation	Xiv
Chapter I: INTRODUCTION	
1.1 Malaria and Its Global Burden.	1
1.2 Major Hurdles In Malaria Treatment And Eradication.	1
1.2.1 The Complex Life Cycle Of The Malaria Parasite.	1
1.2.2 Drug Resistance.	3
1.2.3 Antigenic Variation And Lack Of Effective Vaccine.	4
1.3 Plasmodium Mitochondrion Is A Druggable Target.	4
1.4 DNA Double-Strand Breaks Is Unavoidable In Plasmodium.	9
1.5 Repair Mechanism In The Mitochondria Of Model Organisms.	9
1.5.1 Base Excision Repair (BER).	10
1.5.2 Mismatch repair (MMR)	10
1.5.3 Non-homologous end joining (NHEJ)	10
1.5.4 Homologous recombination (HR)	11
1.6 DNA DSB REPAIR PATHWAYS IN Plasmodium falciparum	13
1.6.1 Homology-directed repair in Plasmodium	14
1.6.2 Alternative -NHEJ in Plasmodium	14
1.6.3 Nucleotide Excision Repair	15
1.6.4 Mismatch Repair	15
1.6.5 Base Excision Repair	16
1.7 Significance Of The Study	22
1.8 Objectives Of This Study.	23
1.9 Aims Of The Ph.D. Work.	24
Chapter 2: MATERIALS AND METHODS	

2.1	Recombinant DNA methods.	25
2.1.1	Bacterial Competent cell preparation	25
2.1.2	Bacterial Transformation	25
2.1.3	Alkaline Lysis Method for Plasmid DNA Isolation	26
2.1.4	Site-Directed Mutagenesis	27
2.2	Yeast Methods	28
2.2.1	Yeast Competent Cell Preparation	28
2.2.2	Yeast Transformation	29
2.2.3	Yeast Two-Hybrid Assay	29
2.3	Recombinant Protein Purification	30
2.4	Western Blotting	32
2.5	Methods in Plasmodium falciparum experiments	33
2.5.1	Washing of Red Blood Cells (RBCs)	33
2.5.2	Thawing of parasites	34
2.5.3	In vitro Parasite Culture Maintenance	34
2.5.4	Parasite Culture Synchronization by Sorbitol Method	35
2.5.5	Transfection in P. falciparum	35
2.5.6	Genomic DNA Isolation From P. falciparum	36
2.6	DNA Damage Induction	37
2.6.1	DSB Induction Using UV	37
2.6.2	DNA Damage by Methyl Methane Sulfonate (MMS)	37
2.7	In vitro Phosphorylation Assay	38
2.8	Indirect Immunofluorescence Assay	39
2.9	Direct Immunofluorescence Assay	39
2.10	PCR-Based Method To Quantify Mitochondrial DNA Damage	40
2.11	Thermolysin Protection Assay	41
2.12	Subcellular Fractionation Of Plasmodium falciparum Culture	41
2.13	MtDNA Immuno-Precipitation in P. falciparum.	42

Chapt	ter 3: Role Of PfBlm And PfRad51 In Mitochondrial DNA Repair	
3.1	Introduction	50
3.2	Results	51
3.2.1	Subcellular Distribution Of Nuclear-Genome Encoded HR Pathway	51
Protes	ins	
3.2.2	Mitochondrial Localization Of PfRad51 And PfBlm	55
3.2.3	Interaction Of PfBlm And PfRad51 With Mitochondrial DNA	59
3.2.3	Stage-specific interaction of PfRad51 and PfBlm with the	61
mitoc	hondrial genome	
3.2.5	Repair Of UV-Induced DNA Double-Strand Break In The Nuclear	64
And S	Mitochondrial Genome	
3.2.6	PfBlm and PfRad51 are Involved In The Repair Of DNA Double-	66
Stran	d Breaks	
3.2.7	Overexpression Of PfBlm and PfRad51 Provides A Kinetic Advantage	69
In Re	pairing Nuclear And Mitochondrial DSBs:	
3.2.8	DNA Damage Induces Organelle Translocation Of PfRad51 And	72
PfBln	n:	
3.2.9	DNA Damage Induces mtDNA Recruitment Of PfRad51 And PfBlm	76
3.2.10	The Amino Acid Residues Of PfRad51 With High Phosphorylation	80
Poten	tial	
3.2.11	1 Effect Of Pfrad51 Double Mutation On Its Subcellular Distribution	82
And T	Foci Formation Activity	
3.3	Summary	86
Chapt	ter 4: PF3D7_0625300 Gene Product Mitochondrial Localization And	
Interd	action With Repair Proteins.	
4.1	Introduction	88
4.2	Results	90
4.2.1	Subcellular Distribution Of PF3D7 0625300 Gene Product	90

4.2.2 Mitochondrial Exclusive Localization Of PfMtDNAP in P.	93
falciparum	
4.2.3 PfMtDNAP Protein Interacts With Plasmodium mitochondrial	95
Genome	
4.2.4 Homologous Recombination Proteins Interact With Mitochondria	97
Specific DNA Polymerase	
4.3 Summary	100
Chapter 5: Discussion	102
References	109
Appendix 1	
A1.1 Stage-specific expression level of endogenous PfBlm and PfRad51	116
proteins:	
A1.2 Cloning of PfRAD51 gene into Plasmodium expression vector pARL	117
[pARLPfRAD51]	
A1.3 Ectopic expression of the dominant-negative mutant of PfRad51K143R	117
A1.4 Cloning of PfRAD51 gene harboring mutation/s into bacterial	119
expression vector	
A1. 5 Expression of recombinant PfRad51 and its mutants	119
A1. 6 Purification of recombinant PfRad51 and its mutants	120
A1. 7 In vitro phosphorylation of PfRad51 and its mutants	120
A1.8 Cloning of PfMTDNAP gene into Plasmodium expression vector pARL	126
[PARL PfMTDNAP]:	
Appendix 2: Synopsis	127

List Of Figures

Figure 1.1: Illustration representing the complete life cycle of Plasmodium	2
falciparum.	
Figure 1.2: Timeline showing the years in which the drugs were first clinically	3
used (the emergence of resistance to them).	
Figure 1.3: Illustration representing Plasmodium mitochondrial genome map	6
with the relative positioning of three protein-coding genes and fragmented	
rRNA genes.	
Figure 1.4: Illustration displays various components of Plasmodium mtETC	8
and the targeted site of potential antimalarial drugs	
Figure 1.5: Illustration display three phases of the homologous recombination	13
repair pathway present in the nucleus and proteins involved in the respective	
events.	
Figure 3.1: Organelle localization of nuclear-encoded repair proteins PfBlm	54
and PfRad51.	
Figure 3.2: Mitochondrial localization of PfBlm, and PfRad51.	57
Figure 3.3: Interaction of PfBlm, and PfRad51 with mitochondrial DNA.	60
Figure 3.4: Stage-specific interaction of PfRad51 and PfBlm with the	64
mitochondrial genome.	
Figure 3.5: Repair of UV-induced DNA double-strand break in the nuclear	65
and mitochondrial genome.	
Figure 3.6: PfBlm and PfRad51 are involved in the repair of DNA double-	68
strand breaks.	
Figure 3.7: Overexpression of PfBlm and PfRad51 provided a kinetic	71
advantage in repairing nuclear and mitochondrial DSBs.	
Figure 3.8: DNA damage induces organelle translocation of PfRad51 and	74
PfBlm.	

Figure 3.9: DNA damage induces mtDNA recruitment of PfRad51 and	78
PfBlm.	
Figure 3.10: The amino acid residues of PfRad51 with high phosphorylation	81
potential	
Figure 3.11: Effect of PfRad51 double mutation on its subcellular	84
distribution and foci formation activity.	
Figure 4.1. Subcellular distribution of PF3D7_0625300 gene product.	92
Figure 4.2. Mitochondrial exclusive localization of PfMtDNAP in P.	94
falciparum.	
Figure 4.3: PfMtDNAP protein interacts with Plasmodium mitochondrial	96
genome.	
Figure 4.4: Homologous recombination proteins interact with mitochondria-	98
specific DNA polymerase.	
Figure 5.1: The model.	103

List Of Tables

Table 1: List of drugs targeting PfETC with their site of action and the	8
mutant gene responsible for the emergence of resistant strains.	
Table 2: List of the proteins involved in BER, NER, HR, NHEJ, MMEJ,	17
MMR pathways known in nuclear and/or mitochondria of Human and P.	
falciparum.	
Table 3: List of primers along with the nucleotide sequence and description of	46
their usage in this work.	
Table 4: List of yeast strains generated in this study and their phenotype	49
description.	

Abbreviations.

DNA

μF Micro Faraday microgram μg microliter μl μM Micro molar aa Amino acid **ADE** Adenine APN1 Apurinic/ apyrimidinic endonuclease-1 **ASBs** Asexual blood stages At-NHEJ Alternate NHEJ **ATP** Adenosine triphosphate **ATQ** Atovaquone **BER** Base excision repair Base pair bp **BSA** Bovine serum albumin Calcium chloride CaCl2 C-NHEJ Classical NHEJ cytochrome C oxidoreductase subunit I **COXI** cytochrome C oxidoreductase subunit III **COXIII** Cyb Cytochrome b Da Dalton Dihydroorotate dehydrogenase **DHODH**

Deoxyribonucleic acid

DSBs Double-strand breaks

dsDNA Double-stranded DNA

DTT Dithiothreitol

EDTA Ethylene diamine tetraacetic acid

Etc et cetera

G3PDH Glyceraldehyde 3-phosphate dehydrogenase

Hct Hematocrit

HDR Homology-directed DNA repair

HJ Holliday junction

HR Homologous recombination

HsmtETC Human mitochondrial electron transport

chain

IPTG Isopropyl β-D-1 thiogalactopyranoside

iRBC infected- RBC

KCl Potassium chloride

kDa Kilo dalton

kV Kilovolt

LB Luria-bertani broth

Leu Leucine

LiOAc Lithium acetate

M Molar

mg Milligram

MgCl2 Magnesium chloride

Min Minute

ml Milli liter

mM Milli molar

MMR Mismatch Repair

MMS Methyl methane sulfonate

MQO Malate-quinone oxidoreductase

MRE 11 Meiotic recombination 11

MRX Mre11-Rad50-Xrs2

mtDNA Mitochondrial DNA

mtDNA-IP Mitochondrial DNA-immunoprecipitation

MWt Molecular weight

NaCl Sodium chloride

NaH2PO4 Sodium dihydrogen phosphate

NaOAc Sodium acetate

NaOH Sodium hydroxide

Ndh2 type 2 NADH ubiquinone-oxidoreductase

nDNA Nuclear DNA

NER Nucleotide Excision Repair

ng nanogram

NHEJ Non-homologous end-joining

Ni-NTA Nickel nitriloacetic acid

OD Optical density

ORF Open reading frame

PARP1 Poly ADP ribose polymerase 1

PBS Phosphate buffered saline

PCIA Phenyl chloroform isoamyl alcohol

PCNA Proliferating cell nuclear antigen

PCR Polymerase chain reaction

PEG Polyethylene glycol

PfmtETC P. falciparum mitochondrial electron

transport chain

PVDF Polyvinylidene fluoride

Qi Ubiquinol reduction site

Qo Ubiquinol oxidation site

Rad2 Radiation sensitive 2

Rad50 Radiation sensitive 50

Rad51 Radiation sensitive 51

Rad52 Radiation sensitive 52

RBCs Red blood cells

RNA Ribonucleic acid

RNase Ribonuclease

RPA Replication Protein A

rpm rotation per minute

rRNA ribosomal RNA

RT Room temperature

Sc Synthetic complete

SDH Succinate dehydrogenase

SDS Sodium dodecyl sulfate

SDS-PAGE Sodium dodecyl sulfate-polyacrylamide gel

electrophoresis

Sec Second

ssDNA salmon serum DNA or single-stranded DNA

TBE Tri borate EDTA

TCA Trichloroacetic acid

TE Tris EDTA

tRNA Transfer RNA

Ura Uracil

UV Ultraviolet

WT Wild type

XRCC4 X-ray cross-complementing factor 4

XRS2 X-ray sensitive 2

YPD Yeast extract peptone dextrose

Chapter 1 <u>INTRODUCTION</u>

1.1 MALARIA AND ITS GLOBAL BURDEN.

Malaria is an ancient health hazard affecting mankind for thousands of years. The earliest documented trace of malaria parasite DNA was found in Egyptian mummies from 500 BC. Since time immemorial, malaria has proven to be one of the most serious infectious diseases affecting more than half of the world's population. Till today, malaria remains an equally infectious disease as seen in the latest WHO annual report which estimates 225 million cases with 4, 09,000 deaths (WHO 2021). Unfortunately, malaria-related mortality is highest in children and pregnant women. Malaria is caused by a unicellular eukaryote of the genus *Plasmodium*. Humans can be infected by five different *Plasmodium* species, namely, *Plasmodium falciparum*, *Plasmodium vivax*, *Plasmodium ovale*, *Plasmodium malariae*, and *Plasmodium knowlesi*. Infection caused by *P. falciparum* is the most lethal as it can affect the central nervous system of humans, and causes cerebral malaria. In the last few decades, a substantial amount of work has been put forward to reduce the global burden of malaria. However, the complete eradication of this infectious disease remains unachievable.

1.2 MAJOR HURDLES IN MALARIA TREATMENT AND ERADICATION.

1.2.1 The complex life cycle of the malaria parasite:

Plasmodium involves two hosts to complete its life cycle which includes vertebrates (human) and invertebrates (mosquito). The infection cycle begins with the bite of a female anopheles mosquito injecting sporozoites into the human body. These sporozoites are transported into the liver via the blood circulation system where they invade hepatocytes and approximately within a week, the sporozoite undergoes exo-erythrocytic schizogony forming mature schizonts. Each mature schizont rupture leads to the release of multiple merozoites into the bloodstream wherein they further infect the erythrocytes and initiate the asexual blood stages (ASBs) of development. During the erythrocytic schizogony, the parasite develops into rings, trophozoites, and finally

schizonts. Once these schizonts mature, rupture leading to the release of multiple merozoites which re-infect healthy RBCs. A fraction of these parasites differentiates into microgametocyte and macrogametocyte which can be taken up by a mosquito vector during the blood meal to propagate the sexual stage of the life cycle. During sexual development, the male and female gametocytes fuse to form a zygote within the mosquito gut. The differentiated motile ookinete invades the midgut wall where it matures into oocyst and further undergoes sporogony to generate sporozoites. The infectious sporozoites migrate to the salivary gland and are ready to be injected into a healthy host during the blood meal (Figure 1.1). Overall it is evident that during the life cycle *Plasmodium* parasite acquires diverse cellular morphologies. Their exceptional ability to adapt and grow in a wide range of host environments possess a major hurdle in developing effective strategies to reduce disease burden and transmission.

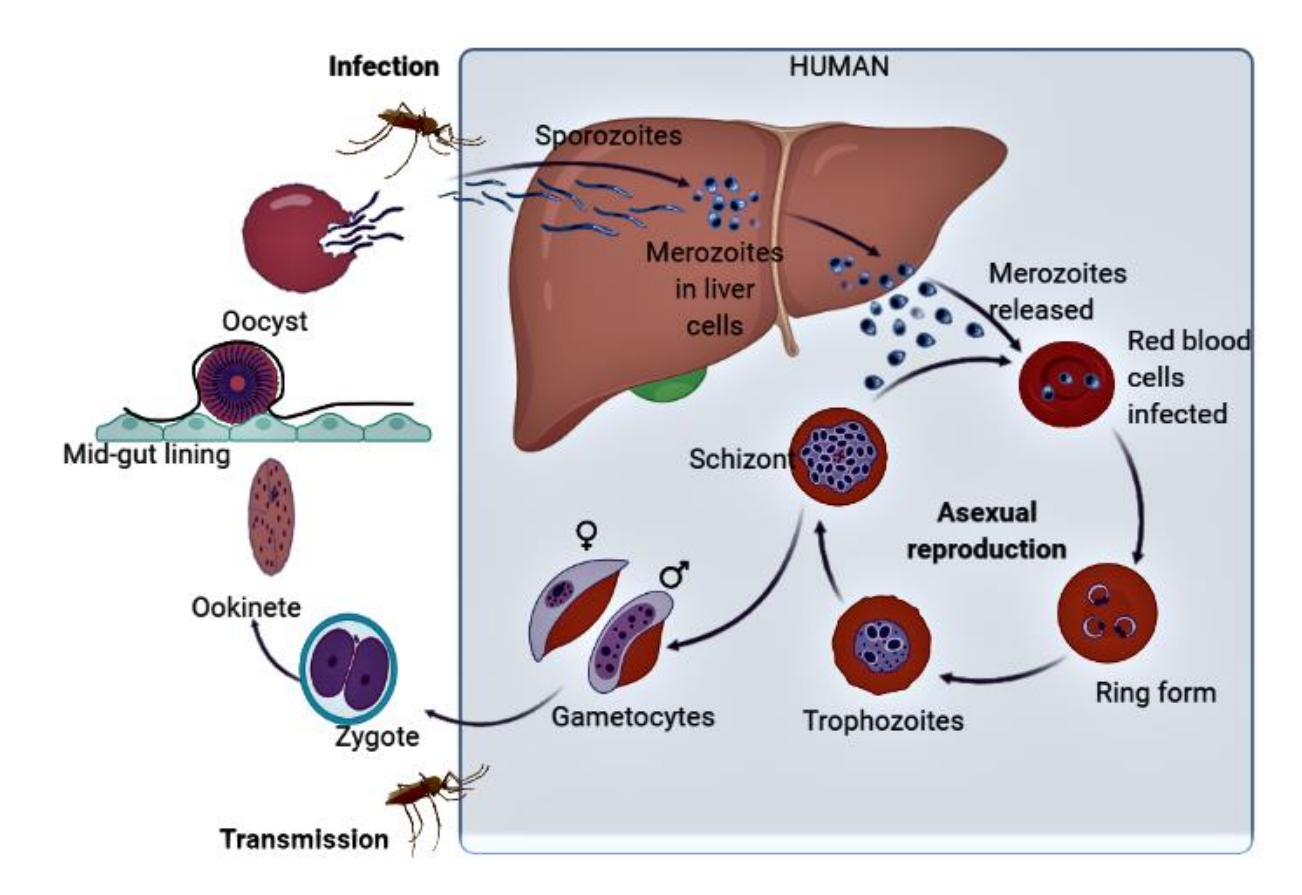


Figure 1.1: Illustration representing the complete life cycle of *Plasmodium falciparum*.

1.2.2 Drug resistance:

Anti-malarial drugs are the primary strategy for controlling malaria globally. In the past, drugs like chloroquine and sulfadoxine-pyrimethamine served as a first-line of treatment for malaria. However, the emergence of chloroquine resistance parasites in Southeast Asia and the outspread of these drug-resistant mutants into India and Africa restricted its usage (Payne 1987). Despite the development of many other antimalarial drugs like mefloquine, atovaquone, pyrimethamine, and proguanil, their usage remains limited due to their high cost and toxicity, however, the later developed artemisinin is utilized for treating malaria. It is also given in combination with other antimalarial drugs and this treatment is known as artemisinin combination therapy. Unfortunately, the rapid development of artemisinin resistance bears a resemblance to the earlier emergence and spread of chloroquine resistance worldwide (Figure 1.2), hence challenging the current strategy to tackle malaria (Dondorp et al. 2009).

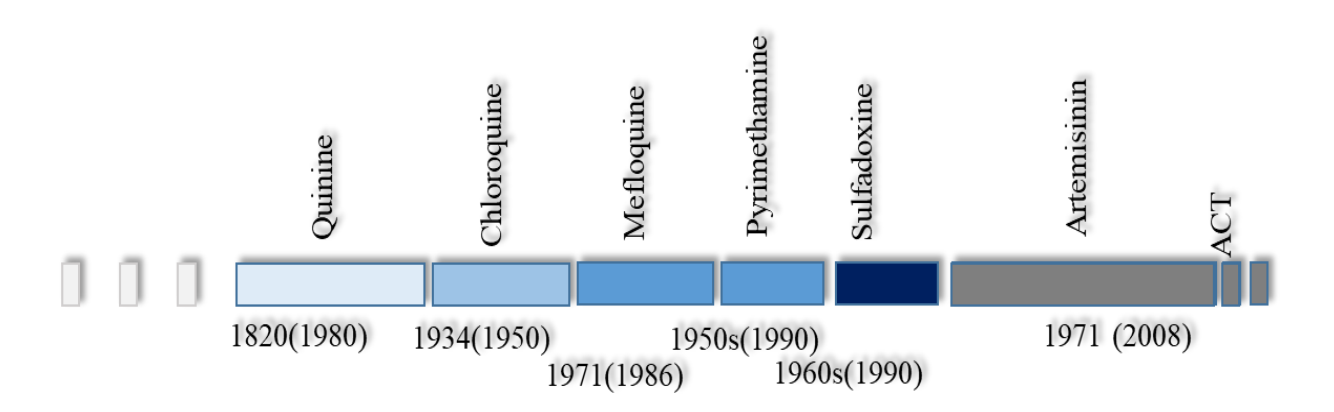


Figure 1.2: Timeline showing the years in which the drugs were first clinically used. The emergence of resistance to each of them is presented within the parenthesis.

1.2.3 Antigenic variation and lack of effective vaccine:

The *P. falciparum* erythrocyte membrane protein 1 (PfEMP1) is a member of the variant surface antigen proteins family. PfEMP1 mediates the cytoadherence function of parasite-infected RBCs (iRBC) to the endothelial membrane leading to parasites' organ sequestration. This protein is encoded by clonally variant 60 var genes per genome that undergo antigenic variation, hence exhibiting a highly polymorphic nature by the virtue of which the malaria parasite is able to evade the immune system and persists in the human host (Baruch et al. 1995; Gardner et al. 2002; Scherf et al. 1998; Smith et al. 1995). The surface antigens like PfEMP1 are being studied for their potential in developing protecting immunity and anti-malaria vaccines. Nonetheless, the wide diversity and plasticity of malarial surface antigens make vaccine development a futile process (Chan et al. 2014). Till date, we lack effective vaccines against malaria.

Considering the rapid emergence of drug resistance and unavailability of vaccines, the plausible solution is to discover new drug targets. For this purpose, an in-depth understanding of *Plasmodium* biology is a prime step.

1.3 Plasmodium MITOCHONDRION IS A DRUGGABLE TARGET.

Mitochondria came into existence as a result of the endosymbiosis of alphaproteobacteria constituting the eukaryotic cell. The mitochondrion is considered the powerhouse of the cell since this organelle is dedicated to perform the tricarboxylic acid (TCA) cycle and electron transport chain (mtETC). Unlike most of the eukaryotic mitochondria that have a typical granular and filamentous morphology, the mitochondrion present in the *Plasmodium* has a unique structure. In the merozoite and ASBs, the mitochondrion maintains a tubular morphology. Whereas during gametogenesis the mitochondrion undergoes morphological changes and adapts elongated structures (Okamoto et al. 2009). These distinctive morphologies during different stages of development are to provide an adequate surface area for supporting

the metabolic processes (Krungkrai 2004). Furthermore, *Plasmodium* mitochondria and its genome are distinct from the human host in many aspects. For instance, a parasite contains a single mitochondrion that has to fulfill all the cellular metabolic needs that are dependent on this organelle. Likewise, parasite mitochondrion has a limited number of the genome (mt-DNA) that is a maximum of 30 in P. falciparum and 100 in P yoelii (Vaidya and Mather 2005). Contrary to this, a human cell can maintain 100 to 600,000 mitochondria, with hundreds to thousands of mtDNA in a mitochondrion. Such a limited number of this mitochondrion and its genome highlights the importance of its faithful propagation and stability in *Plasmodium*. Furthermore, malaria parasites contain the smallest known mitochondrial genome (mtDNA) of size near 6 kb. While the sequence information this genome carries is vastly divergent from the higher eukaryotes including its hosts, but it is highly conserved among the *Plasmodium* spp. Among the *Plasmodium* spp. that infects humans, mtDNA shares more than 90% similarities (Hikosaka et al. 2011). PfmtDNA mainly uses the rolling circle mode of replication resulting in the formation of a linear concatemer that is tandemly arranged in head to tail fashion. The involvement of recombinational events during the replication of mtDNA has been proposed based on the presence of a small fraction of circular oligomers (Preiser et al. 1996). minimalistic parasite mitochondrial genome encodes for merely three electron transport chain proteins namely, cytochrome C oxidoreductase subunit I and III, and cytochrome B. In addition, Plasmodium mtDNA also contains highly fragmented rRNA genes dispersed throughout the genome, which encodes for both small and large subunits of ribosomal RNA (Figure 1.3). However, parasite mtDNA lacks the tRNA gene and therefore, depends on nuclear-encoded tRNA to complete mitochondrial translation machinery. In contrast, the human mtDNA is a 16 kb circular genome replicated by D-loop formation, harboring thirty-seven genes that encode for thirteen proteins, twenty-two tRNAs, and two rRNA.

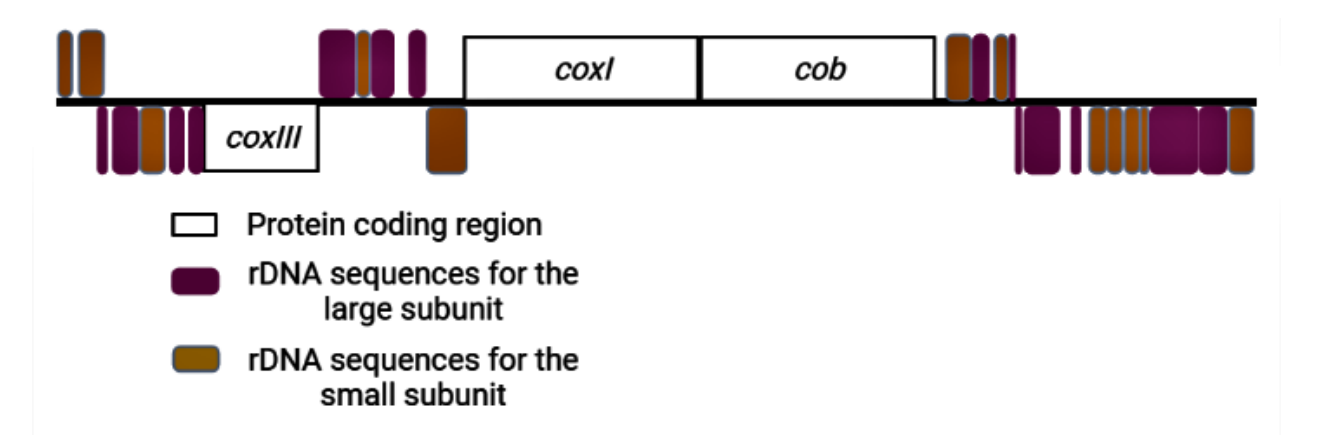


Figure 1.3: Illustration representing *Plasmodium* **mitochondrial genome map.** The relative positioning of three protein-coding genes and fragmented rRNA genes are shown.

The P. falciparum mitochondrial electron transport chain (PfmtETC) also has various dissimilarities with its human counterpart. Firstly, the usage of PfmtETC to generate ATP is stage-specific. Oxidative phosphorylation is active in the sexual mosquito stage but is completely suppressed during asexual blood stages (ASBs). During ABS, the parasite has adapted to use glycolysis for energy generation due to the abundance of glucose in the erythrocyte. Therefore, during the asexual development parasite have a non-cyclic ETC which is proposed to be linked to uncoupled proteins for pumping the proton into the matrix (Ledesma et al. 2002; Uyemura et al. 2004) which otherwise gets pumped in by the action of the ATP synthase complex (Figure 1.4). Secondly, unlike hmtETC, the overall structure and organization of PfmtETC is much simple. For instance, type 2 NADH ubiquinone-oxidoreductase (alternate complex I) of PfmtETC is a single subunit protein solely involved in electron sinking from the cytosolic side to mtETC and lacks the proton translocation function while the human complex I is a multi-subunit protein complex that participates in both electron transport as well as proton efflux. Moreover, the PfmtETC has a malate-quinone oxidoreductase instead of malate dehydrogenase as present in hmtETC.

Distinctive structural features of *P. falciparum* dihydroorotate dehydrogenase (DHODH), alternate complex I, and malate-quinone oxidoreductase are also being examined as potential novel antimalarial drug candidates. Inhibitors of complex III (Q-cycle) like quinolones and atovaquone (ATQ) which are the structural analogs of ubiquinone and are known to compete for the ubiquinol oxidation site (Q₀) of cytochrome b protein. These drugs are used clinically to treat malaria. A point mutation of tyrosine 268 amino acid residue of *Pfcytb* is linked to the emergence of atovaquone resistance. The combination of ELQ-300, which is a competitive inhibitor of ubiquinone reduction site (Qi) and ATQ is successful against the ATQ-resistant parasite. Interestingly, this drug combination significantly reduces the growth of parasite with resistance to either ATQ or ELQ-300 than the monotherapy. The success of these drugs and evolutionary divergence of *Plasmodium* mitochondria from the host suggested its potential as an anti-malarial drug target. Moreover, these extreme dissimilarities in the mitochondrion of host and parasite are the primary reason for targeting this organelle of parasite that could eliminate the off-target effects of drugs in the human cell.

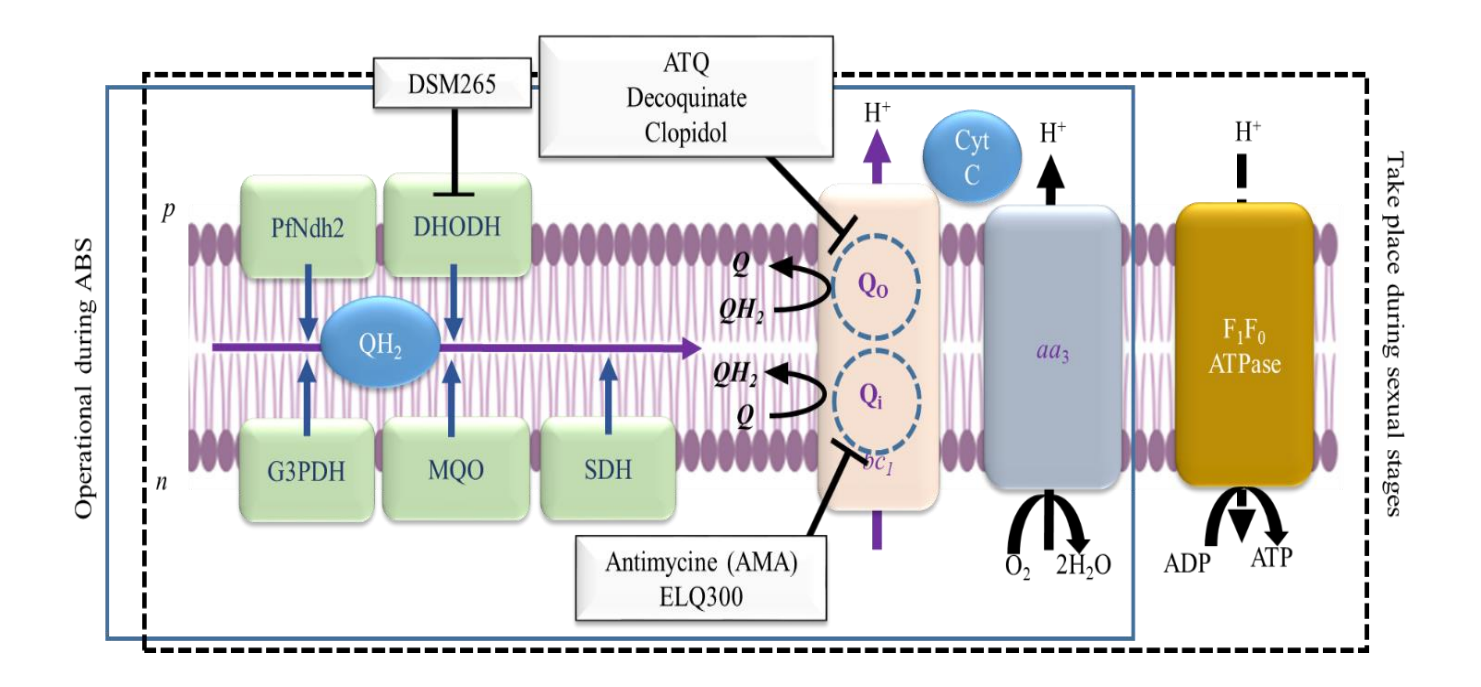


Figure 1.4: Illustration displays various components of *Plasmodium* **mtETC.** The target sites of potential antimalarial drugs are indicated. The black dotted box represents the complete electron cycle and ATP production, blue box shows the electron flow which is active in asexual stages.

Table 1: List of drugs targeting PfETC with their site of action and the mutant gene responsible for the emergence of resistant strains.

Drug	Class Of	Pathway	Site Of	Gene Mutation
	Compound		Action	Linked To Resistance
ATQ	Quinone	ETC	Q ₀ Pocket	PfCytB
ELQ300	Quinone-diaryl ether	ETC	Q _i Pocket	PfCytB

Decoquinate	Quinone	ETC	Q ₀ Pocket	PfCytB
DSM265	Triazolopyrimi dines	Pyrimidine Biosynthesis	DHODH	PfDHODH
Clopidol	Pyridones	ETC	Q ₀ Pocket	PfCytB

1.4 DNA DOUBLE-STRAND BREAKS IS UNAVOIDABLE IN Plasmodium.

DNA damage is unavoidable for the *Plasmodium* parasite as the parasite genome experiences an extraordinary level of DNA double-strand breaks (DSB's). Causative agents for such intense DBSs can be the exogenous sources like ionizing radiation and reactive oxygen species (ROS) generated by the action of antimalarial drugs. Likewise, hazardous free radicals and ROS are produced during endogenous cellular metabolic activity, along with physiological stress such as replication fork arrest and the enzymatic process, which can impair the stability of DNA. Regardless of the source, faithful repair of every single DSB is important for a cell to maintain the continuity of its genome. In the case of unicellular organisms like *Plasmodium*, the repair of such DSB is of at most importance as a single unrepaired DSB can be lethal for the parasite (Frankenberg-Schwager and Frankenberg 1990).

1.5 REPAIR MECHANISM IN THE MITOCHONDRIA OF MODEL ORGANISMS:

Like nuclear genome, independently maintained mtDNA also experiences genotoxic stress. For preserving the nuclear genome integrity, various repair pathways are present which specifically repair the various kind of DNA lesions. Some of these mechanisms are operational whereas others are absent in eukaryotic mitochondria. For example:

1.5.1 Base excision repair (BER): In mitochondria, BER is the major pathway that repairs a range of mtDNA alterations such as base deamination, alkylation, and oxidation. Even though **9** | P a g e

mitochondria are known to lack functional nuclear excision repair (NER), nuclear NER proteins have been found to be localized in mitochondria in addition to the nucleus. However, further investigation revealed that within the mitochondria, the role of these NER proteins is repurposed in BER (Aamann et al. 2010; Kamenisch et al. 2010; Liu et al. 2015). In general, BER begins with the identification of wrongly incorporated or damaged base by the key catalyst of this pathway that is DNA glycosylase which breaks the N-glycosylic bond between the sugar moiety and the base. Several DNA glycosylases also possess lyase enzymatic activity which can cleave the phosphodiester backbone at the 3' end to generate an abasic site. Further, apurinic/apyrimidinic (AP) endonuclease cleaves the 5' phosphodiester bond creating a single nucleotide gap. In the case of DNA glycosylase lacking lyase activity, DNA polymerase gamma removes the deoxyribose-phosphorate moiety that is generated by the action of AP endonuclease. Subsequently, DNA polymerase gamma adds the correct nucleotide at the 3' –hydroxyl moiety, and its ligase activity re-joins the free DNA end to complete the repair process.

- **1.5.2 Mismatch repair** (**MMR**): The existence of MMR in mitochondrial is still questioned as very few essential components of MMR have been documented in mitochondria. On other hand, MMR activity has been reported in the mammalian mitochondrial extract. However, even if MMR does exist in the mitochondrion, certainly there would be a vast difference compared to the nuclear MMR.
- **1.5.3 Non-homologous end joining (NHEJ):** Double-strand breaks (DSBs) are the most deleterious DNA lesion since they disrupt the physical continuity of the genome. To tackle such damage in the nuclear genome, the cell has two highly conserved pathways namely, homology-directed repair (HDR) and non-homologous end joining (NHEJ). Although the canonical NHEJ is absent in the mitochondria, the existence of a microhomology-mediated end joining (MMEJ) mechanism has been confirmed by mitochondrial localization of Mre11 and PARP1. The latter

is a protein involved in MMEJ initiation (Brunyanszki et al. 2016; Dmitrieva et al. 2011). A previous study reported that the human cell mitochondrial extract possesses MMEJ activity against DSBs sharing at least 5 nucleotides or more homology at the broken ends (Tadi et al. 2016).

1.5.4 Homologous recombination (HR): HR-mediated repair is the prominent mechanism for error-free DSB restoration. In general, the HR pathway can be divided into three major events namely presynaptic, synaptic and postsynaptic. In the presynaptic phase, the DSBs are recognized by the MRN/MRX complex comprised of Mre11-Rad50-Nbs1/Xrs2 proteins, and by the nuclease activity of Mre11, the 3' OH single-strand overhang is generated. This singlestranded overhang is stabilized by the binding of RPA which ensures the removal of secondary structures from ssDNA. Further, RPA is replaced by the recombinase protein Rad51 with the assistance of Rad52 protein leading to the formation of the nucleoprotein filament. This is followed by the synapsis in which Rad51 coated ssDNA engages itself into strand seeking for the homologous sequence and anneals with the complementary DNA. This results in the formation of a three-strand structure known as D-loop. The role of Rad54 is to recycle Rad51 onto the 3' overhang while the process of homology search is taking place. The last postsynaptic phase deals with the processing of D-loop intermediated. Since in the DSB, both ends participate in strand invasion which results in the formation of Holliday junction (HJ). The HJ can either be processed by resolvase or dissolvase. With the use of resolvase the end produce could either be crossover or non-crossover. While in the case of dissolvase which involves Blm mediated branch migration and TopoIII facilitated decatenation, the end product is exclusively crossover (Figure 1.5). The presence of genetic recombination in the mitochondrial genomes of fungi, plants, and mammalian cells is well documented (Barr et al. 2005; Shedge et al. 2007). However, the mechanistic details of the HR pathway in mitochondria remained elusive. The role of recombinase protein Rad51 has been reported in mitochondrial copy number maintenance under oxidative stress conditions (Sage et al. 2010; Sage and Knight 2013). Additionally, studies have suggested the function of Rad51 and its paralogs (RAD51C/XRCC3) in safeguarding mtDNA. Similarly, in human cells, a specific mitochondrial helicase called Twinkle has been shown to have a function in the homology-directed repair of mtDNA along with DNA polymerase gamma (Mishra et al. 2018).

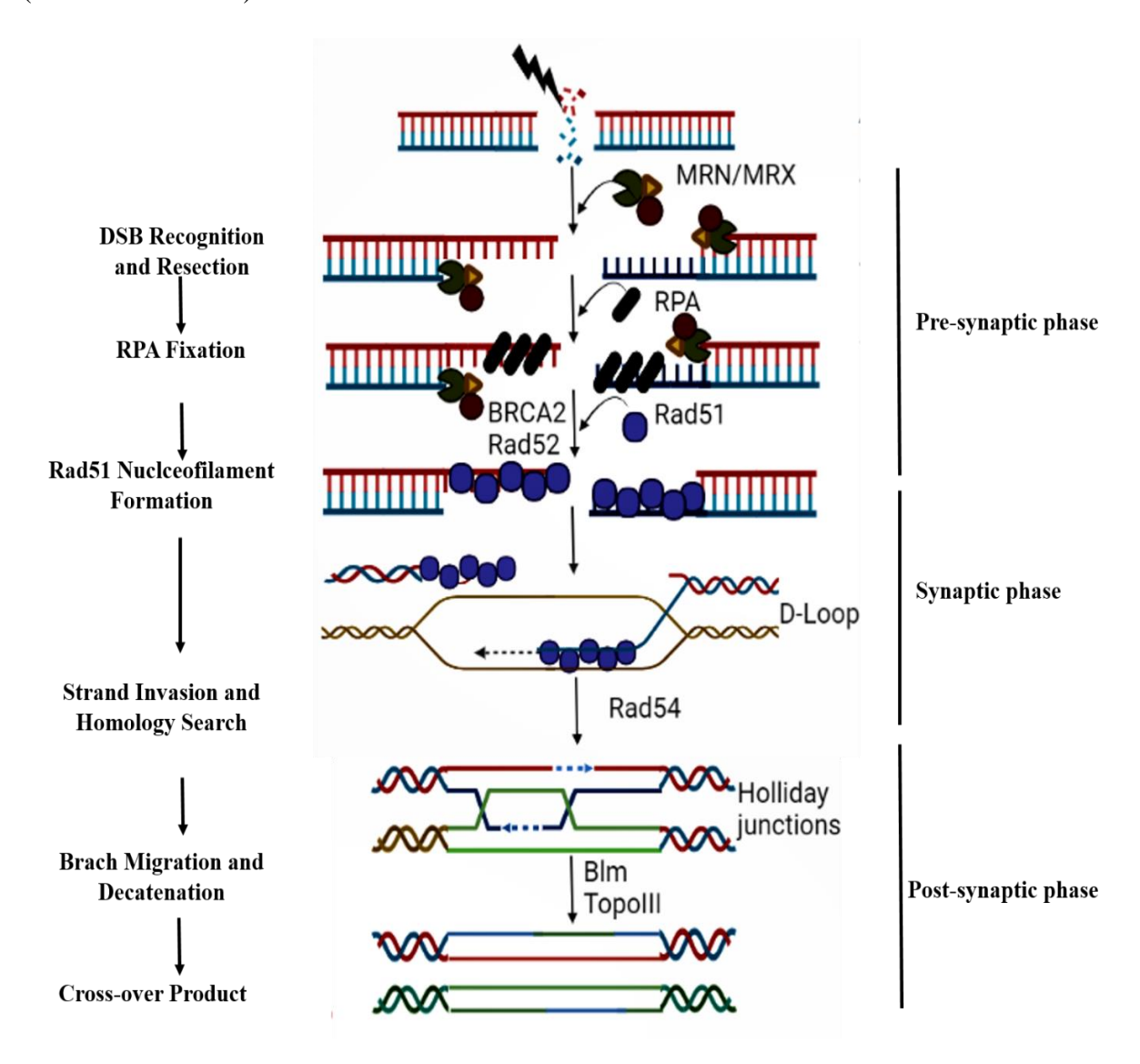


Figure 1.5: Illustration displays three phases of the homologous recombination repair pathway present in the nucleus. Key proteins involved in each step are shown.

1.6 DNA DSB REPAIR PATHWAYS IN Plasmodium falciparum.

Since *Plasmodium* is a unicellular organism even a single DNA DSB could be lethal for it. Hence timely repair of such genomic deformities is crucial for parasite survival. The following mechanisms are involved in *Plasmodium* DSBs repair:

Homology-directed repair in *Plasmodium***:** Several key enzymes of this pathway have been identified in *Plasmodium*. Their function has been shown to be essential for parasite survival. An earlier study has reported that the loss of functional HR pathway abrogated the MMS-induced DSB repair that cannot be compensated by other DNA damage repair pathways. Defective HR mechanism leads to reduced parasite burden in the host, therefore suggesting that HR is the predominant mechanism of repair in *Plasmodium* (Roy et al. 2014). The DNA damage sensor PfalMre11 protein with its conserved nuclease activity was identified in *Plasmodium* (Badugu et al. 2015). The nuclease activity of PfalMre11 enables it to participate in the initial end resection process. Likewise, a key recombinase protein Rad51 has been identified (Bhattacharyya and Kumar 2003) and biochemically characterized in this parasite (Bhattacharyya et al. 2005). An *In vitro* study has established that the recombinant PfRad51 exhibits ATP hydrolysis and strand exchange activity (Bhattacharyya et al. 2005). It was also shown that the inhibition of PfRad51 activity leads to inefficient DNA damage repair leading to decreased parasite survival (Roy et al. 2014; Vydyam et al. 2019). The parasite proteins such as PfRpa1S and PfRpa1L were established as single-strand binding proteins (SSB) and shown to regulate PfRad51 strand exchange activity. Another key enzyme of this pathway namely Rad54 has been identified and shown to promote Rad51 strand exchange activity (Gopalakrishnan and Kumar 2013). Lastly, two DNA helicases, namely, PfBlm and PfWrn were also biochemically characterized in P. falciparum. The knockout of PfWRN has been shown to elevate the rate of mutation rate and resulted in reduced parasite survival (Claessens et al. 2018). A recent study

has shown that functional inhibition of PfBlm severely compromised the nuclear genome repair, hence its direct role in *Plasmodium* DNA repair was thus established (Suthram et al. 2020).

Alternative -NHEJ in *Plasmodium*: Homologs for genes encoding proteins involved in eukaryotic NHEJ, namely, Ku 70, Ku 80, XRCC1, and DNA ligase 4 are not identified in the Plasmodium genome suggesting that the canonical NHEJ is absent in this system (Gardner et al. 2002). Nevertheless, components of Alt-NHEJ have been annotated in the malaria parasite genome. In *Plasmodium*, DSBs have been shown to be repaired by microhomology-directed end joining that includes single-strand overhang resection and newly synthesized nucleotide insertion. Such a mechanism of repair resembles the previously known eukaryotic synthesisdependent microhomology-mediated end joining (SD-MMEJ) pathway (Kirkman et al. 2014). **1.6.3 Nucleotide Excision Repair:** NER is used to repair bulky adducts caused by UV irradiation, chemicals, or ROS. Detection of such DNA lesions in the transcriptionally active genes triggers this pathway by activating TFIIH complex. This multi-proteins complex is involved in both transcription and NER initiation. XPD and p44 are two crucial proteins of this complex and their homologs are present in the *Plasmodium* genome as PF3D7_0934100 and PF3D7_1314900 genes, respectively. In vito study revealed that PfXPD proteins have both ssDNA-dependent ATPase and helicase activity. Interaction of PfXPD with Pfp44 was reported to positively regulate its activity. Additionally, their nuclear localization was in P falciparum

1.6.4 Mismatch Repair: Defective MMR has long been speculated to contribute to elevated SNPs associated with the emergence of drug resistance in *Plasmodium*. Homologs of several genes encoding for MMR pathway proteins have been annotated in the *Plasmodium* genome.

further supported their nuclear function. However, the direct role of these NER proteins in DNA

damage repair is not established yet. Hence, the existence of functional NER in *Plasmodium* for

DNA repair is an open question that needs further validation.

So far only MLH and UvrD proteins are biochemically characterized. PfMLH was reported to have a dual enzymatic activity such as ATPase and endonuclease. Purified PfUvrD protein has shown ATPase and helicase catalytic activity. Expression of these proteins and their nuclear localization has been reported mainly during the schizont and merozoite developmental stages of *P. falciparum* (Ahmad et al. 2012; Tarique et al. 2012).

All the components of NER and MMR pathways found in *Plasmodium* have shown nuclear exclusive localization with no evidence of their mitochondrial presence.

1.6.5 Base Excision Repair: Most of the genes encoding BER components are identified in the *Plasmodium* genome. Three key components of this pathway have been biochemically characterized in *P. falciparum* but their localization to mitochondria/ nuclear is not known (Buguliskis et al. 2007; Casta et al. 2008; Suksangpleng et al. 2014). Except for these three, all others are predicted to localize into mitochondrial. Two main AP endonucleases of this pathway that is PfApn 1 and PfApe 1 have been biochemically characterized in *P falciparum*. PfApn1 has been shown to contain conserved 3' phosphatase activity but lacks 3'-5' endonuclease and NIR functions. Whereas PfApe1 was reported as a multifunctional enzyme that retains 3'-5' endonuclease and NIR functions apart from 3' phosphatase activity. Interestingly, their mitochondrial exclusive localization suggested that the BER pathway is majorly devoted to this organelle repair and has no role in the repair of the nuclear genome.

In general, the knowledge on mitochondrial DNA repair is very limited. Despite being a potential drug target and an indispensable organelle for the parasite survival, so far only one mechanism of DNA repair has been documented in the *Plasmodium* mitochondria. Thus exploring the function of other repair mechanisms in parasite mitochondria would provide new strategies to combat malaria.

Table 2: List of the proteins involved in BER, NER, HR, NHEJ, MMEJ, MMR pathways known in nuclear and/or mitochondria of Human and *P. falciparum*.

Repair	Human		Plasmodium		
Machanism					
	nDNA	mtDNA	nDNA	mtDNA	Gene ID
	Repair	Repair	Repair	Repair	
	UNG1	UNG1	-	-	PF3D7_1415000
	AAG/MAG	-	-	-	PF3D7_1467100
	MYH	-	-	-	PF3D7_1129500
	NTHL1	-	-	-	PF3D7_0614800
	OOG1	OOG1	-	-	PF3D7_0917100
Base Excision Repair (BER)	NEIL1	-	-	-	-
	NEIL2	-	-	-	-
	APE1	APE1	-	PfAPE1 b	PF3D7_0305600
	APE2	APE2	-	-	-
	-	-	-	PfAPN1 ^b	PF3D7_1332600
	DNA Pol γ	-	-	PfDNAPol I ^a	PF3D7_0625300
	DNA Pol β	-	-	-	-
	XPC	-	-	-	-
	Rad23b	Rad23b	-	-	PF3D7_1011700
	XPB/Rad25	-	-	-	PF3D7_1037600
	XPG/Rad2	-	-	-	PF3D7_0206000

		T	T	T	T
Nucleotide Excision Repair	XPD	XPD	-	-	PF3D7_0934100
(NER)	ERCC1	-	-	-	PF3D7_0203300
	XPF	-	-	-	PF3D7_1368800
	CSB	CSB	-	-	-
	CSA	CSA	-	-	-
	P44	-	-	-	PF3D7_1314900
	UVSSA	-	-	-	-
	MRE11	MRE11	PfalMre11	-	PF3D7_0107800
	RAD50	RAD50	Putative Rad50	-	PF3D7_0605800
	NBS1	NBS1	-	-	-
	CtIP	-	-	-	-
	EXO1	-	-	-	PF3D7_0725000
	BLM	-	PfBlm	PfBlm ^a	PF3D7_0918600
	WRN	-	PfWrn	-	PF3D7_1429900
	TopoIIIα	-	PfTopoIII	PfTopoIII ^b	PF3D7_1347100
	RMI1	-	-	-	-
	DNA2	-	Putative DNA2	-	PF3D7_1010200
	RPA1	-	PfRPA1(LS)	-	PF3D7_0409600
			PfRPA1(SS)	-	PF3D7_0904800
	RPA2	-	-	-	-
Homologous recombination	RPA3	-	-	-	-
(HR)	RAD51	RAD51	PfRad51	PfRad51 ^a	PF3D7_1107400
	DMC1	-	Putative DMC1	-	PF3D7_0816800

	RAD52	-	-	-	-
	BRCA2	-	Putative	-	PF3D7_1328200
	RAD54	-	Putative	-	PF3D7_0803400
	DNA Polδ	-	PfDNA Polδ	-	PF3D7_1017000
	PCNA	-	PfPCNA1	-	PF3D7_1361900
			PfPCNA2	-	PF3D7_1226600
	RTEL1	-	-	-	PF3D7_0514100
	XPF	-	-	-	PF3D7_1368800
	ERCC1	-	-	-	PF3D7_0203300
	MUS81	-	-	-	PF3D7_1449400
	EME1	-	-	-	-
	GEN1	-	-	-	PF3D7_0206000
	SPO11	-	-	-	PF3D7_1217100
	-	Twinkle	-	-	PF3D7_1411400
	-	MGME1	-	-	-
	Ku70	-	-	-	-
Nonhomologous end joining (NHEJ)	Ku80	K80 truncated	-	-	-
	DNA ligase IV	-	-	-	-
	DNA-PKs	-	-	-	-
	Artemis	-	-	-	-
	XRCC4	-	-	-	-
	Cernunnos/ XLF	-	-	-	-
	MRE11	MRE11	PfalMre11	-	PF3D7_0107800

	RAD50	RAD50	Putative	-	PF3D7_0605800
	NBS1	NBS1	-	-	-
	CtIP	CtIP	-	-	-
Microhomology-	ATM	-	-	-	-
mediated end joining	XPF	-	Putative	-	PF3D7_1368800
	ERCC1	-	Putative	-	PF3D7_0203300
	FEN1	-	PfFEN1	-	PF3D7_0408500
	DNA Ligase I	-	LigI Putative	-	PF3D7_1304100
	DNA Pol ζ	-	-	-	PF3D7_1037000
	DNA Pol β	-	-	-	-
	DNA Pol η	-	-	-	-
Mismatch Repair (MMR)	MLH	-	-	-	PF3D7_1405400
1	PMS	-	-	-	PF3D7_1117800
	MSH2	MSH2	-	-	PF3D7_0706700
	MSH6	-	-	-	PF3D7_0505500

a- established in this study, b-previously reported, '-' functionally not characterized or absent or unknown

Mutation in mtDNA has been linkered to various neurodegenerative diseases and pathological conditions related to premature aging of the cell. For this reason, the mechanisms involved in safeguarding the mitochondrial genome have been actively pursued in the model organisms. Moreover, it is evident from our literature review that various DNA damage repair pathway is involved in maintaining the integrity of this genome in human cells (Table 2). Likewise, the indispensable nature of mitochondria in *Plasmodium* has been exploited to target this parasite. Key components of most of these mechanisms have been annotated in the *P. falciparum* genome (Table 2). Hence exploring the repair of mtDNA through homologous directed repair besides known BER machinery could give us a novel avenue for developing anti-malarial drugs.

1.7 SIGNIFICANCE OF THE STUDY.

The impact of malaria on global public health and the world economy continues to surge despite the decades of vaccine research and drug development efforts. Resistance to all the commercially available drugs and the lack of an effective malaria vaccine urge for the identification of novel intervention strategies for curbing malaria. Here we uncover the molecular mechanism behind the repair of the most deleterious form of DNA lesions on the parasitic mitochondrial genome. Given that the single-copy mitochondrion is an indispensable organelle of the malaria parasite, we propose that targeting the mitochondrial DNA repair pathways should be exploited as a potential malaria control strategy. The establishment of the parasitic homologous recombination machinery as the predominant repair mechanism of the mitochondrial DNA double-strand breaks underscores the importance of this pathway in *Plasmodium* parasite biology.

1.8 OBJECTIVES OF THIS STUDY.

Plasmodium mitochondrion has been considered an excellent target against malaria. The drugs targeting parasite mitochondria are failing due to the inherent ability of the parasite to attain quick resistance to these drugs. Interestingly, the resistance to drugs targeting mitochondria is associated with the rapid mutations in the proteins involved in mtETC. Therefore, we proposed that targeting Plasmodium mitochondria through other essential housekeeping processes would be an alternative for managing the current scenario of drug resistance in malaria parasites. Thus, in the present study, we seek to explore the repair of the mitochondrial genome. Since HR is the predominant repair pathway in Plasmodium and has a role in mitochondrial genome repair in model organisms, we explored its role in Plasmodium mitochondria stability. For this, we have investigated the existence and function of key components HR in P falciparum mitochondria. We also checked how the external DNA damaging stress modulates mitochondrial localization and mtDNA interaction of HR proteins. Furthermore, we have explored the mitochondrial localization of putative Plasmodium DNA polymerase I and its interaction with HR proteins.

1.9 AIMS OF THE Ph.D. WORK.

- 1) Role of *Plasmodium* homologous recombination machinery in mitochondrial DNA double-strand break (DSB) repair
- Mitochondrial localization of nuclear repair proteins
- Association of HR proteins with mitochondrial genome
- o Mt DNA-IP to identify the interacting mitochondrial locus
- o Stage-specific occupancy of HR proteins
- Role of HR proteins in mitochondrial DSB repair
 - o Kinetics of mitochondrial vs. nuclear DSB repair
 - o Effect of small molecule inhibitor of PfRad51 and PfBlm on mtDNA repair
 - o Mt-DNA repair kinetics in PfRad51 and PfBlm over-expressing parasites
- DNA damage-induced mitochondrial localization of HR proteins
- DSB induced mt-DNA occupancy of HR proteins
- 2) The mitochondrial localization of putative *Plasmodium* DNA polymerase I and its interaction with HR proteins
- Generation of transgenic parasite line episomally expressing putative PfMtDNAP with Cterminal GFP tag.
- Localization of PF3D7_0625300 gene product (putative mtDNAP) into P. falciparum mitochondria
- Association of PfmtDNAP with *P. falciparum* mitochondrial genome
- Mt DNA-IP to identify the interacting mitochondrial locus
- Interaction of PfmtDNAP with repair and replication proteins

Chapter 2 <u>MATERIALS AND METHODS</u>

2.1 Recombinant DNA methods.

2.1.1 Bacterial Competent cell preparation:

An isogenic colony of bacteria was inoculated in the 5 ml LB medium containing the appropriate antibiotic selection and grown overnight in a shaker incubator at 200 rpm rotation and 37°C temperature. The next day, secondary inoculation was given in a 50 ml LB medium containing the suitable antibiotic selection. The cells were grown till the optical density at 600 nm reached 0.5. Cells were harvested by centrifuging the culture at 8000 rpm for 10 minutes at 4 °C. The bacterial pellet was washed by gently re-suspending it in 12.5 ml of ice-cold 0.1 M CaCl₂ solution. Then cells were pelleted down by centrifuging the suspension at 8000 rpm for 10 minutes at 4 °C. Later the cells were again resuspended in 12.5 ml of ice-cold 0.1 M CaCl₂ solution followed by 4-8 hours of incubation on ice. After the incubation, competent cells were harvested by centrifuging the suspension at 8000 rpm for 10 minutes at 4 °C. The resulted cell pellet was re-suspended gently in 2.15 ml ice-cold 0.1 M CaCl₂ solution and 100 μl 100% glycerol. Finally, 100 μl of competent bacterial cell suspension were aliquoted into the pre-chilled microfuge tube and stored at -80 °C.

2.1.2 Bacterial Transformation:

For bacterial transformation vials of competent bacterial cells were taken out from -80°C and thawed on ice for 15 minutes. Plasmid DNA with a preferable amount of 25-50 ng was laid over the cells and incubated on ice for the next 30 minutes. After incubation on ice, cells were subjected to heat shock at 42 °C temperature for a different duration depending upon cell type for example 30 seconds for Top10 cells 45 seconds for BL21 Rosetta cells, or 90 seconds for BL21 pLysS cells. Immediately after the heat shock cell were placed on ice for 1 minute and

later 900 µl of 37 °C pre-warmed LB medium was added to the cells. Next, the cells were incubated at 37 °C for 45 minutes to 1 hour. After this incubation, cells were pelleted down by applying brief spin at top centrifugal speed. Most of the supernatant was discarded leaving approximately 100 ul medium for re-suspending the cells. Lastly, the transformed cell suspension was plated on the LB agar plate containing the appropriate antibiotic selection and incubated at 37 °C for overnight (12- 16 hours).

2.1.3 Alkaline Lysis Method for Plasmid DNA Isolation:

An isogenic bacterial colony was inoculated into a 5- 10 ml LB medium containing suitable antibiotics and grown overnight in a shaker incubator at 200 rpm and 37 °C temperature. The next day, the cells were harvested by centrifuging the culture at 4000 rpm for 10 minutes at room temperature. After the removal of supernatant media completely, the cell pellet was resuspended in 200 µl solution 1 containing 25mM Tri-HCl pH 8 and 10mM EDTA pH 8. This cell suspension was transferred into a fresh 1.5 ml microfuge tube. To this, 200 µl of solution 2 which contains 0.2 mM NaOH and 1% SDS was added and then the samples were mixed thoroughly by inverting the tube multiple times until the cell suspension became vicious which ensures cell lysis. Next, 200 µl solution 3 containing 3M NaOAc pH 5.2 and glacial acetic acid (GAA) was added and mixed very gently for avoiding mechanical shearing of DNA. This mixture was incubated on ice with intermittent mixing every 5 mins until while precipitates started appearing. This turbid solution was centrifuged at 12000 rpm for 10 minutes at room temperature. The resulted supernatant was transferred into a fresh microfuge tube and to this 400 µl of absolute ethanol was added and samples were incubated at -80 °C for 45 minutes. For precipitating the DNA, samples were centrifuged at 12000 rpm for 30 minutes at 4°C. The resulting pellet was washed with 70% ethanol and again centrifuged at 12000 rpm for 5 minutes at 4°C. The supernatant was discarded and pellets were air-dried for 20 minutes. The pellet was resuspended in 50 μ l 1X TE (10mM Tri-HCl ph 8 and 1 mM EDTA pH 8) and then treated with RNase by adding 5 μ l of 10 mg/ml Ranase stock solution. The samples were incubated in the 37 °C water bath for 30 minutes. For PCIA treatment, the volume of samples were made up to 400 μ l using 1X TE to which an equal volume of PCIA solution containing Phenol: Chloroform: Isoamyl alcohol in 25:24:1 ratio was added. For homogenous mixing, the samples were vortexed for 3-5 minutes. To separate the aqueous layer from the organic layer the samples were centrifuged at 12000 rpm for 15 minutes at room temperature. The resulting upper aqueous layer was carefully collected into a fresh microfuge tube and to this 2.2 volume absolute ethanol and 1/3 volume 3 M NaOAc solution was added and incubated at -80 °C for 1-2 hours. The samples were centrifuged at 12000 rpm for 30 minutes at 4 °C for precipitation of the purified plasmid DNA. The pellet was once washed with 500 μ l of 70 % ethanol followed by air-drying the pellet for 20 min. Finally, the DNA pellet was resuspended in 50 μ l of 1X TE solution and kept at -20 °C for long time storage.

2.1.4 Site-Directed Mutagenesis:

All the mutants of Pfrad51 used in this study were generated using the splice overlap PCR-based method. The ORF of this gene was amplified in two fragments and the overlapping flaps of these fragments were harboring the desired mutation. The homologous sequence of overlapping fragments allowed them to anneal and hence acted as the template while amplifying the full-length ORF of the *PfRAD51* gene. The details of primers and their sequence which were used in generating Pfrad51 mutants are listed in table3. The final full-length *Pfrad51* ORFs with the desired mutation were cloned into either bacterial expression vector or *Plasmodium* episomal expression vector (pARL). Single mutant Pfrad51^{S144-A} and double mutant Pfrad51^{S144-A} s319-A

were cloned into pET28a whereas Pfrad51^{S319-A} single mutant was cloned in pGEX6p2. The final clones were sequenced for confirming the desired mutations.

2.2 YEAST METHODS

2.2.1 Yeast Competent Cell Preparation:

An isogenic colony of desired yeast strain was used for giving primary inoculation in 10 ml YPD or YNB medium containing an appropriate amino acid mix. The yeast cells were grown in the incubator shaker at 200 rpm, 30°C for overnight. The next day, OD₆₀₀ of primary culture was measured, and based on the OD, the volume of overnight culture required for secondary inoculum was measured using the following formula:

The volume of primary culture required (ml) =

The final volume of secondary culture (ml) \times desired OD600 of secondary culture OD600 of primary inoculum \times 2²

The culture was incubated in the shaker incubator at 30 °C, 200 rpm till the final OD reached 0.5-0.6. Cells were harvested by centrifuging the culture at 3500 rpm for 5 minutes at 4°C. The resultant supernatant was discarded and the cells were washed with 10 ml sterilized Milli Q water and centrifuged at 3500 rpm for 5 minutes at 4°C. The pelleted cells were re-suspended in 300 µl LiOAc solution containing 1X TE and 1X LiOAc. 200 µl of these competent yeast cells were used for each transformation.

2.2.2 Yeast Transformation:

In a sterile 2 ml microfuge tube, 1-5 μg of sample DNA along with 10 μg of carried DNA (salmon sperm DNA) was added. Competent cells were gently layered over the DNA mix. 1.2 ml PEG solution (containing 1ml 10X LiOAc, 1ml 10X TE, and 8 ml 50% PEG2000) was added

to each tube, this was followed by 30 minutes incubation in a shaker incubator at 30 °C, 200 rpm. Later the cells were subjected to heat shock at 42 °C temperature for 15 minutes. Cells were then pelleted down by centrifuging the suspension at 10,000 rpm for 10 seconds. The cell pellet was re-suspended in 200 µl 1X TE buffer and plated on the YNB agar plates with appropriate amino acid selection. The plates were incubated at 30°C for 3-5 days till the transformed colonies started appearing.

2.2.3 Yeast Two-Hybrid Assay

To study protein-protein interaction, yeast two-hybrid system was used. Firstly, the DNA repair genes PfRAD51 and PfBLM were cloned into the bait vector pGBDU-C1 containing the URA selection marker for fusing a gene to the GAL4 DNA binding domain. Similarly, PfMTDNAP and PfTOPOIII were cloned into the prey vector pGAD-C1 containing LEU selection marker for fusing a gene to the GAL4 activation domain. The final constructs were transformed into a Y2H yeast strain PJ69A4, which resulted in the generation of yeast strains namely, PJY5 (transformed with pGBDU-C1-PfRAD51), PJY6 (transformed with pGBDU-C1-PfRAD51), PJY7 (transformed with pGBDU-C1-empty), PJY8 (Transformed with pGAD-C1-PfMTDNAPOLI), PJY9 (Transformed with pGAD-C1-PfTOPOIII), PJY8 (Transformed with pGAD-C1-empty), PJY10 (Co-transformed with pGBDU-C1-PfRAD51 and pGAD-C1-PfMTDNAPOLI), PJY11 (Co-transformed with pGBDU-C1-PfBLM and pGAD-C1-PfMTDNAPOLI), PJY12 (Co-transformed with pGBDU-C1-PfRAD51 and pGAD-C1-empty), PJY13 (Co-transformed with pGBDU-C1-PfBLM and pGAD-C1-empty), PJY14 (Cotransformed with pGBDU-C1-empty and pGAD-C1-PfMTDNAPOLI), PJY15 (Co-transformed with pGBDU-C1-empty and pGAD-C1-PfTOPOIII), and PJY16 (Co-transformed with pGBDU-C1-PfRAD51 and pGAD-C1-PfTOPOIII). The success of a single transformation was assessed on either Sc –Ura or Sc –Leu single dropout plates. Similarly, co-transformation of bait and prey vectors with/ without inserted gene was examined on Sc –Ura –Leu double dropout plates. Interaction between the test protein was determined by patching the doubly transformed yeast cells on triple dropout plates (Sc –Ura –Leu –His and Sc –Ura –Leu –Ade). The weak interaction was scored by spotting the equal number of doubly transformed yeast cells on Sc – Ura –Leu –His whereas strong interaction was scored on both Sc –Ura –Leu –His/ Ade triple dropout plates. Self-activation of reporter gene promoter (*GAL4* promoter) was determined by scoring the growth of co-transformed yeast strain harboring empty bait and empty prey, empty prey and bait with either *PfRAD51* or *PfBLM*, prey containing either *PfMTDNAP* or *PfTOPOIII* with empty bait on triple dropout plates.

2.3 Recombinant Protein purification:

For purifying wild-type PfRad51 protein, the plasmid *pET101D-PfRAD51* (generated by MKB (Bhattacharyya et al. 2005)) was transformed into *E. coli* expression cell BL21 Rosetta. As reported earlier the maximum expression of recombinant PfRad51 protein was obtained by 1 mM isopropylthiogalactiside (IPTG) induction given at 0.8 OD₆₀₀ for 4 hours at 37 °C, 200 rpm. Likewise, the plasmids *pET28a-Pfrad51*^{S144-A} and *pET28a-Pfrad51*^{S144-A} s319-A were transformed into BL21 Rosetta cells and recombinant protein was induced using 1mM IPTG (Sigma) given at 0.6 OD₆₀₀ for 4 hours at 37 °C, 200 rpm. However, the *pGEX6p2-Pfrad5*^{S319-A} plasmid was transformed into BL21 cell for expressing recombinant PfRad51 ^{S319-A}. Expression of this protein was induced at 1mM IPTG (Sigma) given at 0.6 OD₆₀₀ for 4 hours at 37 °C, 200 rpm. After induction, cells were harvested by centrifuging the culture at 8000 rpm for 8 minutes at 4 °C and can be stored at -80 °C (optional). For purifying recombinant protein with His tag following procedure was used: lysis buffer (containing 50 mM NaH₂PO₄, 200 mM NaCl, 20

mM Imidazole, 50% (v/v) glycerol, 20 mM β-mercaptoethanol, and 2% (v/v) Tween 20) was added to the cells according to the weight of the pellet (3 ml lysis buffer is required for 1 gram cell pellet lysis). Lysozyme with the final concentration of 1 mg/ml was added to the cell suspension and incubated for 45 minutes on ice. PMSF was added to the samples and the samples were sonicated for approximately 20-30 minutes with 10 seconds pulse at 50% amplitude followed by 20 seconds rest on ice. This cell lysate was centrifuged at 10000 g for 45 minutes at 4 °C. The supernatant was collected into the fresh tube and later mixed with the 50% (w/v) pre-equilibrated Ni-NTA bead slurry. For binding, this mixture was rotated for 1 hour at 15-20 rpm in the cold room. Beads were allowed to settle down for 1-2 hours and the loading flow-through was collected. Beads were first washed using washing buffer I (containing 50 mM NaH₂PO₄, 20 mM Imidazole, 50% (v/v) glycerol, 20 mM β-mercaptoethanol, and 2% (v/v) Tween 20) and washing buffer II (containing 50 mM NaH₂PO₄, 150 mM NaCl, 50 mM Imidazole, 50% (v/v) glycerol, 20 mM β-mercaptoethanol, and 2% (v/v) Tween 20). Later, for eluting the bound recombinant proteins elusion buffer I (containing 50 mM NaH₂PO₄, 150 mM NaCl, 250 mM Imidazole, 30% (v/v) glycerol, 20 mM β-mercaptoethanol, and 2% (v/v) Tween 20) was added to the column and fractions were collected in fresh tubes. Similarly, beads were subjected to another round of elution using elution buffer II (containing 50 mM NaH₂PO₄, 150 mM NaCl, 400 mM Imidazole, 30% (v/v) glycerol, 20 mM β-mercaptoethanol, and 2% (v/v) Tween 20).

For purifying PfRad5^{S319-A} tagged with GST, BL21 bacterial cell pellet was resuspended in 2 ml of 1 X PBS pH 8 (containing 10 mMKH₂PO₄, 40 mM K₂HPO₄, 150 mM NaCl). To this, 100 mg/ml lysozyme was added and incubated on ice for 1 hour. Cells were lysed by sonication as described above. Later, 0.1% Triton X-100 was added to the sample and incubated on ice for

30 minutes. The lysate was then centrifuged at 10,000 rpm for 30 minutes at 4°C. The supernatant containing soluble proteins was transferred into a fresh tube. To this, 5 volume of pre-equilibrated Glutathione Sepharose 4B (GST) beads was added and the mixture was incubated on a rocker for 1 hour at room temperatre. This was then centrifuged at 3000 rpm for 1 minute and the loading flow-through was collected into a tube. The bead was washed by adding 5 volumes of washing buffer (containing 10 mM DTT, 2 mM EDTA, 140 mM NaCl, 100 mM PMSF made in 1X PBS). Later the bound recombinant protein was eluted with the help of elution buffer (containing 10 mM DTT, 35 mM reduced glutathione, 0.1% NP40, 10% glycerol made in 1X PBS pH 7)

All the fractions were analyzed on SDS-PAGE for the presence of purified recombinant protein. Elution having the maximum amount of protein was subjected to dialysis in buffer containing 20 mM Tri-HCl pH 8, 1 mM dithiothreitol (DTT), 5% (v/v) glycerol.

2.4 Western blotting:

The protein from different sources such as purified recombinant protein, whole parasite lysate, subcellular fraction samples, and thermolysin protection assay samples was separated on 10-12 % SDS-PAGE followed by blot transfer. For blot transfer, PVDF membranes were first pretreated with 100% methanol for 30 seconds followed by a quick wash with distilled water, and later the membrane was treated with transfer buffer (containing 5.86 grams of glycine, 11.64 grams of Tris base, and 0.75 grams of SDS) for 5 minutes. The semi-dry transfer method was employed for blot transfer at 240 mA constant current for 80 minutes. Followed by transfer, the blot was treated with 5% blocking buffer (containing 5 grams for skimmed milk in 100 ml 1X TBST buffer) for 2 hours on the rocker, at room temperature. Later, the blot was treated with primary antibody and incubated on the rocker overnight at 4°C. The next day, the blot was

washed thrice using 1X TBST (containing 0.2 M Tris base, 9% NaCl pH of buffer adjusted to 7.6, and 0.1 % Tween 20) and later was probed with secondary antibody conjugated with HRP. The blot was then subjected to washing as described above. Followed by blot development using a chemiluminescent HRP substrate (SuperSignal West Pico PLUS; Thermo Scientific) and imaged by using a ChemiDoc Touch imaging system from Biorad. For quantifying, the protein band intensities ImageJ software was used. The primary antibodies used were rabbit anti-PfRad51 (1:5000 dilution) (Roy et al. 2014), rabbit anti-PfBlm (1:5000) (Suthram et al. 2020), rabbit anti-PfalMre11 (1:5000) (Badugu et al. 2015), rabbit anti-HsHistone 3 (1:5000; Imperial Life Sciences), mouse anti- Cytochrome C (1:5000; Abcam), rabbit anti-GFP (1:5000; Abcam) and mouse anti-GAPDH (1:5000; Abcam). The horseradish peroxidase (HRP) conjugated secondary antibodies used in the study were anti-mouse (1:10000; Santa Cruz Biotechnology Inc.) and anti-rabbit (1:10000; Promega).

2.5 Methods in *Plasmodium falciparum* experiments.

2.5.1 Washing of Red Blood Cells (RBCs):

Blood was purchased from the sanjeevani blood bank for experimental use. 10 ml of whole blood was aliquoted in 15 ml centrifuge tube and subjected to centrifugation at 2500 rpm for 20 minutes at room temperature to separate RBCs. The top layer (serum) and intermediate buffy layer were aspirated carefully. The bottom layer containing enriched RBC was washed by resuspending the cells into an equal volume of cold in-complete RPMI medium and centrifuged at 2500 rpm for 20 minutes. Later, the supernatant was discarded and the above-mentioned washing steps were repeated twice. Finally, the washed RBCs were resuspended into an equal volume of cold in-complete RPMI medium to obtain 50% hematocrit and stored at 4 °C.

2.5.2 Thawing of parasites:

A frozen vial of parasites was taken out from the liquid nitrogen storage tank and allowed to thaw by placing the tube in a 37 °C water bath for 5 minutes with continuous monitoring. The vial was properly sterilized using 70 % ethanol and its content was transferred into a 50 ml centrifuge tube. To this, 200 μl of solution I (12 % w/v Nacl) was added drop-wise with gentle mixing, and the cells were allowed to rest for 5 minutes. To this, solution II (1.6% w/v NaCl) was added in a drop-wise manner with intermittent gentle mixing. Later the suspension was centrifuged at 1000 for 10 minutes. The resultant supernatant was aspirated out without disturbing the cell pellet. The pellet was disturbed by gently mixing and to this, solution III (0.9% w/v NaCl, 0.2% w/v glucose) was added in a similar manner as described earlier. The cells were harvested by centrifuging the suspension at 1000 rpm for 10 minutes and the supernatant was discarded. Finally, the thawed parasite-infected RBCs were resuspended in 2 ml of complete medium. To this, 200 μl of washed RBCs (50% hct) was added and the culture was transferred to 6 well plates and grown in the candle jar placed within 37 °C incubator.

2.5.3 *In vitro* parasite culture maintenance:

During the *P. falciparum* culture maintenance, the medium of the culture was preferably changed every day and a new subculture was given every alternative day (depending upon the donor culture parasitemia). For changing the medium the upper layer medium from the plate was aspirated carefully without disturbing the settled cells (infected/ noninfected RBCs) and to this, 4 ml fresh pre-warmed complete RPMI medium was added. The plate was shaken in the rotational motion to mix the cells with the added medium. For determining the parasitemia of the culture, a blood smear was made on a clean slide which was then fixed with 100% methanol.

The slide was next stained with Giemsa stain (Sigma), a nucleic acid stain specifically stains the parasites (infected RBCs). This was visualized under the oil immersion 100X lens of the compound microscope. For subculturing, the donor culture was first mixed well, and depending upon its parasitemia, the required volume of donor culture was transferred to a fresh well of the plate to which 4 ml of prewarmed complete RPMI medium and 0.5 ml of washed blood was added. The plates were transferred into the candle jar placed inside the 37 °C incubator.

2.5.4 Parasite Culture Synchronization by Sorbitol Method:

Parasite culture with more than 60% ring staged parasites with at least 4% parasitemia in total was used for synchronization. The culture was transferred into 15 ml centrifuge tube (per tube 10 ml culture) and centrifuged at room temperature, 2500 rpm for 10 minutes. The resultant supernatant was aspirated out and to the cells, 1 ml of prewarmed sorbitol solution (5% w/v sorbitol) was added. Cells were re-suspended by brief vortexing and then incubated at 37 °C (water bath) for 20 minutes with intermittent mixing. The volume in the tube was made up to 10 ml using prewarmed in-complete media and centrifuged as mentioned above. The culture was washed thrice using in-complete media and finally, the cells were resuspended in prewarmed complete media and kept back in the candle jar at 37 °C.

2.5.5 Transfection in *P. falciparum*:

A cycle prior to the transfection the synchronized parasite culture was fed with fresh blood while maintaining the parasitemia at 2 %. 100 μg of the desired plasmid was resuspended in 50 μl of cold cytomix solution (containing 10 mM K₂HPO₄ pH 7.6, 120 mM KCl, 0.15 mM CaCl₂, 25 mM HEPES pH 7.6, 2 mM EGTA pH 7.6, and 5 mM MgCl₂) and incubated at 4°C overnight a day before transfection. On the day of transfection, 10 ml parasite culture with 8% parasitemia

at the early ring stage (6-10 hpi) was centrifuged at room temperature, 2500 rpm for 10 minutes. The harvested cells were washed twice with pre-warmed cytomix solution and later the cells were resuspended in 1250 µl of cytomix. From this, 350 µl of the cell suspension was added to the tube containing 50µl of DNA and mixed gently. This mixture was then transferred to an electroporator cuvette slowly by avoiding air-bubble formation. The cuvette was then placed carefully into the Bio-Rad Gene Pulsar, by aligning the metallic side of the cuvette with the direction of electrodes. The pulse was given at 0.31kV, 950µF, infinite resistance. Immediately after the electroporation, the content was transferred to the culture plate containing 3 ml of prewarmed complete medium. The remaining cells from the cuvette were collected by washing the cuvette multiple times with 1ml of ice-cold complete medium. To this, 100 µl of fresh blood (50% hct) was added and incubated at 37°C within the candle jar. After 6 hours, medium of the transfected culture was changed. Thereafter every day the media was changed and expansion of the culture was done once parasitemia reaches 2%. The culture was maintained in pyrimethamine drug medium once the parasitemia reaches 4-6% for allowing selective growth of transfectant over the non-transfectant parasite.

2.5.6 Genomic DNA isolation from *P. falciparum*:

Genomic DNA was isolated from 10 ml parasite culture with at least 4 % parasitemia at different time points pre or post UV exposure. Parasites were released from RBC s by saponin lysis and the parasite pellet was resuspended in 75 µl of sterile Milli-Q water and to this 25 µl of lysis buffer (containing 10 mM Tris-HCl pH8, 20 mM EDTA pH8, 0.5% SDS, and 0.1 mg proteinase K) was added. This mixture was thoroughly mixed by vortexing for 5 minutes at every 30 minutes interval during 3 hours of incubation at 37°C. The resulting lysed parasite was subjected

to PCIA treatment to separate the aqueous layer. This top aqueous layer was collected in the fresh microfuge tube and subjected to RNase treatment for 30 minutes at 37°C. Later the samples were again treated with PCIA solution and centrifuged at top speed for 15 minutes to separate the aqueous layer which was collected in the sterile tube. To this 2.2 volume of 100% ethanol and 1/3 volume of 3M NaOAc pH 5.2 was added and the samples were incubated at -80°C overnight. The next day DNA was precipitated by centrifuging the samples at 12000 rpm for 30 minutes at 4°C which was followed by 70% ethanol wash of the DNA pellet and later the pellet was air-dried for 20 minutes. Finally, the isolated DNA was resuspended in 30 µl 1X TE buffer and stored at -20°C refrigerator.

2.6 DNA damage induction.

2.6.1 DSB induction using UV:

To create random DSBs in the *P. falciparum* genome, tightly synchronized trophozoites (24 hours post-invasion) staged parasite with 2% parasitemia (volume of culture varies depending upon the assay type) were used. At the time of treatment, maximum volume of medium from the wells containing parasite culture was aspirated and immediately the cells were exposed to UV light at a dose of 100J/m² (0.01J/cm²) using BIO-LINK® crosslinker (BLX). After the exposure, prewarmed complete medium was added and the culture was harvested at different time points and processed according to the assay.

2.6.2 DNA damage by methyl methanesulfonate (MMS):

The exogenous DNA damage stress was given to 150-200 ml synchronized schizonts (40 hpi). For inducing the DNA damage, 20 ml parasite culture was transferred into 50 ml centrifuge tubes and harvested at 2500 rpm for 10 minutes at room temperature. To each tube 20 ml

complete medium containing 0.05% MMS (i.e. 10 ul 1% MMS in 200 ml complete medium) was added. Then cells were gently resuspended in MMS containing complete medium and transferred back to the culture plates followed by 6 hours incubation at 37 °C within the candle jar. After this incubation, the culture was harvested and subjected to saponin lysis to liberate the parasites and stored at -80°C.

2.7 *In vitro* phosphorylation assay:

For this assay, *P. falciparum* culture was pretreated with 0.05% (v/v) methyl methanesulfonate (MMS) to create DNA damage. 150 ml synchronized schizont staged culture with 8-10% parasitemia was harvested by centrifuging the culture at 3000 rpm for 10 minutes. The RBCfree parasites were generated by treating the infected cells with 2 pack cell volume (PCV) of 0.15% saponin solution for 20 minutes at 37 °C (water bath) with intermittent mixing. Later the parasites were harvested by centrifuging the samples at 3000 rpm for 10 minutes, 4°C. The parasite pellet was washed thrice with cold 1X PBS. The parasite pellet was stored at -80 °C and later used to prepare cell-free extracts containing all the kinases in the parasite system. The parasites were thawed on ice and later re-suspending in 10 volumes of ice-cold lysis buffer (containing 50mM Tris-HCL pH-7.3, 50 mM β-glycerol phosphate, 1 mM DTT, Complete protease inhibitor cocktail, and Phosphatase inhibitor cocktail I). Parasite cells were lysed by multiple rounds of passage through a needle (18 Gnage) and three cycles of liquid nitrogen freeze-thaw. The lysate was centrifuged at 13000g for 30 minutes at 4°C for separating the membrane proteins from soluble proteins. For the *in vitro* phosphorylation assay, 2-5µg recombinant proteins were incubated with either Ni-NTA (for his tagged proteins PfRad51, PfRad51^{S144A}, and PfRad51^{S144A/S319A}) or GST(for GST tagged PfRad51^{S319A}) beads for 1-2 hours in the cold room. The beads were washed thrice using 1X PBS/ NP40 buffer for 5 minutes on the rocker at 4 °C. To this, 100-200 μ g parasite lysate along with kinase buffer (containing 20 mM Tris-HCl pH-7.5, 1 mM DTT, 25 μ M ATP, 10 mM MgCl₂, 40 mM KCl, 1 mM NaF, 1 mM Na₂VO₄) and γ^{32} ATP (2 μ Ci) were added. Incubated the samples at 30 °C for 30 minutes. After incubation 5 beads were washed three times with 1X PBS/ NP40 buffer for 5 minutes on the rocker at 4 °C. 2X Laemmle buffer was added to the beads and boiled for 10 minutes. Later separated the proteins on 10% SDS-PAGE. The gel was dried and exposed to the membrane in the radioactive cassette. Scanned the cassette in typhoon radioactive scanner.

2.8 Indirect Immunofluorescence assay:

Synchronous trophozoite/ schizont staged parasites harboring *PfBlm-GFP*, *PfRad51-GFP*, or *PfMtDNAP* were fixed using 4% formaldehyde (Sigma). Membrane permeabilization was performed using 1:3 chilled acetone: methanol, followed by 1-hour blocking using 3% BSA. Parasites were probed with mouse anti-Cytochrome C (Abcam), and rabbit anti-GFP (Abcam) primary antibodies for 1 hour at 37°C followed by three washes with 1X PBST. Cells were then treated with the secondary antibody cocktail containing Alexa fluor 488 conjugated goat anti-rabbit IgG (green), Alexa fluor 594 conjugated rabbit anti-mouse IgG (red), and Hoechst 33342 (blue) (Invitrogen), and subsequently washed thrice with 1X PBST. Finally, parasites were mounted using anti-fade (Life technologies). Fluorescence microscope Nikon Eclipse NiE AR was used for analyzing and capturing the green and red fluorescence of GFP and CytC, respectively.

2.9 Direct Immunofluorescence assay:

The Synchronous parasites harboring *PfBLM-GFP*, or *PfRAD51-GFP* were harvested. Parasites were stained with 60 nM MitoTracker red dye and DAPI (5mg/ml) for 30 minutes at 37°C. Cells were washed thrice with 1X PBS. Fluorescence microscope Axio Observer Z1 with Apotome,

Carl Zeiss was used for analyzing and capturing the levels of green, blue, and red fluorescence of GFP, DAPI, and MitoTracker, respectively.

2.10 PCR-based method to quantify mitochondrial DNA damage:

The ring staged parasites were pretreated with a sublethal dose of the inhibitors, such as ML216 (1 μM), BO2 (1μM), and Atovaquone (0.3 nM). Pre-treated parasites were irradiated with 100 J/m² UV light at the trophozoite stage. Post DNA damage, the mock-treated and drug-treated parasites were cultured in the respective drug medium for 48 hours. Samples were collected from pre-and post-UV treatment at every 12-hour intervals. Genomic DNA was isolated from harvested parasites and the amount of total DNA was quantified using the SYBR green I dyebased standard plot method. An equal amount of DNA was used as a template to amplify longand short-range fragments. Primer set OMKB540 along with OMKB541 and OSB251 with OSB252 were used to amplify mitochondrial specific long (5967 bp) and short (290 bp) PCR products, respectively. Similarly, OMKB463 with OMKB464 and OSB94 with OSB95 were used to amplify nuclear specific long (7200 bp) and short (269 bp) PCR products, respectively The long PCR products were subjected to DNA sequencing to ascertain that they are derived from the mt-genome. Further, the amount of DNA in the PCR products was quantified using SYBR green I dye. Fluorescence intensities from the short-range PCR products were used to normalize the data. The equation used to calculate percent DNA damage at any given time was 1- (fluorescence intensity of long-range PCR product/fluorescence intensity of short rang PCR product) X N X 100, where N factor represents the ratio of long-range PCR amplicon size and short-range PCR amplicon size (for mitochondria N is 20.57 and nucleus N is 26.76). The percent of DNA damage was considered 0% in UV untreated control and 100% in 0 hours post UV sample. The GraphPad Prism software was used to plot the percent residual damage at each time point.

2.11 Thermolysin protection assay:

For thermolysin protection assay, a previously described methodology was used with minor modification (Kehr et al. 2010). 240 ml synchronized trophozoite stage parasite culture was lysed using saponin and washed with 1X PBS. The parasite cultures were then divided into four equal parts and re-suspended into 100 µl of assay buffer (50 mM HEPES-NaOH, pH 7.4, 5 mM CaCl₂, 300 mM sorbitol) containing either no detergent (control), 0.05% Digitonin, 0.05% Digitonin with 10 mM EDTA or 1% Triton X-100 (1.3 mg digitonin was dissolved in 100ml sterile MilliQ water). After incubation on ice for 10 minutes, simultaneously, the total protein content in the lysate was determined using the Bradford protein estimation method. And accordingly, thermolysin protease (4 mg lyophilized thermolysin was dissolved in 100 µl of buffer containing 50 mM Tris HCl pH8 0.5 mM CaCl) was added to the samples (25µg per 1mg parasite protein) and incubated on ice for 1 hour. Reactions were stopped by adding 4X Laemmli buffer, samples were boiled and separated on SDS-PAGE followed by western blotting.

2.12 Subcellular fractionation of *Plasmodium falciparum* culture:

For subcellular fractionation, 80ml of synchronized *Plasmodium falciparum* 3D7 with 8-10% parasitemia was treated with 0.15% (wt/vol) saponin to get RBC free parasite. The standard protocol for subcellular fractionation was used with slight modifications (Chalapareddy et al. 2014). The parasite pellet was first washed with 5ml of ice-cold buffer I (0.34 M Sucrose, 15 mM NaCl, 0.2 mM EDTA, 0.2 mM EGTA, 15 mM Tri HCl pH 7.4, 0.2 mM PMSF). Later, resuspended in 5ml of buffer II (buffer I containing 0.1% Triton X100) followed by 30 minutes incubation on ice. Cells were homogenized using a Dounce homogenizer and tight-fitting pestle

(30 complete strokes were given). Next, the parasite lysate was subjected to centrifugation at 600 X g for 10 minutes at 4°C for harvesting nuclear fraction. The obtained supernatant containing cytoplasm and organelle was collected in a fresh 15ml centrifuge tube. For preparing the organelle fraction the supernatant was centrifuged at 12000 X g for 30 minutes at 4°C. Nuclear and organelle pellets were washed twice using buffer I for removing cytoplasmic contamination. Finally, these pellets were resuspended into 100 μl of 4X Laemmli buffer and the samples were boiled and separated on SDS-PAGE followed by western blotting.

2.13 MtDNA Immuno-precipitation in P. falciparum.

50 ml of tightly synchronized *P. falciparum* culture with high parasitemia were used for mtDNA IP as described below either with or without cross-linking. The RBC-free parasite was prepared using the conventional saponin lysis method. This was followed by the crosslinking of the parasites by resuspending the pellet in 3.65 ml of pre-warmed 1X PBS and to this 50µl of 37% formaldehyde (final concentration 0.5%) was added and incubated on Rocker for 10 minutes at room temperature for the crosslinking (Bozdech et al. 2013). To stop the reaction, 300ul of 1.67 M glycine (prepared in 1X PBS) was added and the parasites were incubated on ice for 5 minutes. Later the cells were harvested by centrifuging at 4000g at room temperature for 5 minutes. The supernatant was discarded and the parasite pellet was washed once with ice-cold PBS. The resulted parasite pellet was frozen in liquid nitrogen and stored at -80°C and later processed as mentioned below. Firstly, the CL or NCL (cross-linking/Non-cross-linking) parasite pellet was thawed on ice. Then the cells were resuspended in 2ml of cold lysis buffer (containing 10 mM HEPES pH 7.9, 10 mM KCl, 0.1 mM EDTA pH 8, 0.1 mM EGTA pH 8, 1 mM DTT, protease inhibitor) and incubated on ice for 1 hour with intermittent mixing. To this, Nonidet-40 with a final concentration of 0.25% was added. Later subjected to homogenization for complete lysis using Dounce homogenizer and tight-fitting pestle (200 strokes for rings and early trophozoites, 100 strokes for late trophozoites and schizont was given). After lysis, the parasite lysate was transferred to fresh 1.5 ml microfuge tubes (1 ml per tube) and then centrifuged at 14000 rpm for 10 minutes 4°C. The supernatant was discarded and the pellet in each tube was re-suspended in 125 µl of SDS lysis buffer (containing 1% SDS, 10mM EDTA pH8, 50mM Tris HCl pH8 supplemented with PI, PMSF, DTT). The DNA was then sheared using Elma water bath sonicator, sonication of the chromatin solution was performed for 6 sessions (10 seconds burst and 5 min rest) at 37 Hz frequency. The DNA solutions from all the tubes were pooled in a single tube and were 10 fold diluted by adding 2250 µl of DNA dilution buffer (0.01% SDS, 1.1% tritonX100, 1.2 mM EDTA, 16.7 mM Tris HCl pH8, 150mM NaCl, PI, PMSF). The DNA shearing was monitored by running the DNA solution on the agarose gel. For the pre-cleaning of the DNA solution, 190 µl of equilibrated protein A agarose beads with the equilibration buffer (0.1% BSA, 0.1% Na azide, 1X TE) was added to it and incubated on the rocker, 4°C for 2 hours. The protein A agarose beads were removed by spinning the DNA solution at 2500 rpm, 4°C for 10 seconds. The supernatant was transferred to a fresh tube and for each immunoprecipitation, 400µl and input 250µl of DNA solution was used. For immunoprecipitation 10 µl of antibodies against PfRad51 (generated in the laboratory), PfBlm (generated in the laboratory), GFP (Abcam), CytC (Abcam), and IgG (Invitrogen) were added to the DNA solution and incubated on the rocker, 4°C for overnight. The next day 45µl of equilibrated protein A agarose beads were added to the DNA solution containing the respective antibodies and incubated on the rocker, 4°C for 2 hours. The samples were then centrifuged at 7000 rpm for 10 seconds. The supernatant obtained was stored at -20°C and was used as IP supernatant samples. The bound beads were then subjected to washing on the rocker at 4°C for

5 minutes with 1ml of each of the following cold buffers. The wash buffers were discarded after each wash by centrifuging the sample at 7000 rpm for 10 seconds: (A) Low salt immune complex wash buffer (containing 0.1% SDS, 1% Triton X100, 2mM EDTA, 20mM Tris HCl pH8, 150mM NaCl). (B) High salt immune complex wash buffer (containing 0.1% SDS, 1% Triton X100, 2mM EDTA, 20mM Tris HCl pH8, 500 mM NaCl). (C) LiCl immune complex wash buffer (containing 0.25 M LiCl, 1% NP-40, 1% Deoxycholate, 1 mM EDTA, 10 mM Tris HCl pH 8). (D) 1X TE (containing 10 mM Tris HCl pH 8 and 1 mM EDTA).

After the washing step, the beads were resuspended in 500µl of 1X TE buffer and transferred into a fresh microfuge tube, this step was repeated to collect residual beads. Further to elute the immune complexes freshly prepared 250µl of SDS/NaHCO3 (1% SDS, 0.1M NaHCO3) buffer was added to the beads, mixed by vortexing followed by incubation on a rocker at 4°C for 15 minutes. The samples were spun and the supernatant was transferred into a fresh microfuge tube and the elution step was repeated once more with the beads. The samples were again spun and the supernatant was collected and combined with supernatant obtain in the previous elution step. For reverse HCHO crosslinking, 20µl of 5M NaCl was added to the eluted immune complexes (pellet fraction), 2.5µl to 300µl of IP supernatant fraction and 10µl to the input. The samples were mixed by vortexing, given a short spin. Then samples were incubated at 65°C for 5 hours. Further samples were spun briefly and then transferred into fresh tubes. To this 2.2 volume of absolute ethanol was added and then kept for precipitation at -20°C for overnight.

The next day, samples were centrifuged at 12000 rpm, 4°C for 30 minutes followed by 70 % ethanol wash of the resulting DNA pellet for 5 minutes. The pellet was then air-dried for about 5 minutes and re-suspended in 100µl of 1X TE followed by incubation on ice for 10 minutes.

Later the samples were subjected to proteinase K treatment by adding 25μl of 5X proteinase K buffer (50mM Tris HCl pH8, 25mM EDTA, 1.25% SDS) along with 1.5μl of proteinase K (20mg/ml) and incubated at 42°C for 2 hours. After incubation, 175μl of TE was added to the IP pellet fraction and 275μl of TE to the input and the IP supernatant fraction. An equal volume of PCIA (phenol: chloroform: Isoamyl alcohol -25:24:1) was added to the samples, mixed by vortexing for 3 minutes, and then centrifuged at the top speed, RT for 10 minutes. The upper aqueous layer was then collected in a fresh microfuge tube. The organic extraction step was repeated for the input and the IP supernatant fraction once more. 5μg of glycogen, 1/10 volume of 3M sodium acetate, and 2.2 volume of absolute ethanol were added to the samples and kept for precipitation at -20°C for overnight. The samples were spun at 12000 rpm, 4°C for 30 minutes, and the pellet was washed with 70 % ethanol for 5 minutes. The pellet was air-dried and the IP pellet fraction was resuspended in 150μl of TE, input in 250 μl of TE, and IP supernatant fraction in 300μl of TE.

Table 3: List of primers along with the nucleotide sequence and description of their usage in this work.

Name 5'GAGTGGATTAAATG FP 669 Kb upstream COXIII gene used to amplify mitochondrial specific long-range PCR product in repair kinetics experiment and 'A' fragment mtDNA-IP 2020) OMK541 ATTGTTCTACATTACG AGATACC RP 702 Kb upstream COXIII gene used to amplify mitochondrial specific long-range PCR product in repair kinetics experiment and F' mtDNA-IP 2020) OMK614 CATAACATTTTTTAGT CCATGC FP used to amplify 'B' fragment in mtDNA-IP CCCATGC This study (Bansod et a applify 'C' fragment mtDNA-IP) OMK615 CTGGCCTACACTATA AGAACG RP used to amplify 'C' fragment mtDNA-IP (Bansod et a applify 'C' fragment mtDNA-IP)	
CCCAGCC3' amplify mitochondrial specific long-range PCR product in repair kinetics experiment and 'A' fragment mtDNA-IP OMK541 ATTGTTCTACATTACG RP 702 Kb upstream COXIII gene used to amplify mitochondrial specific long-range PCR product in repair kinetics experiment and F' mtDNA-IP OMK614 CATAACATTTTTAGT FP used to amplify 'B' fragment in mtDNA-IP This study CCCATGC OMK615 CTGGCCTACACTATA RP used to amplify 'C' fragment mtDNA-IP (Bansod et a	
PCR product in repair kinetics experiment and 'A' fragment mtDNA-IP OMK541 ATTGTTCTACATTACG RP 702 Kb upstream COXIII gene used to amplify mitochondrial specific long-range PCR product in repair kinetics experiment and Tr' mtDNA-IP OMK614 CATAACATTTTTAGT FP used to amplify 'B' fragment in mtDNA-IP This study CCCATGC OMK615 CTGGCCTACACTATA RP used to amplify 'C' fragment mtDNA-IP (Bansod et a	al.
'A' fragment mtDNA-IP OMK541 ATTGTTCTACATTACG RP 702 Kb upstream COXIII gene used to amplify mitochondrial specific long-range PCR product in repair kinetics experiment and F' mtDNA-IP OMK614 CATAACATTTTTAGT FP used to amplify 'B' fragment in mtDNA-IP This study CCCATGC OMK615 CTGGCCTACACTATA RP used to amplify 'C' fragment mtDNA-IP (Bansod et a	
OMK541 ATTGTTCTACATTACG RP 702 Kb upstream COXIII gene used to AGATACC amplify mitochondrial specific long-range PCR product in repair kinetics experiment and F' mtDNA-IP OMK614 CATAACATTTTTAGT FP used to amplify 'B' fragment in mtDNA-IP CCCATGC TGGCCTACACTATA RP used to amplify 'C' fragment mtDNA-IP (Bansod et a	
AGATACC amplify mitochondrial specific long-range PCR product in repair kinetics experiment and F' mtDNA-IP OMK614 CATAACATTTTTAGT FP used to amplify 'B' fragment in mtDNA-IP This study CCCATGC OMK615 CTGGCCTACACTATA RP used to amplify 'C' fragment mtDNA-IP (Bansod et a	
PCR product in repair kinetics experiment and 'F' mtDNA-IP OMK614 CATAACATTTTTAGT FP used to amplify 'B' fragment in mtDNA-IP CCCATGC OMK615 CTGGCCTACACTATA RP used to amplify 'C' fragment mtDNA-IP (Bansod et a	al.
T' mtDNA-IP	
OMK614 CATAACATTTTTAGT FP used to amplify 'B' fragment in mtDNA-IP This study CCCATGC OMK615 CTGGCCTACACTATA RP used to amplify 'C' fragment mtDNA-IP (Bansod et a	
CCCATGC OMK615 CTGGCCTACACTATA RP used to amplify 'C' fragment mtDNA-IP (Bansod et a	
OMK615 CTGGCCTACACTATA RP used to amplify 'C' fragment mtDNA-IP (Bansod et a	J
AGAACC 2020)	al.
AUAACU 2020)	
OMK616 CTACTGGTTTAGAAG FP used to amplify 'D' fragment mtDNA-IP (Bansod et a	al.
TTGATAC 2020)	
OMK617 TACTGGAATAGAGGA RP used to amplify 'D' fragment in mtDNA-IP (Bansod et a	al.
TAACAAG 2020)	
OMK618 GTTATCCTCTATTCCA FP used to amplify 'E' fragment in mtDNA-IP (Bansod et a	al.
GTAGC 2020)	
OMK619 CATACATCCTAACAT RP used to amplify 'E' fragment in mtDNAIP (Bansod et a	al.
TAATAACG 2020)	
OMK620 CGCTGACTTCCTGGC FP used to amplify 'F' fragment in mtDNA-IP (Bansod et a	al.
TAAAC 2020)	
OMK621 CCGCCTAGGTTTTCC RP used to amplify PfRad51 for cloning into This study	y
TCATAATCTGCTAT pARL vector	
OMKB276 5'AAGAATTGGGACA RP GFP confirmatory primer This study	V
AACTCC3'	'

CHAPTER 2 MATERIALS AND METHODS

OMKB463	5'TCAGTCGACATGTT	FP used to amplify nuclear specific long-range	(Suthram et al.
GAATGATATGAA		PCR product in repair kinetics experiment	2020)
	TAAAAAAG3'		
OMKB464	5'TCAGTCGACTCAAC	RP used to amplify nuclear specific long-range	(Suthram et al.
	CTATGTAACCTTTAC	PCR product in repair kinetics experiment	2020)
	ACTTC3'		
OMKB471	5'GCTAAAGTATGACA	PfRad51 ^{S144A} FP used in site directed	This study
	TAGTTGAGCTTTTCCT	mutagenesis	
	G3'		
OMKB472	5'GGTGAATTTCGTAC	PfRad51 ^{S144A} RP used in site directed	This study
	AGGAAAAGCTCAACT	mutagenesis	
	A3'		
OMKB473	5'GGAATCATAAATTT	PfRad51 ^{S319A} FP used in site-directed	This study
	TGCAGATTCGAGCTT	mutagenesis	
	CTCCCCT3'		
OMKB474	5'GGAAATATTTCAAT	PfRad51 ^{S319A} RP used in site directed	This study
	TAATCCG3'	mutagenesis	
OMKB598	GGGGTACCGGATGAA	FP (KpnI) used to amplify PfRad51 for	This study
	ACAAGCAAATACAAA	cloning into pARL vector	
	AG		
OMKB621	CCGCCTAGGTTTTTCC	RP (AvrII) used to amplify PfRad51 for	This study
	TCATAATCTGCTAT	cloning into pARL vector	
OMKB745	5'GACGGTACCATGAA	FP (KpnI) used to amplify PfMtDNAP for	This study
	ATTGTTTGATTCATTT	cloning into pARL vector	
	TTTAAAC3'		
OMKB756	5'GACCCTAGGTGAAG	RP (AvrII) without stop codon used to amplify	This study
	ACTCCTTGTAGACTC	PfMtDNAP for cloning into pARL vector	
	C3'		
OSB176	5'CATCCCATAGCAAG	FP Upstream COXIII gene used to amplify	(Bansod et al.
	TATCATAG3'	'C' fragment mtDNAIP	2020)
OSB251	5'GACGCATCTCTACA	FP within COXIII gene used to amplify	This study
	AACTACAGAG3'	mitochondrial short-range PCR and 'A'	
		fragment mtDNAIP	

CHAPTER 2 MATERIALS AND METHODS

OSB252	5'GACTTATTCTGAAT	RP COXIII gene used to amplify	This study
	AGAATAAGAACTC3'	mitochondrial short-range PCR and 'B'	
		fragment mtDNAIP	
OSB502	5'ATCGGATCCATGAA	FP (BamHI) used to amplify PfMtDNAP for	This study
	ATTGTTTGATTCATTT	cloning into pGAD-C1 Y2H plasmid	
	TTT3'		
OSB503	5'ATCGTCGACTTATG	RP (SalI) used to amplify PfMtDNAP for	This study
	AAGACTCCTTGTAGA	cloning into pGAD-C1 Y2H plasmid	
	CTCC3'		
OSB94	5'CTGTAACACATAAT	FP used to amplify nuclear specific short-range	(Suthram et al.
	AGATCCGAC3'	PCR product in repair kinetics experiment	2020)
OSB95	5'TTAACCATGGTTAT	RP used to amplify nuclear specific short-range	(Suthram et al.
	CATCATTATTTC3'	PCR product in repair kinetics experiment	2020)

FP: Forward primer, RP: Reverse Primer

Table 4: List of yeast strains generated in this study and their phenotype description.

1.	PJY5	MATa trp1-901, lue2-3, 112 ura3-52, his3-200, gal4Δ, gal80Δ, LYS2::GAL1-HIS3 gAL-ADE2, met::GAL7-lacZ, pGBDU- C1/PfRad51, pGADC1/PfmtDNAP
2.	РЈҮ6	MATa trp1-901, lue2-3, 112 ura3-52, his3-200, gal4Δ, gal80Δ, LYS2::GAL1-HIS3 gAL-ADE2, met::GAL7-lacZ, pGBDU- C1/PfBlm, pGADC1/PfmtDNAP
3.	PJY7	MATa trp1-901, lue2-3, 112 ura3-52, his3-200, gal4Δ, gal80Δ, LYS2::GAL1-HIS3 gAL-ADE2, met::GAL7-lacZ, pGBDU-C1/PfRad51, pGADC1/empty
4.	РЈҮ8	MATa trp1-901, lue2-3, 112 ura3-52, his3-200, gal4Δ, gal80Δ, LYS2::GAL1-HIS3 gAL-ADE2, met::GAL7-lacZ, pGBDU-C1/PfBlm, pGADC1/empty
5.	РЈҮ9	MATa trp1-901, lue2-3, 112 ura3-52, his3-200, gal4Δ, gal80Δ, LYS2::GAL1-HIS3 gAL-ADE2, met::GAL7-lacZ, pGBDU-C1/empty, pGADC1/PfmtDNAP
6.	PJY10	MATa trp1-901, lue2-3, 112 ura3-52, his3-200, gal4Δ, gal80Δ, LYS2::GAL1-HIS3 gAL-ADE2, met::GAL7-lacZ, pGBDU- C1/PfRad51, pGADC1/PfTopoIII
7.	PJY11	MATa trp1-901, lue2-3, 112 ura3-52, his3-200, gal4Δ, gal80Δ, LYS2::GAL1-HIS3 gAL-ADE2, met::GAL7-lacZ, pGBDU-C1/empty, pGADC1/PfTopoIII
8.	PJY12	MATa trp1-901, lue2-3, 112 ura3-52, his3-200, gal4Δ, gal80Δ, LYS2::GAL1-HIS3 gAL-ADE2, met::GAL7-lacZ, pGBDU-C1/empty, pGADC1/empty

Chapter 3

<u>ROLE OF PfBlm AND PfRad51 IN MITOCHONDRIAL DNA</u>

<u>REPAIR</u>

3.1 INTRODUCTION.

Plasmodium falciparum being a unicellular parasite DSB repair pathway has been proven as an excellent target against it since a single unrepaired DBS could potentially be life-threatening to this parasite (Frankenberg-Schwager and Frankenberg 1990). In addition to the nuclear genome, being an apicomplexan Plasmodium parasite contains two additional organelle-genomes namely, mitochondrial and the plastid called apicoplast. These organelles show maternal inheritance and carry a reduced DNA genome. The function of these organelles is essential for parasite propagation in both the mosquito and human hosts. Blocking the housekeeping cellular processes of these organelles such as replication, transcription, and translation is found to be detrimental for parasite survival and growth.

Although the replication and repair of the extra-chromosomal DNA present in the organelle are independent of the nuclear genome maintenance, they heavily rely on nuclear-encoded proteins for these processes, since mtDNA is devoid of genes encoding for replication and repair proteins.

During its life cycle, the parasite encounters an enormous amount of DNA damaging stress. Similar to the nuclear genome, the organelle DNA is also endangered by this genotoxic stress. The central player of HR, PfRad51 possesses the canonical ATP hydrolysis, and strand-exchange activities (Bhattacharyya et al. 2005). Small molecule inhibitors that block the ATPase activity or the homodimerization of PfRad51, displayed a profound effect on the DSB repair of the nuclear genome (Vydyam et al. 2019). In *P. berghei*, depletion of Rad51 resulted in the complete abrogation of DSB repair, implying that the HR pathway is the predominant DSB repair mechanism (Roy et al. 2014). PfalMre11 has been identified and characterized as a dual functioning protein involved in DNA damage sensing and resection (Badugu et al. 2015). The

important role of one of the RecQ helicases, PfBlm has recently been appreciated in DNA repair (Suthram et al. 2020). Chemical inhibition of PfBlm blocked DSB repair in this parasite, subsequently making parasites hyper-sensitive to the DNA-damaging agents. Such DNAdamage sensitivity can be reversed by the overexpression of PfBlm protein in the parasite (Suthram et al. 2020). PfBlm was found to interact with PfRad51, PfalMre11, and PfTopoIII (Bansod et al. 2020; Suthram et al. 2020), implying the existence of a 'recombinosome' complex in the parasite. PfTopoIII, a protein located in both nucleus and mitochondria, has been found to provide a growth advantage to the hydroxyurea (HU)-arrested parasites (Bansod et al. 2020). At present it is inarguable that the mtDNA is more vulnerable to DSBs and its repair is not optional however is an essential cellular process for which eukaryotic cell is known to devote various repair machinery. The function of BER has been established as predominant repair machinery in the mitochondria of model organisms. So far, BER is the only repair pathway found to be functional in *Plasmodium* mitochondria. However, BER machinery is incapable of handling DSBs, yet the repair of such most catastrophic DNA lesions is essential for preserving genomic continuity. In the last few decades, recombination-mediated repair has gained immense appreciation for its function in mtDNA stability (Boesch et al. 2011; Mishra et al. 2018; Sage et al. 2010; Sage and Knight 2013; Tadi et al. 2016). Hence, it is not unreasonable to investigate the possible role of nuclear-genome encoded HR proteins in the parasite mitochondrial DSBs. In this aim, we have developed an inducible system that facilitated both the creation of random DSBs in the mtDNA as well as nDNA and follow-up on the repair of these breaks. The model additionally provided feasibility to monitor the entry and exit of different factors before the induction of DSBs, during the repair process, and after the repair of mtDNA.

3.2 RESULTS.

3.2.1 Subcellular distribution of nuclear-genome encoded HR proteins.

Since P. falciparum mtDNA is at risk of oxidative stress-induced DSBs and it does not encode for repair proteins, we sought to investigate whether nuclear-encoded homologous recombination proteins have a role in rectifying such breaks. In general, the HR pathway has five steps namely, double-strand break resection, strand invasion/ exchange, DNA synthesis, branch migration, ligation, and Holliday junction (HJ) resolution. In this parasite, the three HR proteins including, PfalMre11 (DSB resection), PfRad51 (strand invasion), and PfBlm (HJ resolution) (Badugu et al. 2015; Bhattacharyya et al. 2005; Suthram et al. 2020) have been shown to be essential for the repair of nDNA DSBs (Figure. 3.1 A). Here, we studied the organelle localization of the aforementioned proteins in malaria parasites under favorable condition. To this end, we have employed sub-cellular fractionation followed by the western blotting technique. This methodology is based on the fact that each sub-cellular component has variable size and densities and hence the application of differential centrifugal force can purify fractions corresponding to the nucleus, mitochondria, cytoplasm, etc. Sub-cellular fractionation was performed using late-trophozoite stage parasites due to the high expression of these repair proteins in that stage (Appendix figure. A1). We observed that PfBlm and PfRad51 proteins were present in both the nucleus and organelle. However, PfalMre11 was exclusively seen in the nuclear but not in the organelle fraction. Here, P falciparum histone 3 (Pf H3), P falciparum Cytochrome C (PfCytC), and P falciparum glyceraldehyde-3 phosphate dehydrogenase (PfGAPDH) proteins were used as a nuclear, mitochondrial, and cytoplasmic marker, respectively (Figure 3.1B). The abundance of PfCytC protein in the organelle fraction suggested the enrichment of mitochondria in this fraction. Moreover, the exclusive presence of PfCytC in organelle and PfH3 in nuclear fraction shows the purity of these fractions and roles out cross-contamination. Similarly, the lack of PfGAPDH in both confirms the lack of cytosolic contamination in these fractions. Altogether this data suggested organelle localization of PfBIm and PfRad51 but not PfalMre11 in addition to their nuclear presence.

Organelle fraction prepared from this apicomplexan parasite includes proteins from mitochondria as well as apicoplast organelle. Hence, to investigate mitochondrial existence HR proteins we tested their protection from a metalloprotease named thermolysin with/ without the presence of variable detergents. This approach relies upon the action of digitonin, which is a steroidal saponin also known as saraponin. It can differentially permeabilize various sub-cellular membranes. The selective lysis by this non-ionic detergent is governed by its required binding to cholesterol to permeabilize the membrane, thus the total cholesterol content of a membrane determines its lysis. Since mitochondrial membrane cholesterol content is very low, digitonin does not act on it. In the protease protection assay, the late-trophozoite staged parasites were subjected to thermolysin digestion post permeabilization. We observed protection of PfRad51 and PfBlm along with the mitochondrial marker PfCytC, while the cytoplasmic and nuclear marker protein bands disappeared in the test reaction which includes the treatment with digitonin followed by protease digestion. Digestion of entire sub-cellular protein including mitochondrial protein was seen in the control reaction owing to the complete cell lysis by the action of anionic detergent TritonX-100, hence exposing all the cellular protein to thermolysin. On the other hand, in the negative controls containing either EDTA inactivated protease or lacking the enzyme in the reaction mix, we observed that proteins of all the subcellular compartments were protected (Figure 3.1C). Overall, this result suggested that a portion of PfRad51 and PfBlm proteins reside within the parasite mitochondria apart from their usual nuclear residence.

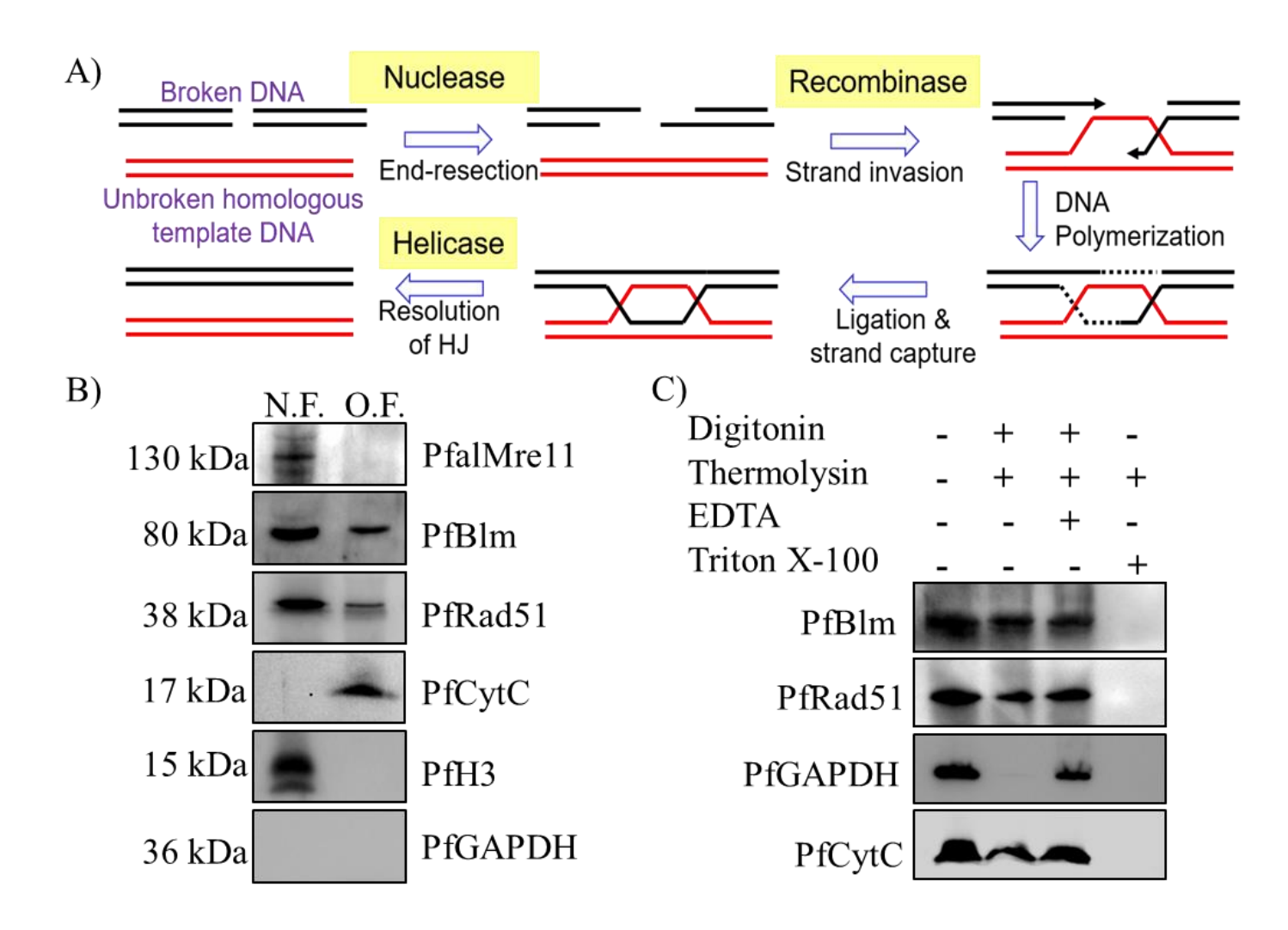


Figure 3.1: Subcellular distribution of nuclear-genome encoded HR proteins.

(A). Diagrammatic representation of five key steps of homologous recombination pathway. (B). Western blot displaying the presence of PfBlm, PfRad51, and PfalMre11 in the organelle (O. F.) or nuclear (N. F.) fractions using specific antibodies against them. PfCytC and PfHistone H3 serve as mitochondrial and nuclear markers, respectively. The subcellular localization study was performed with parasite from the trophozoites (28 hpi) stage. (C) Western blots representing the protease protection of repair proteins: PfBlm and PfRad51 form thermolysin digestion upon

membrane-permeabilization with digitonin but not with Triton X-100. EDTA was used as a quencher of the thermolysin activity. Various treatments are marked at the top. PfGAPDH and PfCytC serve as cytosolic and mitochondrial markers, respectively.

3.2.2 Mitochondrial localization of PfRad51 and PfBlm:

For the visual validation of mitochondrial localization of PfBlm and PfRad51, we sought to tag the repair proteins with green fluorescence protein (GFP) followed by immunofluorescence assay. To this end, we have cloned the full-length *PfRad51* gene into *Plasmodium* transfection vector pARL between KpnI and AvrII restriction sites. The expression of the inserted gene is under PfCRT promoter control. As the GFP tag was needed to fuse at the C-terminal end of the protein hence we have omitted the stop codon from the reverse primer sequence which was used to amplify PfRad51. The precision of the PfRad51-GFP-pARL construct was examined by double-digestion with KpnI and AvrII restriction enzyme and Sanger sequencing (Appendix figure. A2). Subsequently, the plasmid construct was transfected into P. falciparum 3D7 laboratory strain to generate a transgenic line. The expression of PfRad51-GFP in the transfected lysate was checked using the western blotting technique. Since the size of GFP protein is approximately 30kDa and PfRad51 is 38kDa, thus the protein band we observed in the western blot around 68kDa corresponds to the GFP tagged PfRad51 fusion protein. Moreover, the absence of a corresponding protein band in 3D7 parasite lysate further confirms that this protein band is certainly PfRad51-GFP present exclusively in transfectant lysate (Figure 3.2A). We have used previously reported parasite strains for investigating the localization of PfBlm-GFP protein (Suthram et al. 2020). Furthermore, their mitochondrial localization was established

using an indirect immunofluorescence assay. Immunofluorescence assay was performed on formaldehyde-fixed trophozoite or schizont stage parasites using the anti-GFP antibody. Anti-CytC antibody was used as a mitochondrial marker and Hoechst dye was used to stain the nucleus. A clear overlap was observed between the signals of GFP-tagged proteins (green) and mitochondrial marker (red) confirming their presence in the parasite mitochondria in both the trophozoite and the schizont stage (Figure. 3.2B). As expected GFP-tagged PfRad51 or PfBlm proteins were also found in the parasite nucleus. IFA with untagged parasite line (3D7) using anti-GFP antibody served as a negative control. The use of the pre-immune sera against the transfectant parasites served as an additional negative control. In the negative controls, the green fluorescence signal was missing owing to the lack of GFP fusion protein, while the mitochondrial marker and nuclear dye signal were unaffected, hence validating the experimental procedure and the specificity of the green signal. Taken together, these results indicate the mitochondrial localization of PfRad51 and PfBlm and suggest a likely role of these proteins in the mitochondrial biology of the malaria parasites.

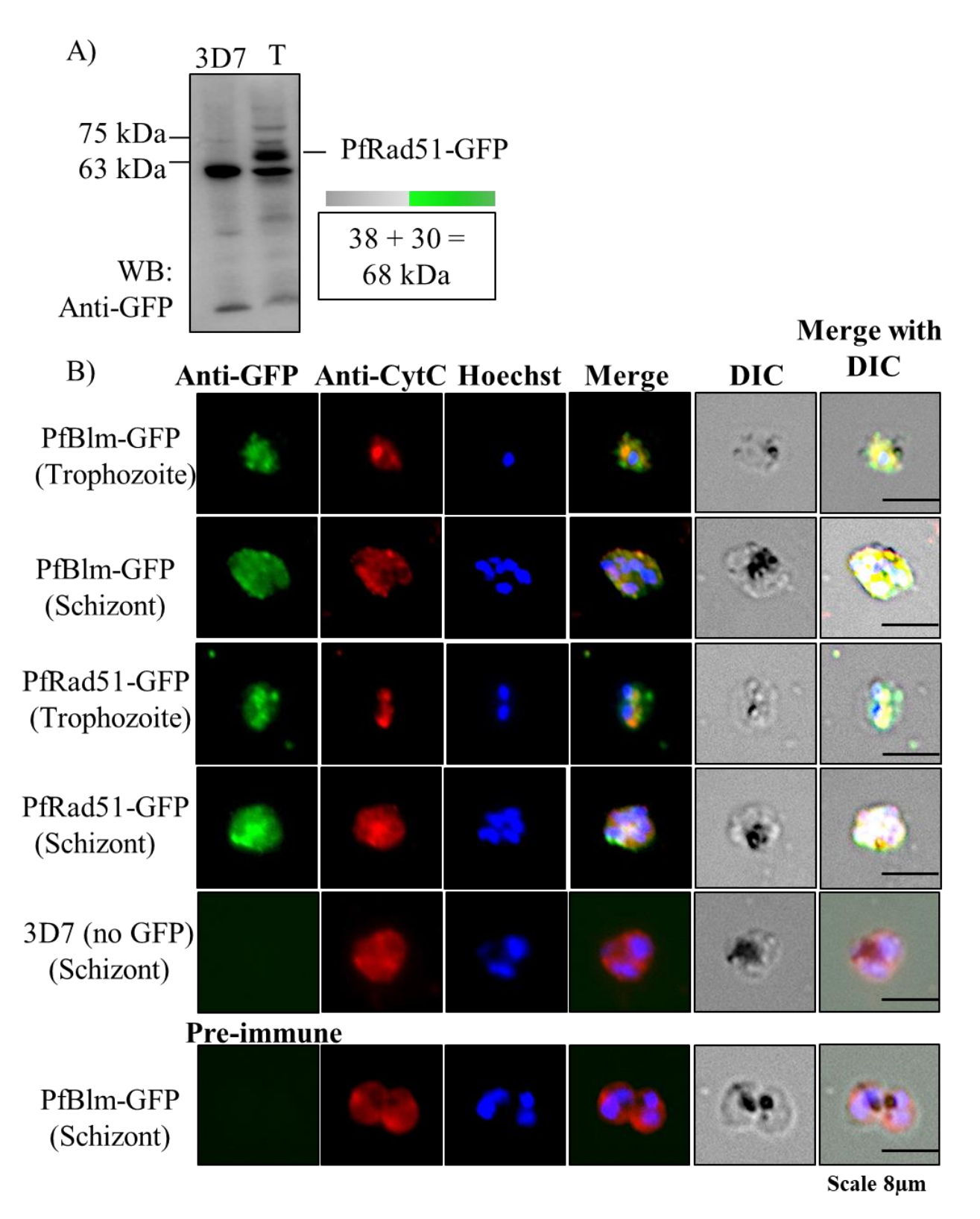


Figure 3.2

Figure 3.2: Mitochondrial localization of PfBlm, and PfRad51. (A) Western blot displaying the expression of PfRad51-GFP protein in the transfected (T) parasite line and not in the untransfected (3D7) parasite line. The molecular weight markers are indicated on the left. (B) Immunofluorescence images displaying localization PfBlm-GFP, and PfRad51-GFP (Green) to mitochondria (Red) and/or nucleus (Blue) of *Plasmodium falciparum* parasite. Anti-CytC antibody and Hoechst dye were used to stain the parasite mitochondria and nucleus, respectively. IFA using anti-GFP in 3D7 and pre-immune sera in PfBlm-GFP transfected parasite served as the experimental negative controls. IFA was performed with trophozoites and schizonts parasite as indicated.

3.2.3 Interaction of PfBlm, and PfRad51 with mitochondrial DNA:

Nuclear repair proteins are known to bind to the nuclear genome to facilitate DNA damage repair. To investigate such interaction of PfBlm, and PfRad51 with mitochondrial DNA (mtDNA), we performed mtDNA-immunoprecipitation (mtDNA-IP). We have used a set of six specific primers encompassing the entire mitochondrial genome to map the association of the aforementioned proteins with mt-genome (Figure. 3.3A). Specific antibodies against PfBlm and PfRad51 were used to immunoprecipitate formaldehyde cross-linked and mechanically sheared generating approximately 1kb mtDNA. PfCytC, which is a soluble protein with no known DNA binding ability along with immuno-globin (IgG) antibody assisted mtDNA-IP was used as the negative control for this experiment. To rule out the non-specific binding of proteins upon parasite lysis, we performed mt-ChIP without formaldehyde cross-linking and referred to it as non-cross-linked mtChIP. Occupancy of PfBlm and PfRad51 were investigated with the synchronous trophozoite-stage parasites. We observed the PCR amplification of each A-F loci in PfBlm and PfRad51 immunoprecipitated pellets, but not in PfCytC and IgG-IP (Figure. 3.3B), suggesting the specific interaction of repair protein to mtDNA. Furthermore, in the non-crosslinked IP samples including PfBlm and PfRad51, we did not find PCR amplification of any mitochondrial loci which rules out the possibility of nonspecific binding of the repair proteins. Altogether, with findings, we have established that the PfBlm and PfRad51 interact with the mtDNA, and such association was observed throughout the 6 kb mitochondrial genome.

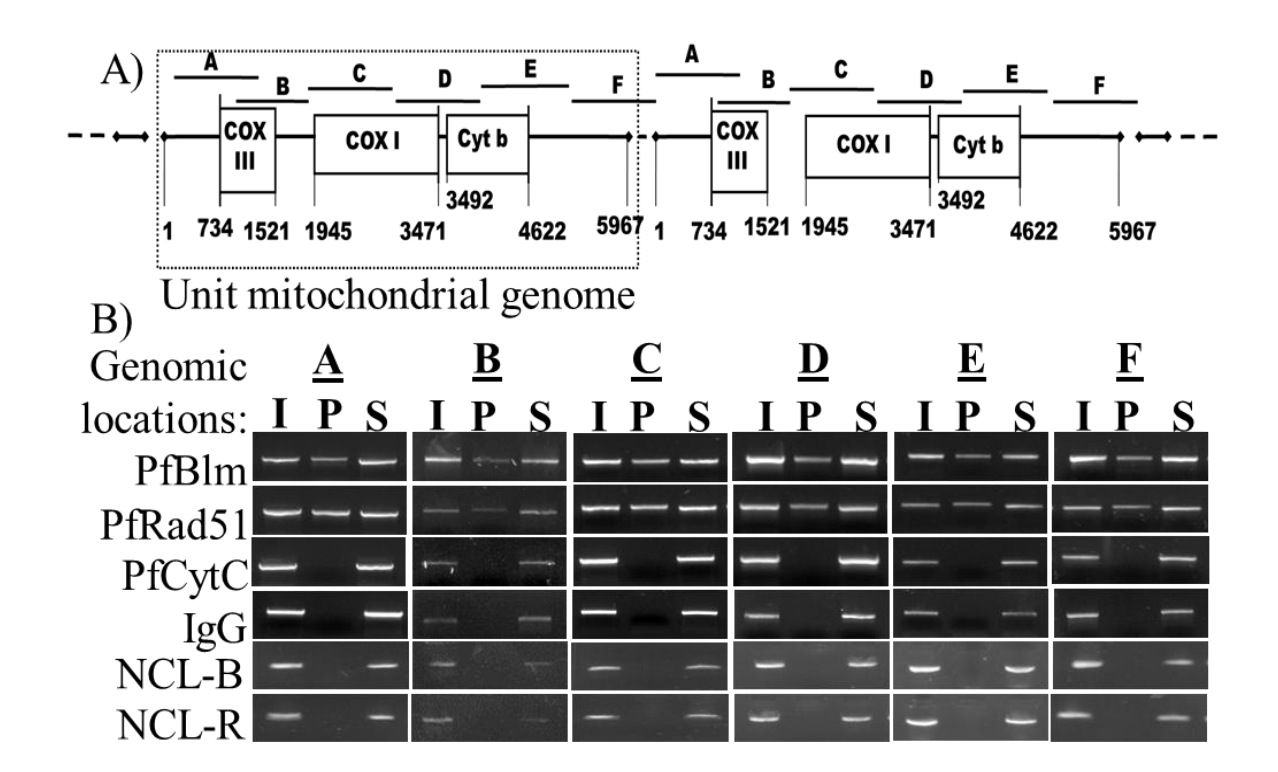


Figure 3.3: Interaction of PfBlm and PfRad51 with the mitochondrial genome. (A) The pictographic representation of *P. falciparum* linear concatemeric form of 6-kb mitochondrial genome arranged in head to tail fashion. This mtDNA map also notifies the relative positioning of three mitochondrial genes: *COXIII*, *COXI*, and *CYB*; and six DNA fragments encompassing the entire genome, named as A to F used in this study. (B) Agarose gels display the occupancy of PfBlm or PfRad51 proteins on the mitochondrial genome (A-F) by mtDNA-IP, using specific antibodies against them. IP with CytC and IgG antibodies served as experimental negative controls. I, P, and S stand for input mt DNA, immuno-precipitated mt DNA, and supernatant, respectively. NCL-R and NCL-B display non-cross-linked mito-DNA IP data, using anti PfRad51 (R) and PfBlm (B) antibodies.

3.2.4 Stage-specific interaction of PfRad51 and PfBlm with the mitochondrial genome:

The expression of PfBlm, and PfRad51 proteins are at the peak during schizont ABSs of the parasite, owing to their higher requirement during this mitotically active parasite stage. Mitochondrial metabolic activity such as pyrimidine synthesis, ETC along with mtDNA replication occurs during the later stages of the parasite. Thus, during these developmental stages parasite, mitochondrial genome stability is challenged by replication fork arrest and high load of oxidative stress. Therefore, we sought to examine the effect of parasite asexual development on the occupancies of PfBlm and PfRad51 repair protein at the mtDNA. To do so, we have used tightly synchronized ring, trophozoite, early schizont, mid-schizont, and late schizont asexual blood stages of the parasite and investigated the association of these repair proteins at all the six loci of mtDNA. We found that the relative occupancy of PfBlm and PfRad51 at all mtDNA loci were higher in schizonts than rings and early trophozoite stages. The data was normalized against corresponding IgG-mtDNA-IP values. The relative occupancy at given points was measured with respect to total input mtDNA. Overall, this result suggested that the occupancy of both the repair proteins at all loci increased as the parasite progresses to mature stages (Figure 3.4A and B). The mature stages of the asexual parasites are not only active in DNA replication but are also expected to experience a higher propensity for DNA damage due to increased metabolic activity. Thus, our finding on the mature stage-specific occupancy of both PfRad51 and PfBlm on the mtDNA indicates the involvement of these two nuclearencoded proteins in mtDNA replication and/or repair.

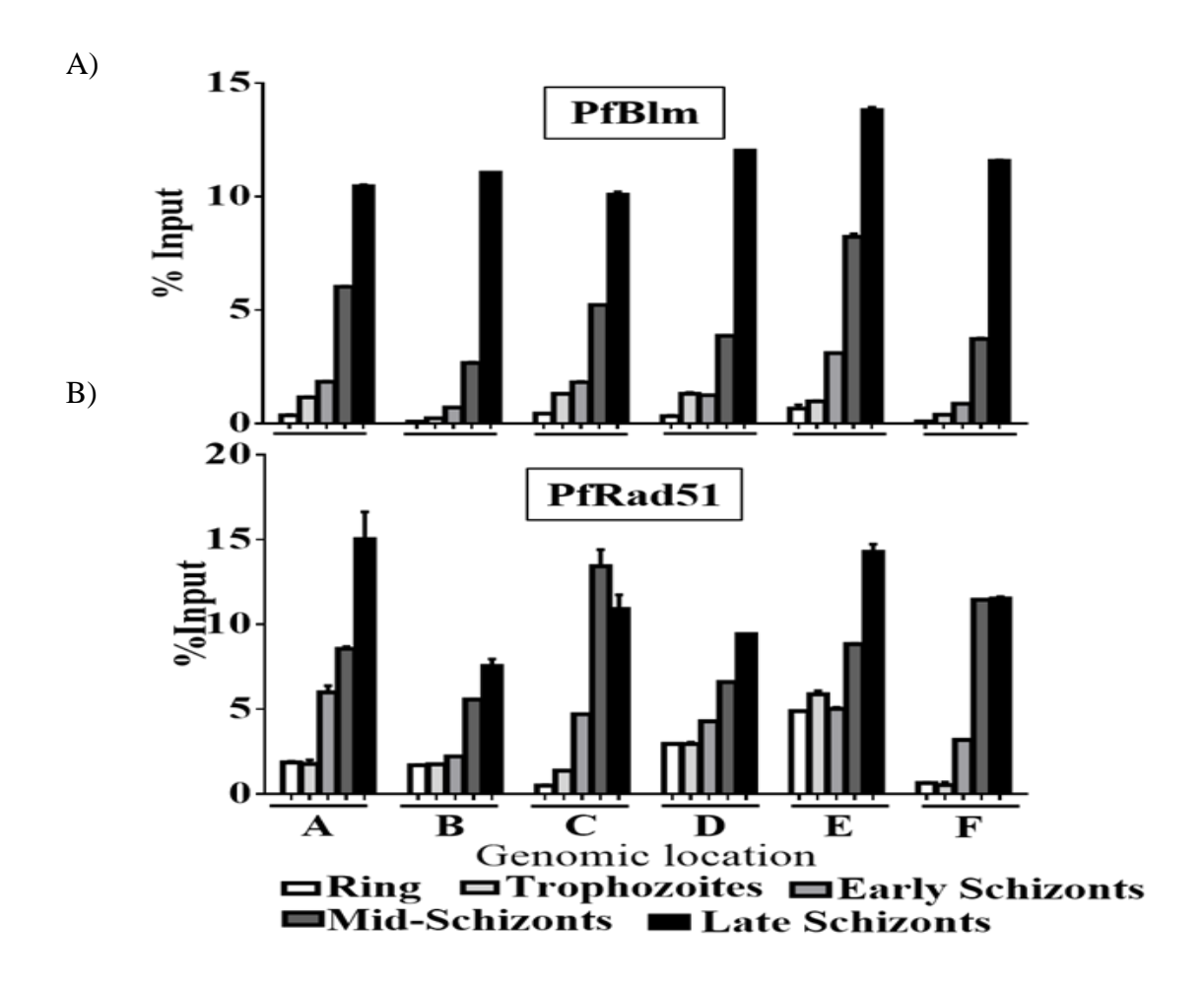


Figure 3.4: Stage-specific interaction of PfRad51 and PfBlm with the mitochondrial genome. (A) and (B) display the relative occupancy (in terms of % input) of PfBlm, and PfRad51 as quantified by qPCR throughout the mitochondrial genome (A-F), in rings (10-12 hpi), trophozoites (28 hpi), early schizonts (32 hpi), mild schizonts (38 hpi), and late schizonts (44-48 hpi) stages of the parasite. Data represent the mean ±SEM of three repeats. Data were normalized using respective IgG-IP values.

3.2.5 Repair of UV-induced DNA double-strand break in the nuclear and mitochondrial genome:

In order to study the DNA damage repair kinetics, we have designed a strategy to induce and monitor the repair of nuclear and mitochondrial DSB in real-time. Firstly, we checked the effect of different doses of UV irradiation (50, 100, 125, and 150 J/m²) on nuclear DSB repair. We found the dose-dependent effect of UV irradiation on DSB induction. 50 J/m² UV dose had a negligible effect on parasite growth and no detectible DNA DSB induction. Whereas, the treatment with 125 and 150 J/m² UV light the parasite viability sharply reduced with a very high degree of DNA DSB induction. The parasite could not repair such a high dose of UV-induced DSB and eventually lead to cell death. The 100 J/m² UV dose resulted in decreased parasite viability and significant induction of DNA double-strand breaks as compared to the control parasite (Figure 3.5 A). Therefore, in our studies, we have used 100 J/m² UV dose to induce DNA DSBs. We have developed a PCR-based assay system to study the damage and its repair in P. falciparum nDNA and mtDNA. This method is based on the principle that a longer region of the genome is likely to experience UV-induced DNA breaks and as a result, will not yield a PCR amplicon until and unless such DNA breaks are repaired. On the other hand, a very short region of the genome could be amplified even under DNA damaging conditions as this region is less likely to harbor any break. Thus, a short-range PCR amplicon of size 290 bp from the mtDNA and 269 bp from the nDNA could be used to normalize the data obtained from the longrange PCR amplicon (5967 bp of mtDNA and 7200bp of nDNA) (Fig. 3.5 B). Post-UVirradiation parasites were harvested at the 0th hour of the DNA damage and thereafter at every 12-hour time interval, followed by genomic DNA isolation and PCR amplification. To this end, we have first compared the repair kinetics of the damaged mitochondrial DNA and the nuclear

DNA. We found that more than 50% of nuclear genome DSBs were repaired within 12 hours and almost complete repair was attained by 24 hours post UV irradiation. A similar repair kinetics profile was observed for mitochondrial DSB repair wherein complete repair was achieved within 24 hours after DNA damage induction (Figure 3.5B).

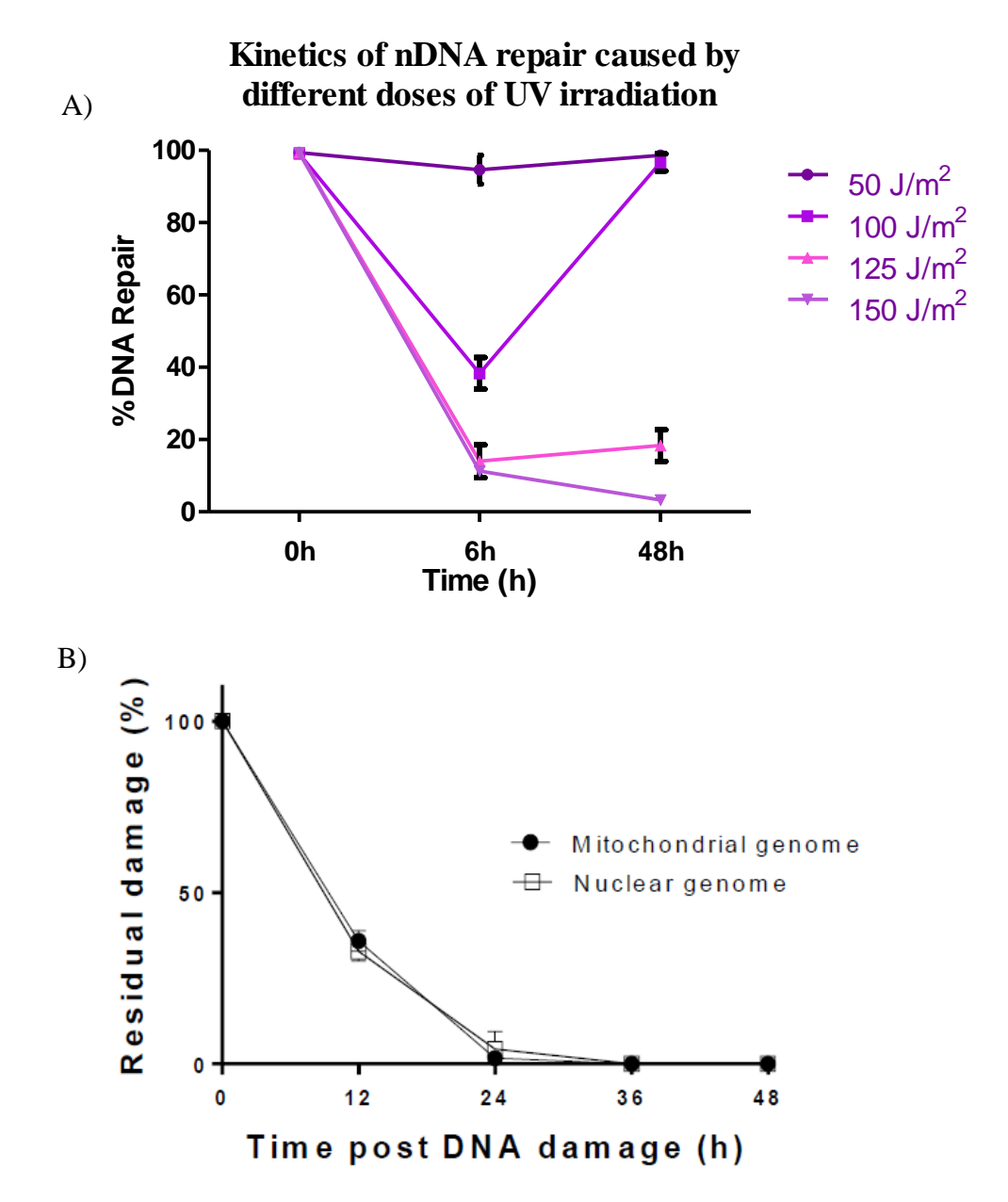


Figure 3.5: Repair of UV-induced DNA double-strand break in the nuclear and mitochondrial genome. (A) The nuclear DNA DSB induction by different doses of UV was assayed and plotted in terms of % DNA Repaired at indicated time points after irradiation. (B) Repair of the mitochondrial DNA or the nuclear DNA was assayed with specific primer sets. The percent residual damage at indicated time points was plotted using GraphPad Prism. Error bar represents the mean fluorescence intensity ± SEM of three experimental repeats.

3.2.6 PfBlm and PfRad51 are involved in the repair of DNA double-strand breaks:

In order to test our hypothesis that PfRad51 and PfBlm could be involved in the repair of DSBs in the mitochondrial genome, we have used chemical inhibitors specific to these two proteins and investigated for any impairment in DNA repair activity in the mitochondrial genome. The outcome of this approach was compared with the nuclear DBSs repair kinetics. We have used small molecular inhibitors that are BO2 against PfRad51 and ML216 against PfBlm. Their inhibitory effect on the respective protein has been established in previous studies (Suthram et al. 2020; Vydyam et al. 2019). Firstly, we have titrated the BO2 concentration that can block PfRad51 activity to an extent that can be tolerated by the parasites. While the treatment with 0.5 μM BO2 had a negligible effect on the parasite growth and nDNA DSB repair, the nDNA repair kinetics was similar to the untreated parasite. On other hand, in treatment with 5 µM BO2 we could not detect any long-range PCR amplicon in the later time points. Moreover, parasite treatment with 1 µM BO2 had shown encouraging phenotype wherein the parasite growth was mildly affected while the DSB repair was effectively blocked (Figure 3.6A). Since the IC₅₀ value of ML216 has been reported to be 10 μM which is close to BO2 IC₅₀ (8 μM) (Suthram et al. 2020; Vydyam et al. 2019), therefore we have used a 1 µM concentration of these drugs in our repair kinetics studies. To this end, the parasite cultures were pre-treated with the sub-lethal doses of the drugs (1µM). Cells were maintained in the drug-containing medium during and after the DNA damage, and the kinetics of DNA repair was determined. We observed that the treatment with BO2 and ML216 disrupted the mitochondrial DSB repair since we could not find any restoration of DSB till 24 hours, moreover the damage was persistent till 48 hours, and that eventually lead to parasites death (Figure 3.6B). However, the DNA repair was unaltered in the case of mock-treatment wherein the parasites were maintained in a medium containing the

solvent that is DMSO without any drug. Atovaquone which is a chemical inhibitor of cytochrome bc1 complex of electron transport chain, with no known effect on DSB repair, was used as a negative control. Certainly, the treatment with a sub-lethal dose of Atovaquone (0.3mM) did not affect DNA repair, since the damaged DNA was repaired by 24 hours post UV irradiation as observed for the mock-treated parasites. Similar to mtDNA DBS abrogation caused by these chemical inhibitors, we observed that the repair of nDNA DSBs was also severely impaired by the treatment with BO2 as well as ML216 (Figure 3.6C). The long-range PCR product of this assay was sequenced to ascertain that the amplicons were mitochondrial genome-specific. The kinetics of mtDNA DSB repair in mock-treated and ATQ-treated control parasites was unaffected. In total, this result suggested that these repair proteins are involved in both nuclear and mitochondrial DSB repair.

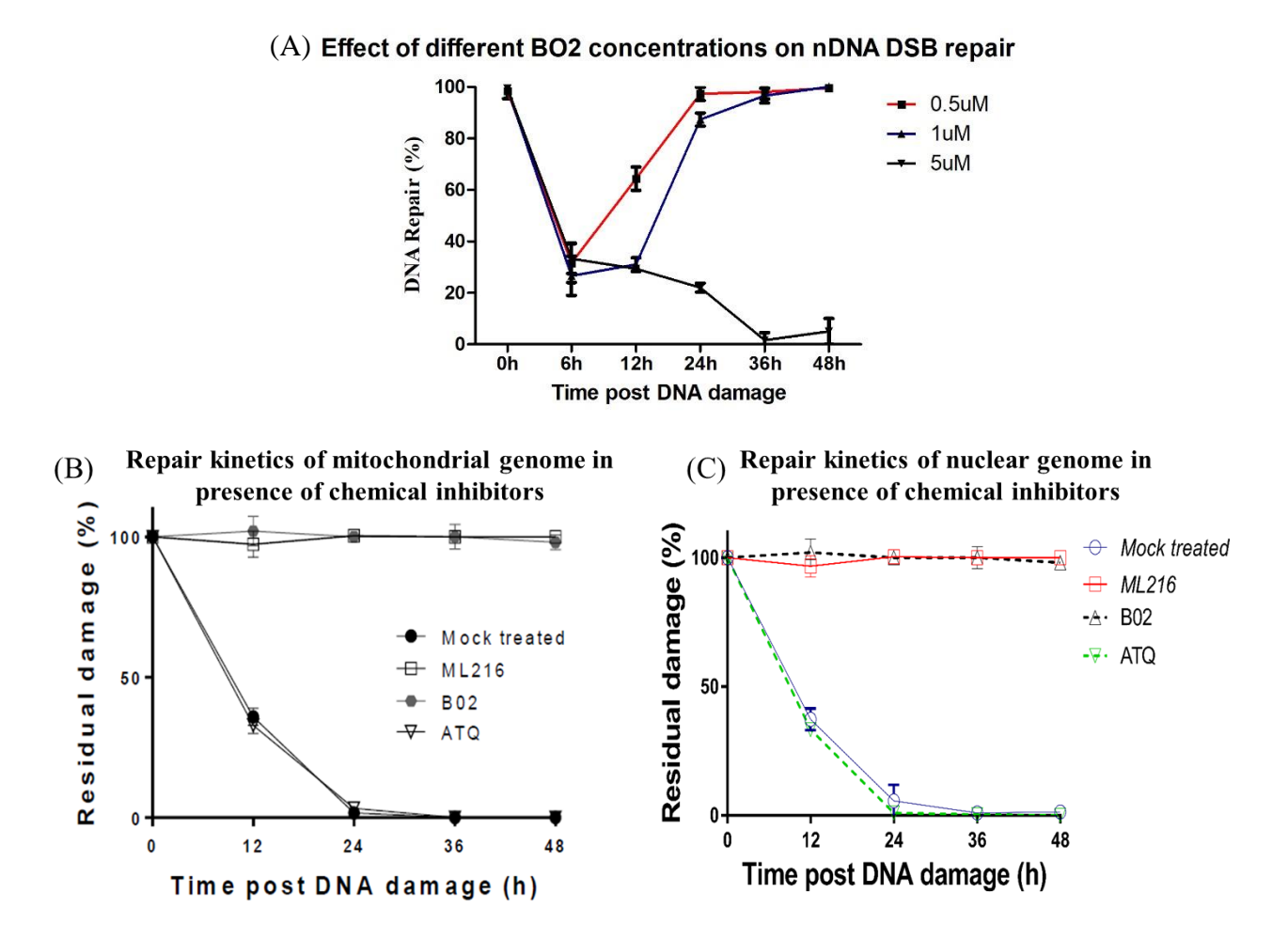


Figure 3.6: PfBlm and PfRad51 are involved in the repair of DNA double-strand breaks.

(A) The graph represents the effect of different BO2 concentrations on nuclear DSB repair kinetics. Parasite cultures were maintained in a medium containing either 0.5, 1, or 5 μM BO2 concentrations, before and after UV exposure. The graph shows the percentage of DNA repair at indicated time point. (B) And (C) Graphs representing the mitochondrial and nuclear repair kinetics, respectively. In both, the assay *In-vitro* cultures of *P. falciparum* were pre-treated with ML216, BO2, or Atovaquone (ATQ) at the sub-lethal concentrations. The mock-treated parasite (grown in the drug-free complete medium) along with drug-treated parasite cultures were UV-irradiated. Post-DNA damage cells were grown with or without the respective drugs (ML216, B02, or ATQ) for 48 hours. We have used a different set of long-range and short-range primers 68 | P a g e

from mtDNA and nDNA loci. The percent residual damage at indicated time points was plotted using GraphPad Prism. Error bar represents the mean fluorescence intensity \pm SEM of three experimental repeats.

3.2.7 Overexpression of PfBlm and PfRad51 provides a kinetic advantage in repairing nuclear and mitochondrial DSBs:

Our hypothesis predicts that the overexpression of these two DSB repair proteins would have a positive effect on the DSB repair. In order to test that we have created two parasite lines each expressing either PfRAD51 or PfBLM genes from an episomal plasmid pARL. We have compared the repair kinetics of the wild-type 3D7 strains and the two parasite lines harboring extra copies of either of the genes (p-RAD51 and p-BLM). Significantly faster repair kinetics of nDNA and mtDNA were observed for each of the two transgenic parasite lines. For mitochondrial genome, it was observed that at the end of 18 hours post DNA damage, in the wild-type 3D7 strain only 74% repair was achieved, but in the transgenic strains, (86-87) % repair was completed (Figure 3.7A). In the case of the nuclear genome, we found that the DSB repair in the 3D7 parasite was 75% while in the transfectant parasites overexpressing either PfRad51 or PfBlm proteins the repair % increased to 90% by 18 hours post UV irradiation (Figure 3.7 B). The experiment was repeated more than 3 times with transgenic parasite strains and we found that the increase in repair efficiency in both PfBLM and PfRAD51 expressing strains are statistically significant. In order to ascertain that such increased efficiency is due to the expression of the additional copies of the respective genes, we have created two more parasite lines expressing the mutant versions of the genes. Earlier it was reported that the helicase-dead mutant of PfBLM (Pfblm-K83R) could not confer any survival advantage to the

MMS treated parasites as opposed to the parasites expressing additional copies of the wild-type *PfBLM* gene (Suthram et al. 2020). We have included this parasite line in our study as a control. Similarly, the expression of a mutant version of *PfRAD51* (*PfRAD51K143R*) had a dominant-negative effect on the wild-type *PbRAD51* and rendered such parasites more vulnerable to MMS treatment (Roy et al. 2014). For this study, we have created the *PfRAD51* dominant-negative *P. falciparum* line by expressing the *PfRad51K143R* mutant allele from an episomal plasmid PfCENv3. The overexpression of mutant *PfRad51K143R* was confirmed using the western blotting technique (Appendix figure. A3). This parasite line has also served as a control for our experiments. It was observed that the *Pfblm-HD* expressing parasite line did not confer any faster repair of mtDNA or nDNA. As expected in the *Pfrad51-DN* line the DSB repair of both nuclear as well as mitochondrial genome was completely abolished (Fig. 3.7A and B). Taken together, our findings establish the pivotal roles of the nuclear-encoded HR proteins in the DSB repair of both nuclear and mitochondrial genomes.

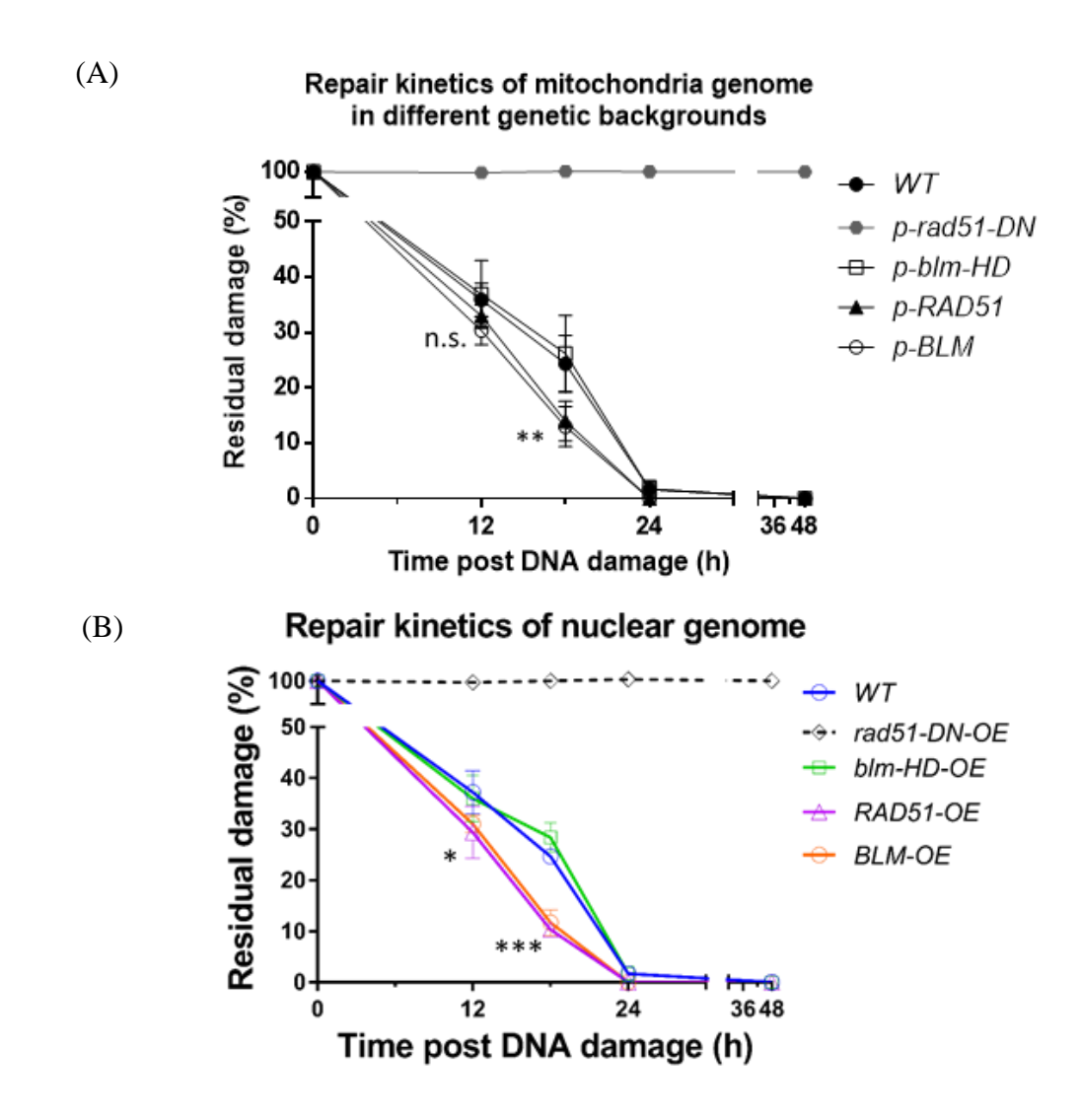


Figure 3.7: Overexpression of PfBlm and PfRad51 provided a kinetic advantage in repairing nuclear and mitochondrial DSBs. (A) and (B) The graphs display the kinetics of mtDNA and nDNA repair, respectively, in 3D7 parasite (*WT*) and parasite expressing *PfRad51-GFP* (p-*PfRad51*), *PfBlm-GFP* (p-*PfBlm*), a dominant-negative mutant of *PfRad51K143R* (p-*rad51-DN*), or helicase dead mutant of *PfBlmK83R* (p-*blm-HD*) from episomal plasmids. Twotailed student *t*-test was used to calculate the *P*-values (** *P*-value <0.01, and n.s. *P*-value >0.05).

3.2.8 DNA damage induces organelle translocation of PfRad51 and PfBlm:

We investigated the organelle and nuclear import of PfRad51 and PfBlm and compared the outcome with the overall expression of these repair proteins at the whole parasite level in response to the UV-mediated DSBs. We reasoned that if these two proteins are directly involved in repairing the DSBs, they are likely to be imported to a higher extent into the mitochondria and nucleus. To this end, P. falciparum cultures at the trophozoite stage were subjected to 100J/m² UV radiation to induce random DSBs. Parasites were collected at 0 hours, 6 hours, 12 hours, 24 hours, and 40-hour time-points post UV irradiation, and they were used to prepare whole cell, nuclear, and organelle fraction lysates. Extracted proteins from these samples were subjected to western blot analysis using specific antibodies against PfRad51 or PfBlm proteins. We found a gradual increase in the organelle import of both the repair proteins till 12 hours, thereafter a sharp increase in their translocation was observed till 24 hours post DNA damage induction, their organelle level remains unaltered afterward (Figure 3.8 A and B). In the organelle import study, the mitochondrial protein PfCytC, which is also nuclear-encoded and imported to the mitochondria, acted as a loading control as it is not related to the DNA damage response. The nuclear protein PfH3 acted as a negative control for this experiment. In the case of nuclear import of PfRad51 and PfBlm in response to DBSs, we have normalized the data using nuclear marker PfH3. We found that the nuclear levels of these proteins during the initial 6 hours were unchanged. However, a sharp increase was observed thereafter until 24 hours post DNA damage, subsequently, the elevated nuclear levels of these proteins were maintained in the nuclear fraction (Figure 3.8C and D). Next, we investigated the DSB induced expression of PfRad51 and PfBlm at the whole parasite level. Consistent with the previous reports we found a significant increase in their expression in response to DNA damage stress (Bhattacharyya and

Kumar 2003; Suthram et al. 2020). We observed a gradual increase in the expression of both the proteins from 6 hours till 40 hours after DNA damage (Figure 3.8 E and F). Here PfActin was used to normalize the data. Interestingly, the expression kinetics of these proteins in whole parasite extract was proportional to their nuclear and mitochondrial import kinetics. Thus, our findings establish that DNA damage stress induces increased expression of PfBlm and PfRad51 and their nuclear and mitochondrial transport.

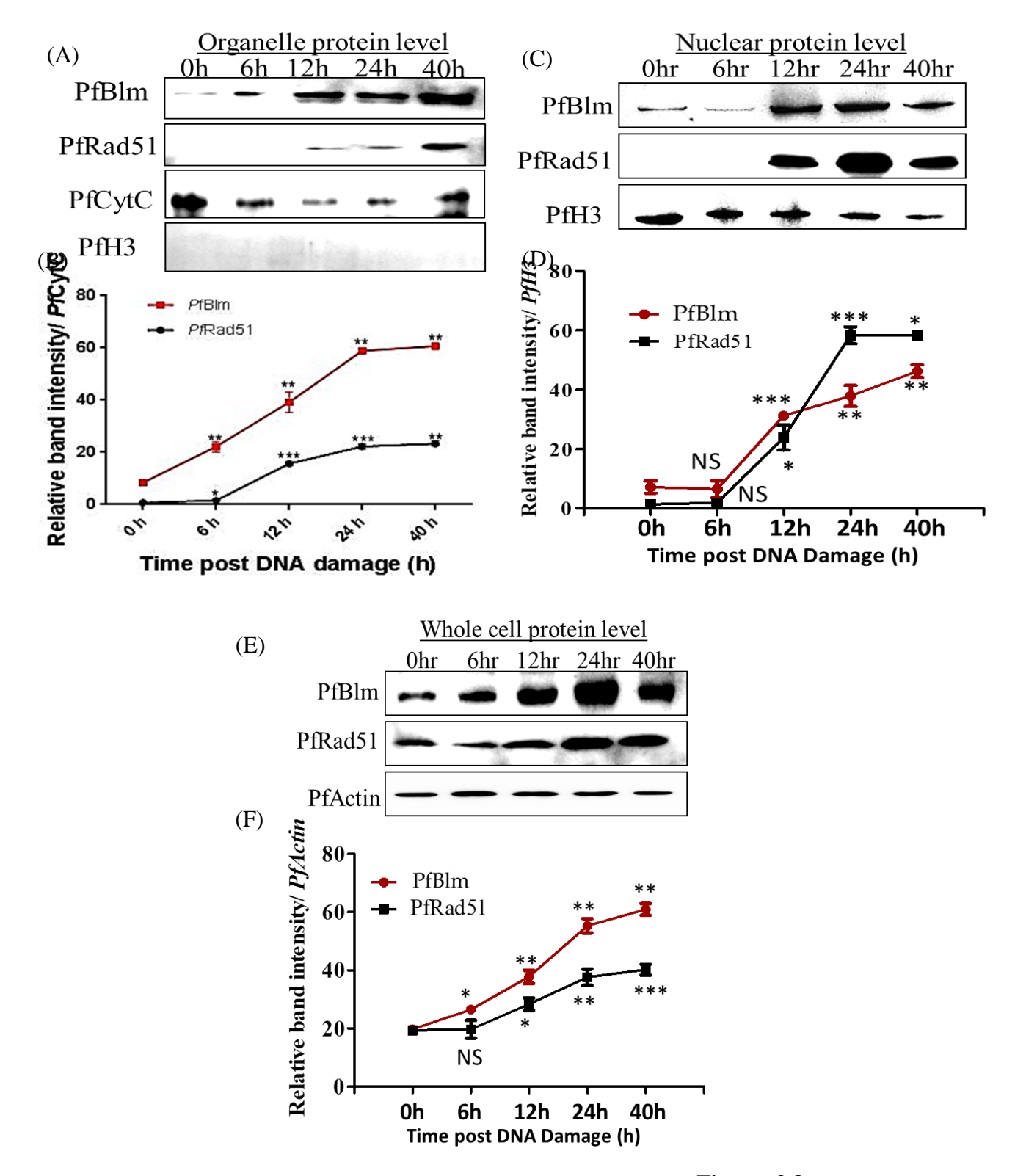


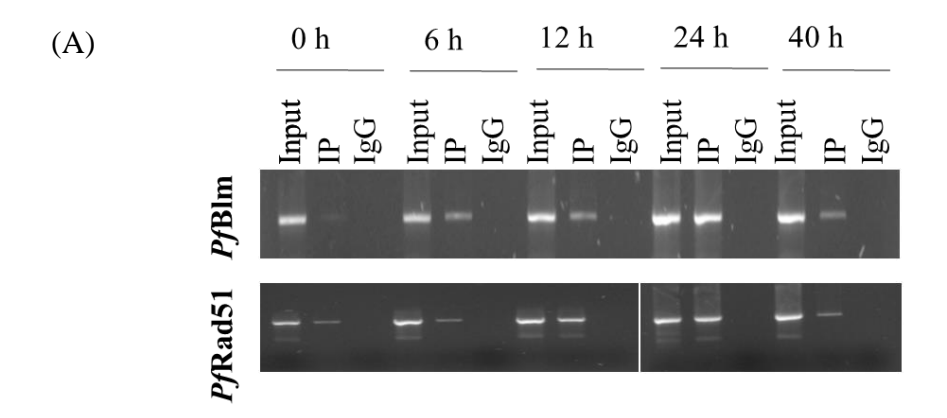
Figure. 3.8

Figure 3.8: DNA damage induces organelle translocation of PfRad51 and PfBlm. (A) (C) and (E) the Western blots showing the levels of PfBlm and PfRad51 proteins in the organelle, nuclear, and whole-cell (WC) fractions at the respective time points post DNA damage, respectively. Tightly synchronous trophozoite staged parasite were subjected to UV radiation and parasite at indicated time points were used to prepare subcellular fractions. (A) In the case of organelle import, PfCytC a mitochondrial marker was used as a loading control and the nuclear marker (PfH3) shows the purity of the organelle fraction. (C) Nuclear data was normalized using nuclear marker protein PfH3. (E) PfActin was used as a loading control for whole-cell proteins. (B), (D), and (F) Represents the band intensities of PfBlm and PfRad51 normalized against corresponding loading control in the organelle, nuclear, and WC fractions. Image J software was used to quantify the band intensities in the western blots of the three experimental repeats. Data represent the mean band density ± SEM. Two-tailed student *t*-test was used to calculate the *P*-values (* *P*-value <0.05, ** *P*-value <0.01, *** *P*-value<0.001).

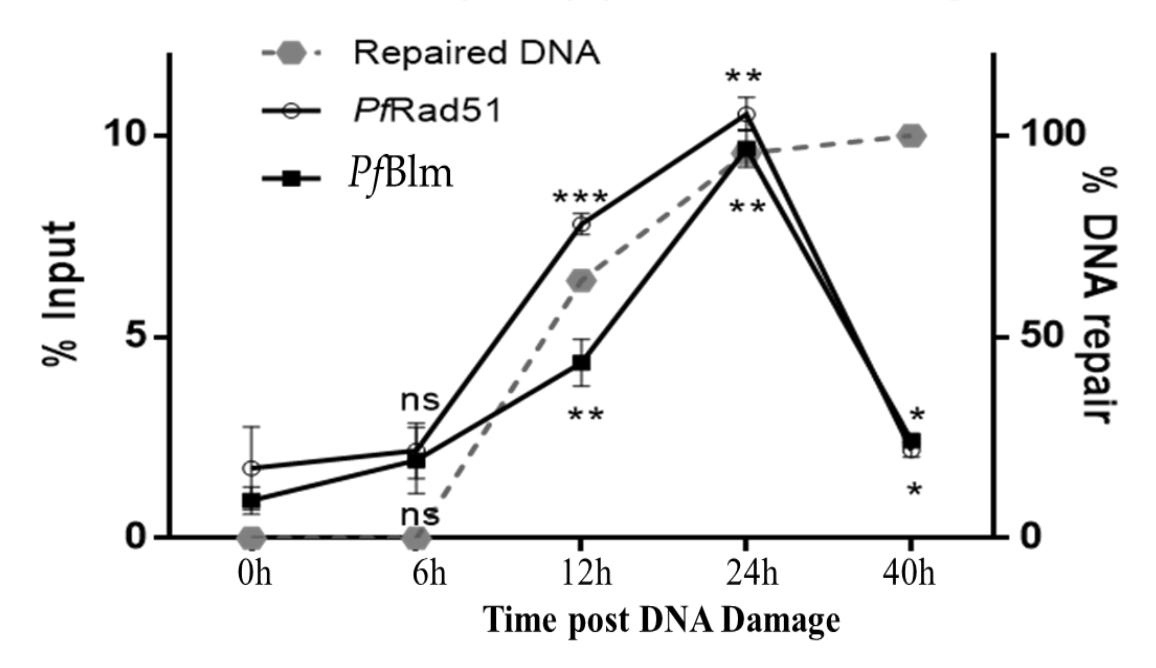
3.2.9 DNA damage induces mtDNA recruitment of PfRad51 and PfBlm:

Further, we investigated whether the increased import of PfRad51 and PfBlm are correlated with increased occupancy of these proteins onto the damaged mtDNA. To this end, we have determined the time-kinetics of the recruitment of PfRad51 and PfBlm at the mtDNA by performing mtDNA-IP experiments. Similar to the previous study, the trophozoite stage parasites were subjected to 100J/m² UV radiation to induce random DSBs. Parasites were collected at 0 hours, 6 hours, 12 hours, 24 hours, and 40-hour time-points post UV irradiation, and they were used for mtDNA-IP using specific antibodies against PfBlm and PfRad51. The relative occupancy of PfBlm and PfRad51 proteins on mtDNA were found to be increased significantly after 12 hours post DNA damage, with no significant change during the initial 6 hours. The recruitment of these HR proteins was further seen to be significantly elevated, and at the end of 24 hours, it reached a peak. Thereafter, the occupancy of these repair proteins was reduced to the basal level at the end of the 40-hour time-point (Figure. 3.9A and B). Rivetingly, the pattern of the recruitment kinetics was found to be parallel with the DNA repair kinetics, and the peaks of both the kinetics coincided at the 24th-hour post DNA damage (Figure. 3.9B). These findings provide evidence for the direct role of PfRad51 and PfBlm in the repair of damaged mtDNA. To validate the faster repair kinetics exhibited by the parasite lines ectopically expressing GFP tagged PfRad51 or PfBlm, we investigated the recruitment of both recombinant proteins to mtDNA at 0 and 24 hours post UV irradiation (Figure, 3.9C). As expected, we noted a markedly enhanced recruitment of both the proteins at 24 hours post DNA damage. Taken together, our findings suggest that in response to mtDNA damage, PfRad51 and PfBlm translocate to the mitochondria and are recruited at the damaged sites in mtDNA during the first 12-24 hours, a duration that coincides with the time required for the completion of the mtDNA

repair. However, once the damage is repaired, these proteins dislodged themselves from the DNA, but still reside within the mitochondria, at least up to the 40-hour time-point.



(B) Relative occupancy post DNA Damage



(C) Relative occupancy post DNA damage

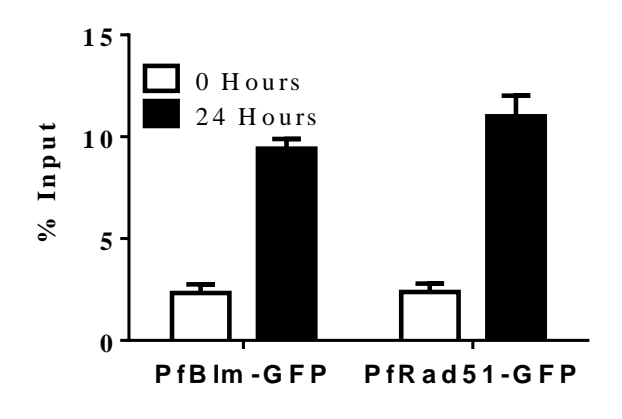
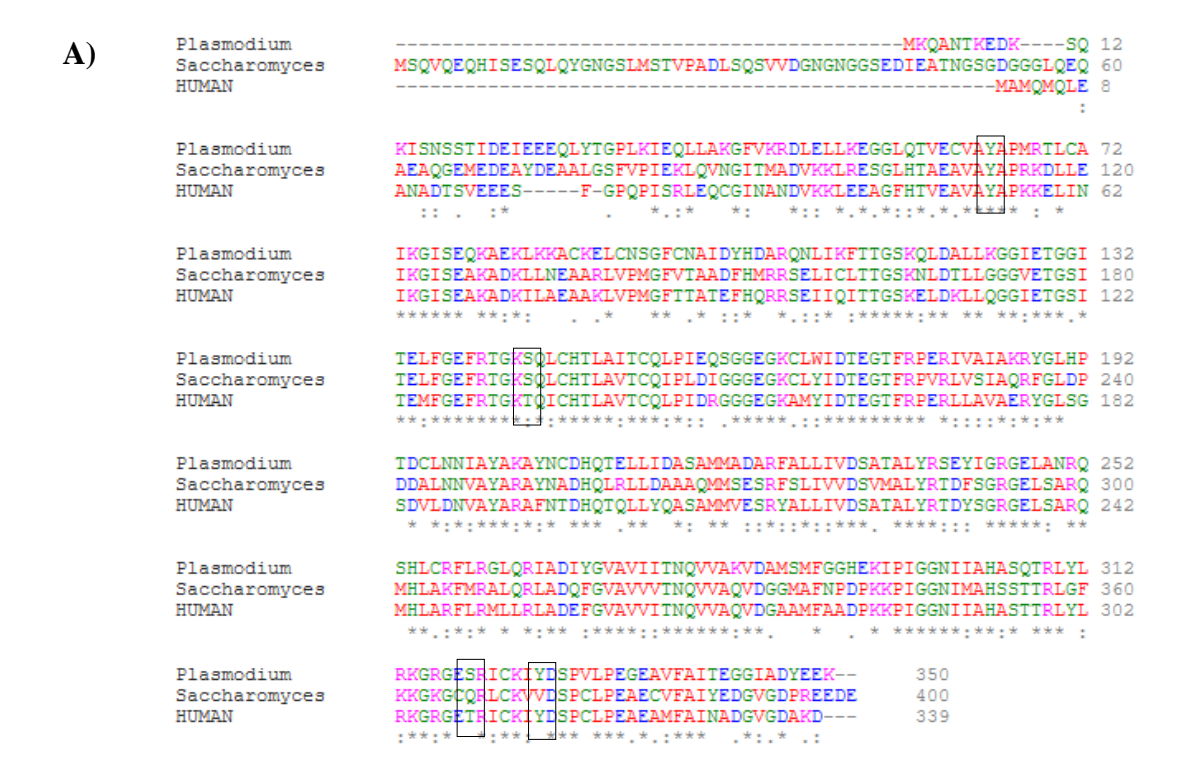


Figure. 3.9

Figure 3.9: DNA damage induces mtDNA recruitment of PfRad51 and PfBlm. (A) Agarose gels represent PCR amplification of the mitochondrial locus A in the following samples: input mtDNA (Input), PfBLM- or PfRad51-immunoprecipitated mt-DNA (IP), and rabbit immunoglobulin G immuno-precipitated mtDNA (IgG) at the indicated time points post UV irradiation. The upper and lower panel displays the recruitment of PfBlm and PfRad51 proteins to mtDNA post DNA damage. (B) The plot displays the kinetics of the relative occupancy of PfBlm and PfRad51 to mtDNA (locus A) upon DNA damage. The precipitated mtDNA was quantified by qPCR and is expressed in terms of % input in the left Y-axis. Data were normalized against respective IgG-IP values. The repair kinetics of the damaged mtDNA is represented as the dotted line on the right Y-axis. (C) The bar graph represents the DNA damage-induced enrichment of GFP tagged PfBlm and PfRad51 to mtDNA at 0 and 24 hours post UV treatment. Error bar represents mean ± SD (n=3). * P-value <0.05, ** P-value <0.01, *** P-value <0.001, and n.s. P-value >0.05.

3.2.10 Prediction of amino acid residues of PfRA51 with high phosphorylation potential:

Previous reports from model organisms have suggested that the Rad51 undergoes various kinds of posttranslational modification which consequently regulate different functional aspects of this protein (Milena Popova 2011). In humans, Rad51 phosphorylation has been shown to regulate its nuclear localization and subsequently stimulates Rad51 mediated foci formation (Slupianek et al. 2011). Since phosphorylation is the most extensively characterized PTM in *Plasmodium*, therefore, we sought to explore the possible residues of PfRad51 which are most likely to undergo phosphorylation. To check that we have employed conserved residue analysis using clustalOmega software and Netphos III bioinformatics tools for predicting the residues with high phosphorylation potential. In the multiple sequence alignment study, we have found four conserved residues in PfRad51 whose corresponding residues are known to get phosphorylated in model organisms. First, Ser192 of ScRad51 which regulates DNA binding and ATPase activity of this protein is conserved as Ser144 in PfRad51. Similarly, Tyr54, Tyr315, and Tyr309 residue of HsRad51 are conserved in PfRad51 as Try64, Tyr325, and Ser319 (Figure 3.10A). Additionally, our phosphorylation prediction analysis has also shown high phosphorylation potential for these four residues (Figure 3.10 B). These findings narrowed down our search for residues that are likely to be phosphorylated in PfRad51.



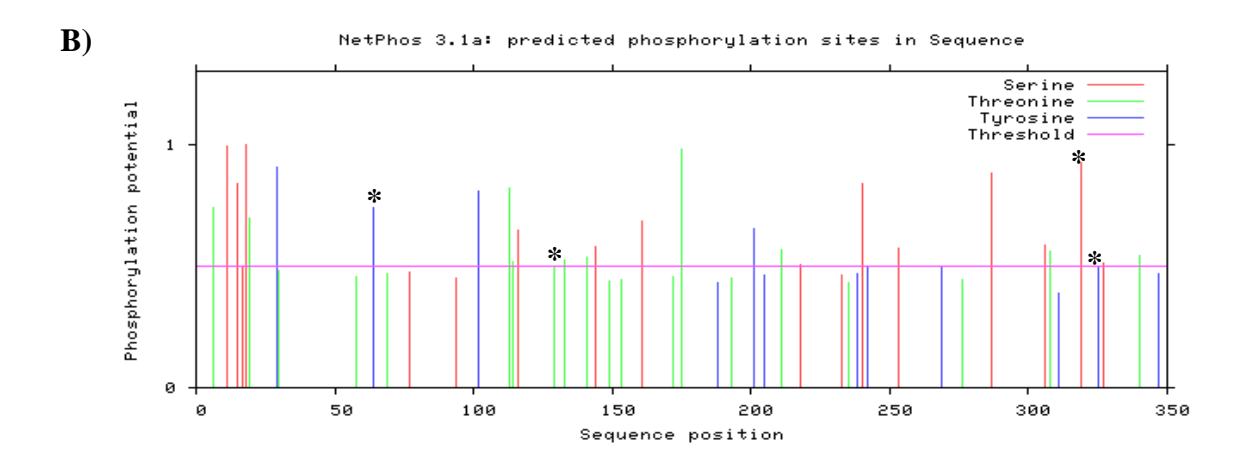


Figure 3.10: The amino acid residues of PfRad51 with high phosphorylation potential. (A)

The multiple sequence alignment between *P falciparum*, *S. cerevisiae*, and Human Rad51 proteins represents the conserved amino acid residues. The black box emphasizes the conserved PfRad51 residues with high phosphorylation potential. (B) The NetPhos3 graph shows the predicted phosphorylation residues of PfRad51. Here, the pink horizontal line is indicating the

threshold phosphorylation potential score. The star mark shows the peaks corresponding to S144, Y64, S319, and Y325 residues.

3.2.11 Effect of Pfrad51 double mutation on its subcellular distribution and foci formation activity:

Since the *Plasmodium* genome lacks gene encoding for tyrosine kinases, hence we chose Ser144 and 319 for further examination. To this end, we generated single and double mutants of the PfRad51 gene using site-directed mutagenesis. These mutants are cloned into pET28a bacterial expression vector and the final constructs were sequenced to ascertain appropriate amino acid alteration and cloning (Appendix figure 4). We have purified these recombinant Pfrad51 mutants along with wild-type protein to perform in vitro phosphorylation assay (Appendix figure 6). However, we could not find an effect of mutations on Pfrad51 phosphorylation owing to the presence of a nonspecific signal overlapping with the signal emitted by radiolabeledphosphorylate PfRad51 (Appendix figure 7). We took an alternative approach to find out the effect of double mutation of Pfrad51, wherein we sought to investigate its subcellular localization and foci formation activity of mutant Pfrad51 within the parasite. To this end, we have generated a parasite strain overexpressing Pfrad51^{S144-A/S319-A} double mutant from an episomal plasmid pARL. The expression of this mutant protein was verified using the western blotting technique (Figure 3.11 A). We have compared the subcellular localization and foci formation activity of the wild-type PfRad51-GFP with the parasite strain expressing double mutant of *Pfrad51-GFP*. We have used immunofluorescence assay to investigate nuclear and mitochondrial localization of GFP-tagged wild-type and mutant Pfrad51 protein. In this assay live parasites were stained with mitochondrial dye (Mitotracker), and nuclear dye (DAPI). We found that the green signal coming from GFP tagged PfRad51 and its double mutant colocalizes with the signals emitted from mitochondria (Red) as well as the nucleus (Blue). Both proteins showed comparable nuclear and mitochondrial distribution with no noticeable change in their colocalizing fluorescence signal (Figure 3.11 B (I Vs III) and C (I Vs III)). Similarly, PfRad51 mediated foci formation was also unaffected by these mutations (Figure 3.11 B (II Vs IV) and C (II Vs IV)). Altogether our results showed that the mutations at S144 and S319 residues in PfRad51 do not affect its nuclear and mitochondrial translocation and foci formation activity.

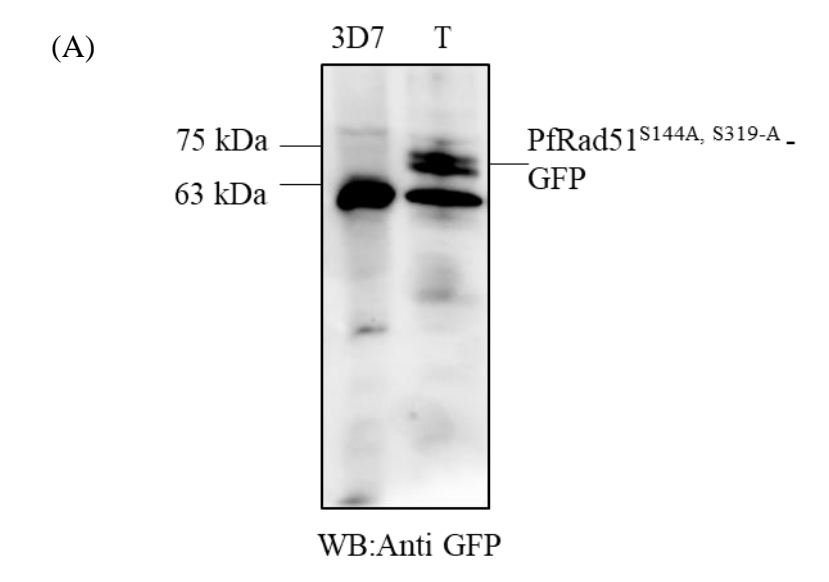


Figure 3.11

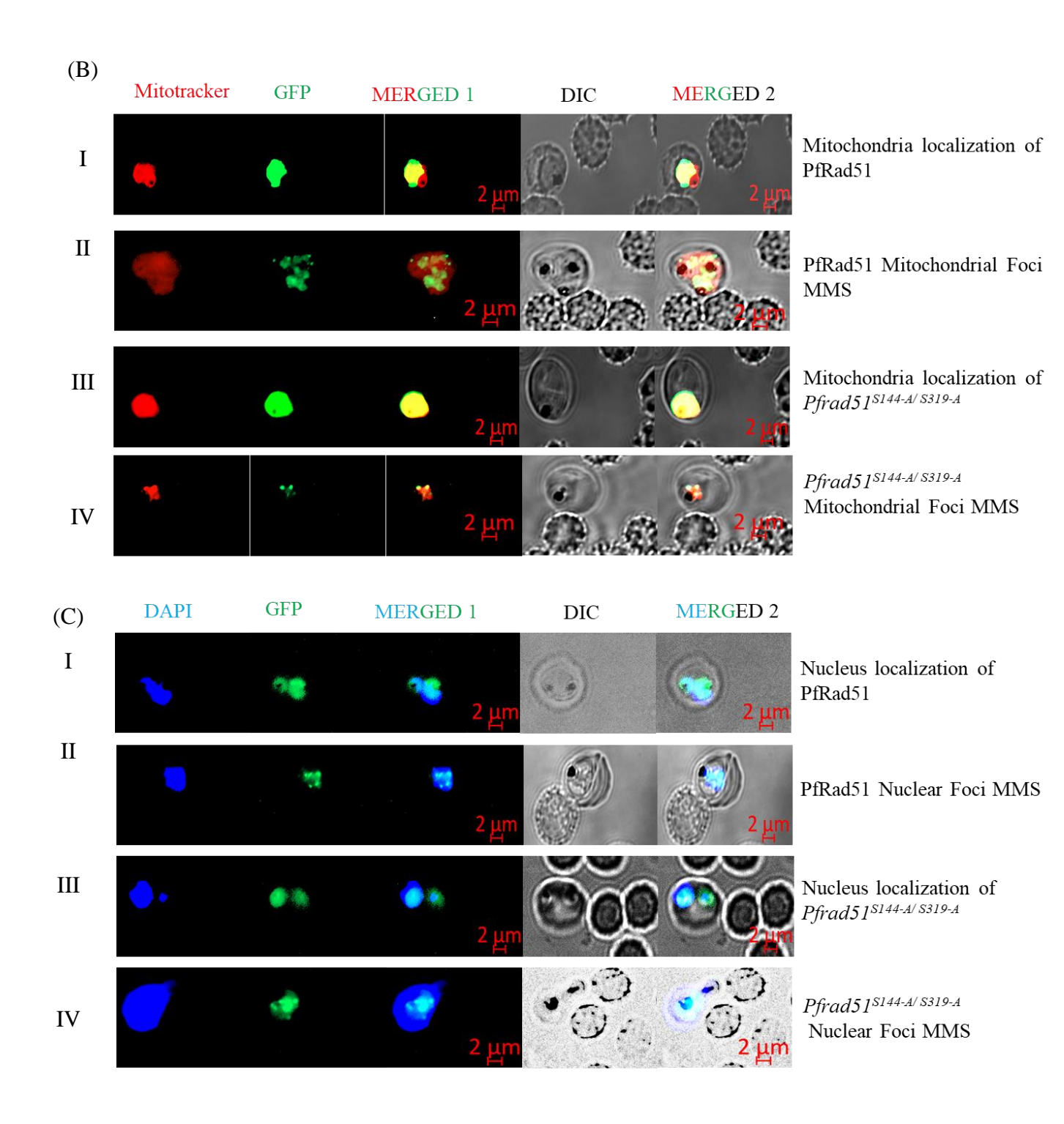


Figure 3.11: Effect of Pfrad51 double mutation on its subcellular distribution and foci formation activity. (A) Western blot displaying the expression of *Pfrad51*^{S144A/S319A}-*GFP*

protein in the transfected (T) parasite line and not in the un-transfected (3D7) parasite line. (B) Immunofluorescence images displaying mitochondrial localization and MMS-induced foci formation activity of wild type and double mutant PfRad51-GFP. (C) IFA images display the nuclear localization and MMS-induced foci formation activity of wild type and double mutant PfRad51-GFP. Green, red and blue signal represents fluorescence emitted by GFP tagged PfRad51(WT/mutant) protein, Mitotracker Red staining mitochondria, and DAPI staining nucleus.

3.3 Summary

In this chapter, we have shown the organelle presence of two HR proteins namely, PfBlm and PfRad51. While the DNA damage sensor PfalMre11 has shown nuclear exclusive presence. Mitochondrial localization of PfBlm and PfRad51 was established in addition to their typical nuclear presence. PfBlm and PfRad51 proteins showed association with the mtDNA in a stagespecific manner, and such association was observed throughout the 6 kb mitochondrial genome. We found that the mtDNA occupancy by PfBlm and PfRad51 increased significantly in the mature asexual parasite stages as compared to the rings stage. In the later stages of development, the parasite genome is likely to be predisposed to DNA damage owing to highly active metabolic and genome duplication activity. Thus, our finding that the occupancy of both PfRad51 and PfBlm on the mtDNA elevates multiple folds in the schizont stages indicates the involvement of these two nuclear-encoded proteins in mtDNA replication and/or repair. It was evident from our results that blocking PfBlm and PfBlm activity with the use of chemical inhibitors impaired both mitochondrial and nuclear DNA DSB repair. Moreover, overexpression of these HR proteins provided a kinetic advantage by enhancing the DSB repair at a given time point. Therefore, our data established the direct role of these HR proteins in the mtDNA DSB repair which was correlating with their nuclear genome repair functions. Since PfBlm and PfRad51 are involved in mtDNA DSB repair this implies that their mitochondrial import and mtDNA association would increase under DNA damaging stress conditions. Indeed, our finding showed that DNA damage does induce elevated mitochondrial localization and more importantly, increased mtDNA occupancy of these repair proteins. The maximum interaction PfBlm or PfRad51 with mtDNA was observed during 12 to 24 hours after DSB induction and also during this time we have monitored the maximum mtDNA repair. This finding suggested that the

occupancy kinetics of HR protein and mtDNA repair kinetics coincide, providing additional evidence of their function in parasite mitochondria genome repair. Although we could not establish the role of phosphorylation in regulating PfRad51 function, it is clear that these two serine residues are nonessential for PfRad51 mediated DNA-damage foci formation and its import to nucleus and organelle. Overall this work has established that the *P. falciparum* possesses functional homologous recombination in its mitochondria.

Chapter 4 <u>PF3D7_0625300 GENE PRODUCT MITOCHONDRIAL</u> <u>LOCALIZATION AND INTERACTION WITH REPAIR</u> <u>PROTEINS.</u>

PF3D7_0625300 GENE PRODUCT MITOCHONDRIAL LOCALIZATION AND INTERACTION WITH REPAIR PROTEINS.

4.1 INTRODUCTION.

Plasmodium mitochondrion is a key organelle shown to be essential for parasite survival. It is the subcellular compartment involved in mtETC and several other metabolic pathways. This parasite is not dependent on its mtETC for ATP generation, instead uses glycolysis as a primary energy source due to the abundance of glucose in the host. Since the salvage pathway for synthesizing pyrimidine is absent in Plasmodium, the parasite depends on the de novo pathway for the synthesis of this biomolecule. The pyrimidine biosynthesis pathway is further linked to mtETC at the level of ubiquinone. Due to such vital role of Plasmodium mitochondria, it has been considered as a potential target for anti-malarial drug development. The success of atovaquone as the antimalarial drug is proof of this concept. However, the rapid emergence of resistance to this drug suggests the need to explore other targets. Our finding of functional HR repair mechanism in this organelle has presented an additional pathway that can explore for its potential as a therapeutic target.

Synthesis of the new complementary DNA strand with the help of DNA polymerase enzyme is required to complete the HR-mediated repair. A minimalistic recombinosome complex must consist of a recombinase for catalyzing strand exchange and homology search, a DNA polymerase for filling the DNA gap, and a DNA helicase for resolving the end product. So far, we have found the function of a recombinase (PfRad51) and DNA helicase (PfBlm) in the *Plasmodium* mitochondrial. In humans, DNA polymerase gamma which is a mitochondrial-specific DNA polymerase has been shown to be involved in repairing mtDNA DSBs along with Rad51 and a mitochondrial-specific DNA helicase called Twinkle. In a previous study by Prtmiter et. al. it was shown that the *Plasmodium* mitochondrial extract harbors DNA polymerase activity. However, the gene encoding this protein remains elusive. In the same

PF3D7_0625300 GENE PRODUCT MITOCHONDRIAL LOCALIZATION AND INTERACTION WITH REPAIR PROTEINS.

study, the authors have observed that the partially purified DNA polymerase from *Plasmodium* mitochondria was resistant to aphidicolin which categorizes it as either β or γ type DNA polymerase. Further, its activity was found to be inhibited by α -ethylmaleimide suggesting that this *Plasmodium* DNA polymerase is more like eukaryotic DNA polymerase γ (Chavalitshewinkoon-Petmitr et al. 2000)

Gene with plasmoDB ID PF3D7_0625300 has been annotated as putative DNA polymerase I. In a previous study, this gene was identified as a member of the type A family DNA dependent DNA polymerase based on conserved domain analysis (Reesey 2017). This family comprises DNA polymerases that share homology to *E. coli* polymerase I and have a role in filling the DNA gaps during DNA recombination, repair, and replication. The conserved catalytic domain of *PfDNAP*, human DNA polymerase γ and *Saccharomyces cerevisiae* DNA polymerase γ fall under type A DNA polymerase. In model eukaryotes, DNA polymerase gamma (Pol γ / PolG) holds sole responsibility for both mtDNA replication and repair (Graziewicz et al. 2006; Pavlov et al. 2006). Interestingly, putative PfDNAP has shown sequence divergence from its human host mtDNA polymerase γ indicating its potential to be explored as an antimalarial target. A previous study has shown that the knockout of the PF3D7_0625300 gene resulted in a significant reduction in the mitochondrial copy number, suggesting a possible role of this gene product in *Plasmodium* mitochondrial genome replication. However, its localization to mitochondria and function in mtDNA repair remained unknown.

With this prior knowledge, we revisited the sequence of *P falciparum* DNA pol I to analyze the presence of mitochondria targeting signal sequence and conserved catalytic domains. This nuclear-encoded gene is predicted to be a mitochondrial DNA polymerase (mtDNAP) in *P. falciparum* owing to a very high score by the software predicting mitochondrial localization

PF3D7_0625300 GENE PRODUCT MITOCHONDRIAL LOCALIZATION AND INTERACTION WITH REPAIR PROTEINS.

(Mitoport-II score = 96%). This gene remained as a putative mtDNAP due to the lack of biochemical and genetic studies. Moreover, an alignment study revealed that PF3D7_0625300 shares homology with DNA polymerase I of *Babesia microti* which is reported to be involved in organelle biogenesis. Similar to the malaria parasite, *Babesia microti* is also an apicomplexan parasite that infects human RBCs. Therefore, we were curious to check the subcellular distribution of PF3D7_0625300 gene product. In this chapter, we have explored the mtDNA association of PfDNAP with the reasoning that the polymerase enzyme must bind to its DNA substrate. We also studied its interaction with the known mitochondrial repair and replication proteins.

4.2 RESULTS

4.2.1 Subcellular distribution of PF3D7_0625300 gene product:

To establish the mitochondrial localization and function of putative DNA Pol I (PfMtDNAP) primary step is to be able to track this protein within the parasite cell. For this purpose, we tagged PfMtDNAP with GFP and express it in the parasite. To this end, we have cloned the full-length PF3D7_0625300 gene into *Plasmodium* expression vector *pARL*. Expression of the GFP fusion protein is under the control of constitutive promotor of *PfCRT*. The plasmid contract was transfected into the *P. falciparum* laboratory strain (3D7). The expression of episomally GFP tagged PfMtDNAP in the transfectants was examined by the western blotting technique (Figure 4.1.A). We found a discrete protein band around 162 kDa which is the expected size of GFP tagged PfMtDNAP protein in transfectant parasite but not in 3D7 lysate, confirming successful expression of this protein. Next, we have investigated the subcellular distribution of PfMtDNAP using cellular fractionation followed by western blotting (Figure 4.1.B). We found that the

CHAPTER 4

PF3D7_0625300 GENE PRODUCT MITOCHONDRIAL LOCALIZATION AND INTERACTION WITH REPAIR PROTEINS.

protein band corresponding to PfMtDNAP in the western blot was exclusively present in the organelle but not in nuclear fraction. The abundance of PfCytC a mitochondrial marker protein has suggested the enrichment of mitochondria in the organelle fraction. While the lack of nuclear marker PfH3 and cytoplasmic marker PfGAPDH rules out any cross-contamination in the organelle fraction. Our result confirmed the organelle-specific presence of PfMtDNAPol suggesting its role in the organelle.

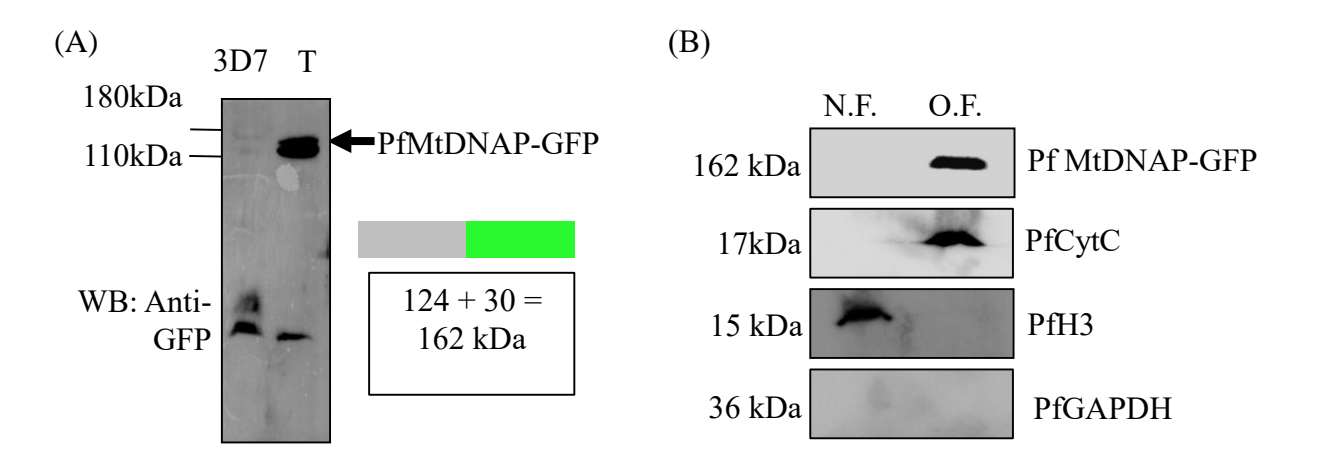
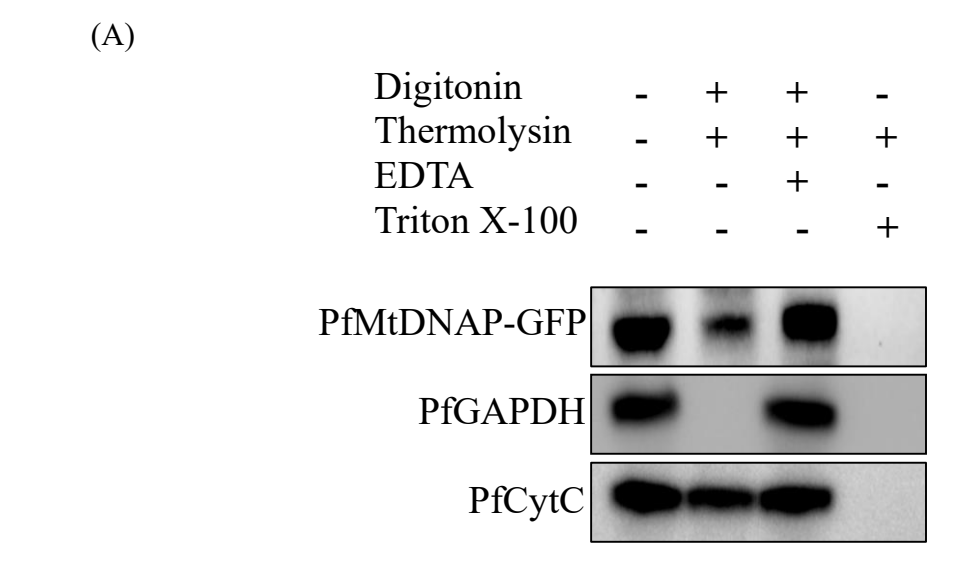


Figure 4.1. Subcellular distribution of PF3D7_0625300 gene product. (A) The western blot displays the expression of PfMtDNAPol tagged with GFP in 3D7 and transfected parasites (T). Marker is depicted on the left side. The arrow on the right side marks the protein band of interest. (B) Western blot displaying the level of PfMtDNAP protein in organelle (O. F.) and in nuclear (N. F.) fractions using specific antibodies against GFP. PfCytC and PfHistone H3 serve as mitochondrial and nuclear markers, respectively. The subcellular localization study was performed with a parasite from the trophozoites (28 hpi) stage.

4.2.2 Mitochondrial exclusive localization of PfMtDNAP in P. falciparum:

We then intended to examine the mitochondrial presence of PfMtDNAP, for which we have used a thermolysin protection assay. As explained earlier that the mitochondrial proteins are protected from the digestive action of this protease since digitonin does not permeabilize the mitochondrial membrane (Figure 4.2. A). In this assay, the synchronized trophozoite parasite was subjected to variable reaction conditions, and the effect of protease on the proteins was checked using the western blot technique. We found that the PfMtDNAP protein band was unaffected by the protease activity of thermolysin after digitonin-mediated permeabilization. As expected PfGAPDH and PfH3 which are the cytosolic and nuclear markers were completely digested (Figure 4.2. A). Hence this result suggested the mitochondrial presence of PfMtDNAP in *P. falciparum*.

We further validated the mitochondrial presence of this protein using an indirect immune fluorescence assay. As described earlier, the trophozoite and schizonts cells were used to examine the subcellular localization of PfMtDNA- GFP using anti-GFP antibody conjugated with a green fluorophore. For mitochondrial and nuclear probing we have used anti-PfCytC antibody conjugated with a red fluorophore and Hoechst dye, respectively. We found a clear overlap of green signal from GFP tagged PfMtDNAP and mitochondrial red signal, suggesting localization of PfMtDNAP into parasite mitochondrial. Moreover, PfMtDNA signal did not colocalize with the nuclear signal (Figure 4.2.B). This observation was in complete agreement with our subcellular fractionation data which also suggested the mitochondrial exclusive localization of PfMtDNAP.



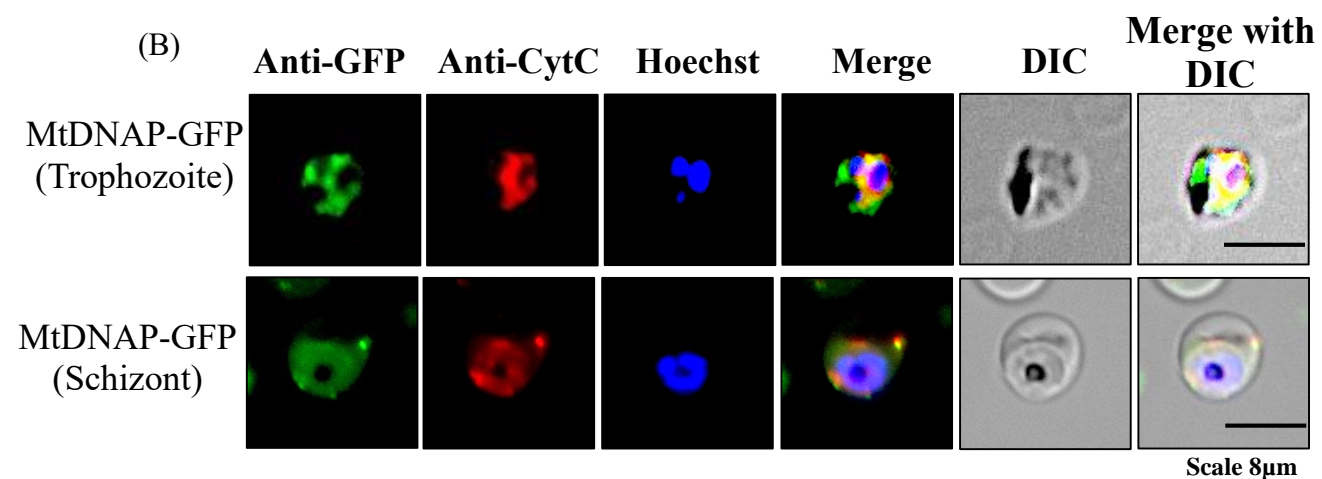


Figure 4.2. Mitochondrial exclusive localization of PfMtDNAP in *P. falciparum*. (A) The western blots show the effect of thermolysin on the PfMtDNAP, PfGAPDH (cytosolic protein), and PfH3 (nuclear protein) in the indicated reaction conditions. (B) Immunofluorescence images displaying localization PfMtDNAP-GFP, to mitochondria (Red) and/or nucleus (Blue) of *Plasmodium falciparum* parasite. Anti-CytC antibody and Hoechst dye were used to stain the parasite mitochondria and nucleus, respectively. IFA was performed with trophozoites and schizonts parasite as indicated.

4.2.3 PfMtDNAP protein interacts with *Plasmodium* mitochondrial genome:

Being a DNA-dependent DNA polymerase, PfMtDNAP must associate itself with the mitochondrial genome. Therefore, we sought to inspect the recruitment of this protein on mtDNA using anti-GFP mtDNA IP. We investigated the degree of its associates throughout the mitochondrial genome. We found PCR amplification of A-F loci in the GFP-assisted mtDNA IP samples (Figure 4.3A). While in the negative control (IgG mtDNA) we did not find such PCR amplification. Further, upon quantifying the absolute PCR product from each locus using SyBR green we found that the occupancy of PfMtDNA varies throughout the mtDNA(Figure 4.3B). Unlike PfRad51 and PfBlm, the mtDNA interaction of PfMtDNAP was found to be more predominant with the second half of the mt genome (loci E and F). Hence our results are in agreement with our hypothesis that the PfMtDNA polymerase does interact with mtDNA. Taken together, it appears that PF3D7_0625300 encodes for DNA polymerase that likely targets the parasite mitochondria. Within mitochondria, its association with mtDNA suggests that the mitochondrial genome is a possible substrate of this DNA- dependent DNA polymerase enzyme.

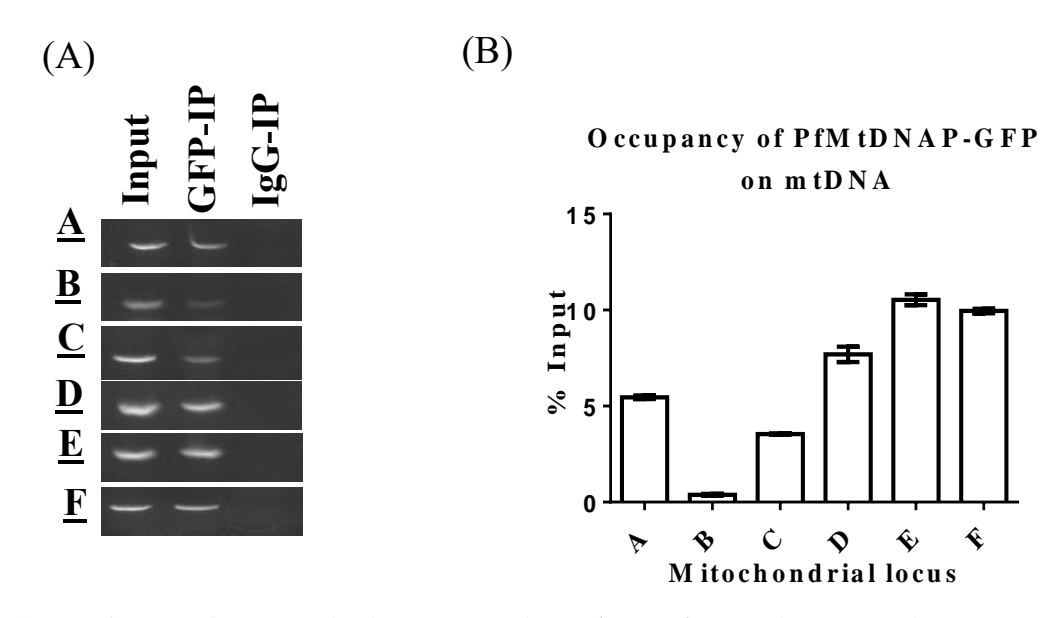


Figure 4.3.: PfMtDNAP protein interacts with *Plasmodium* mitochondrial genome. (A) Agarose gels depict the association of PfMtDNAP-GFP protein with the mitochondrial genome (A-F loci) by mtDNA-IP, using anti-GFP antibody. IP with IgG antibody served as experimental negative controls. Here, Input, GFP-IP, and IgG-IP denote; Input mtDNA, anti-GFP immuno-precipitated mt DNA and, anti-IgG immuno-precipitated mt DNA, respectively. The bar graph displays the relative occupancy of PfMtDNAP-GFP on mtDNA fragments A-F in terms of % input. Data were normalized using respective IgG-IP values.

4.2.4 Homologous recombination proteins interact with mitochondria specific DNA polymerase:

As mentioned earlier that during the third step of HR (Figure. 3.1A) the invaded strand is extended by a coordinated action of DNA polymerase, recombinase, and helicase, we sought to investigate whether PfRad51 and PfBlm are also engaged with the mitochondrial DNA polymerase. Yeast two-hybrid assay was employed for protein-protein interaction studies. PfBLM or PfRAD51 were cloned in the bait vector containing the GAL4 DNA binding domain and URA3 selectable marker. PfMtDNAP was cloned in the prey vector harbouring GAL4 activation domain and LEU2 selectable marker. The co-transformed PJ694A yeast cells were analysed on synthetic complete agar plates (without Leucine, Uracil, and, Histidine or without Leucine, Uracil and, Adenine) for the expression of reporter gene HIS3 or ADE2, where expression of HIS3 scores for both strong and weak interactions and ADE2 scores for only strong interactions. It was observed that the interaction between repair proteins and PfMtDNAP was weak in nature (Fig. 4.4.A). We further investigated the interaction between PfRad51 and PfTopoIII, as PfTopoIII was reported to be localized in *P. falciparum* mitochondria (28). A strong interaction was observed between PfRad51 and PfTopoIII (Figure 4.4.A). Earlier, both PfTopoIII and PfRad51 were found to interact with PfBlm (Bansod et al. 2020; Suthram et al. 2020). Thus, it is likely that PfMtDNAP, PfRad51, PfBlm, and PfTopoIII could be parts of a multi-protein complex (Figure 4.4.B). Our localization studies reiterate the possibility that such a complex may exist within the mitochondria.

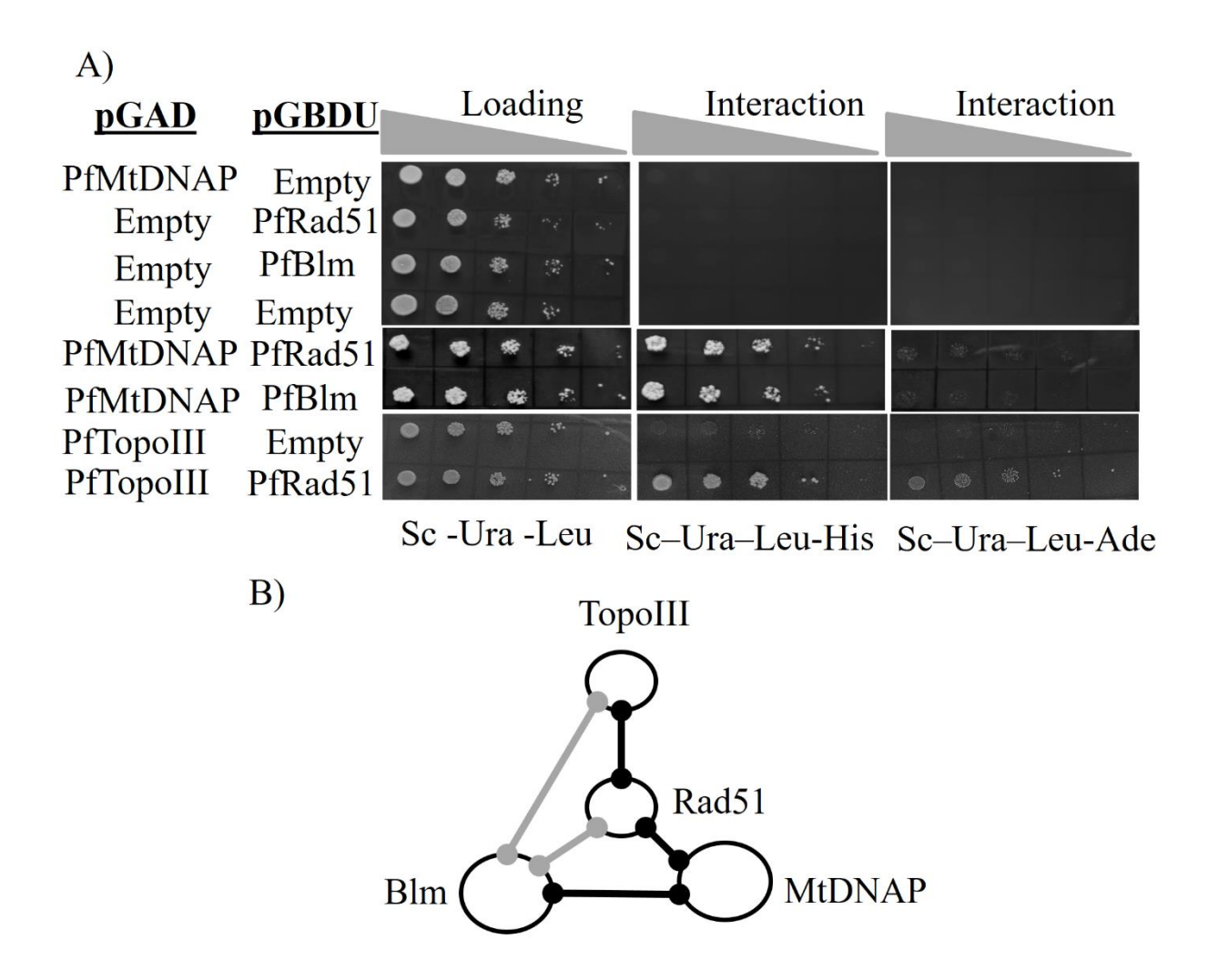


Figure 4.4: Homologous recombination proteins interact with mitochondria-specific DNA polymerase. (A) Yeast-two-hybrid analysis showing interactions between different parasite proteins. PfBlm and PfRad51 were fused with GAL4 DNA-binding domain of the bait vector pGBDU-C1. Likewise, PfMtDNAP and PfTopoIII were fused with the GAL4 activation domain (GAL4-AD) of the prey vector pGAD-C1. Interactions of the fusion proteins were examined in PJ69-4A yeast strain containing *ADE2* and *HIS3* reporter genes under the *GAL4* promoter. An equal number of transformed yeast cells and their ten-fold serial dilutions were spotted on Sc – Uracil –Leucine agar plates to establish the expression of the fusion proteins. Simultaneously,

CHAPTER 4

PF3D7_0625300 GENE PRODUCT MITOCHONDRIAL LOCALIZATION AND INTERACTION WITH REPAIR PROTEINS.

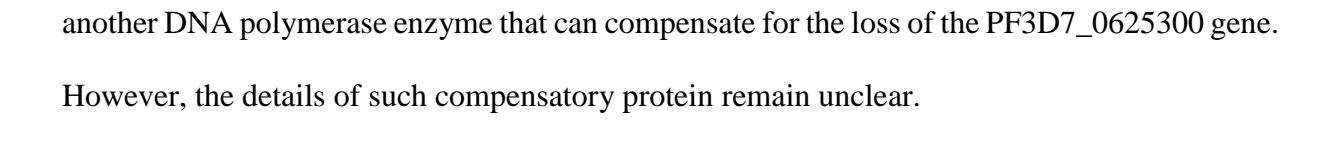
yeast cells were spotted on Sc –Uracil –Leucine –Histidine and Sc –Uracil –Leucine –Adenine triple dropout agar plates to assess the protein-protein interactions. Interaction of empty prey vector and PfBlm or PfRad51; empty bait vector and PfMtDNAP or PfTopoIII were used as experimental negative controls. (B) A pictorial representation of the putative 'recombinosome' complex involved in the repair of mtDNA. The black connecting lines represent protein-protein interactions established in this study, whereas the grey connecting lines represent previously reported protein interactions.

PF3D7_0625300 GENE PRODUCT MITOCHONDRIAL LOCALIZATION AND INTERACTION WITH REPAIR PROTEINS.

4.3 SUMMARY.

The existence of DNA polymerase activity in the *Plasmodium* mitochondria is long being documented. Based on its antibiotic sensitivity profile this *Plasmodium* protein was anticipated to be like eukaryotic DNA polymerase γ. PF3D7 0625300 gene was believed to carry the genetic information to encode mitochondrial DNA polymerase based on its sequence similarity with DNA polymerases family A proteins of other systems. This speculation was confirmed by the knockout study which has shown that knockout PF3D7 0625300 gene reduced mtDNA copy number. Our report on the mitochondrial exclusive localization of the PF3D7 0625300 gene product provided direct evidence that this gene product is the mitochondrial DNA polymerase. Hence this protein qualifies to be called *Plasmodium* mitochondrial DNA polymerase (PfMtDNAP). In the present study, we have documented the association of PfMtDNAP throughout mtDNA at varying degrees. The reason behind such biased occupancy of PfMtDNAP on mtDNA is not clear yet. Additionally, our finding indicates that mtDNA is likely a substrate for this enzyme. In general, DNA polymerases of the DNA-dependent DNA polymerase family A are shown to be involved in mitochondrial DNA repair. Such involvement of PfMtDNAP in mitochondrial genome repair was indirectly established by its ability to associate with repair proteins namely PfBlm and PfRad51. These repair proteins are known to interact with the mitochondrial replication protein that is PfTopoIII. These protein-protein interaction reports indicate the possibility of the formation of a multiprotein recombinosome complex within the *Plasmodium* mitochondria. However, the existence of such complex within the parasite system needs additional validation. As noted previously, the knockout of this could reduce the copy number by 70 % and the remaining mtDNA was found to be sufficient for parasite survival and growth. In other words, this finding suggested the possible existence of

CHAPTER 4 PF3D7_0625300 GENE PRODUCT MITOCHONDRIAL LOCALIZATION AND INTERACTION WITH REPAIR PROTEINS.



Chapter 5

<u>DISCUSSION</u>

5 DISCUSSION.

The homologous recombination (HR) pathway has not only been implicated in the repair of chromosomal DNA double-strand breaks (DBSs) of the malarial parasites but also is the predominant mechanism in this parasite. The extrachromosomal mitochondrial genome of this parasite is even more vulnerable to the DSBs, however, nothing is known about the proteins involved in the repair of the mitochondrial genome. We investigated the involvement of the nuclear-encoded HR proteins in the repair of the mitochondrial genome as this genome does not code for any DNA repair proteins.

The contribution of homologous recombination in *Plasmodium* mitochondrial genome stability has been unclear. Several lines of evidence presented in this study have demonstrated the existence of a functional DSB repair mechanism in *P falciparum* for its mitochondrial genome stability. First, we found mitochondrial localization of two major nuclear-encoded HR proteins, namely, PfRad51 and PfBlm, in addition to their nuclear presence. Second, these proteins have shown mtDNA association, and their binding to mtDNA was maximum in the metabolically active and DNA damage-prone mature stages of ASB parasites. Third, we found that the repair of UV-induced DSBs repair in both mitochondrial and nuclear genomes was severely compromised upon inhibiting the function of PfBlm and PfRad51 using small molecule inhibitors. This was further validated by the genetic study using a dominant-negative mutant of PfRad51, wherein we found that the repair of nDNA, as well as mtDNA DBSs, were completely suppressed in the parasite harboring Pfrad51^{K143R} mutant protein. Fourth, we found maximum recruitment of these proteins to mtDNA between 12-24 hours post DSB induction which was also the time duration when we observed maximum mtDNA repair. Thus, the occupancy of these two repair proteins on the damaged mtDNA coincided with the mitochondrial DNA damage repair kinetics. Fifth, our experiments established putative PfDNAPolI as the mitochondrial DNA polymerase (PfmtDNAP) in *P falciparum* by demonstrating its mitochondrial exclusive localization and mtDNA association. Finally, PfRad51 and PfBlm proteins were found to interact with the mitochondrial DNA polymerase (PfmtDNAP) and topoisomerase (PfTopoIII). A previous study has shown the mitochondrial presence of PfTopoIII and its association with mtDNA. PfTopoIII was also found to offer survival benefits to the parasite suffering from HU-induced replication blockage and DNA damage (Bansod et al. 2020).

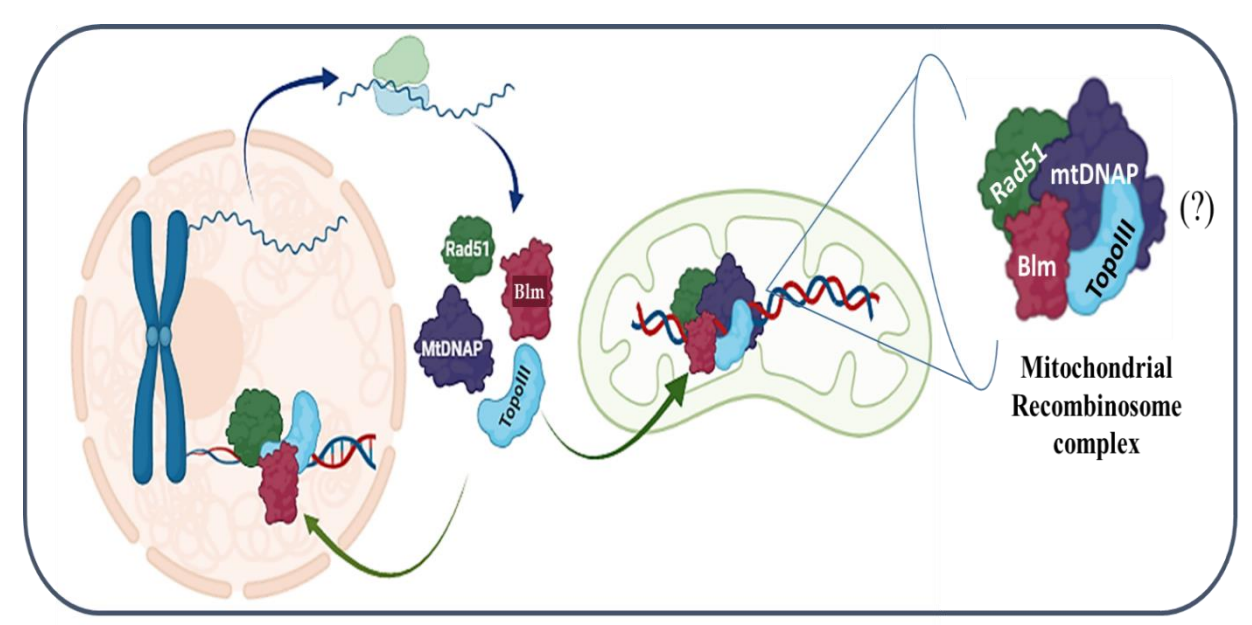


Figure 5.1: The model. A pictorial representation of the proposed model depicting transcription and cytosolic translation of repair and replication proteins within *Plasmodium*. The distribution of these protein products from the cytoplasmic pool to the nucleus and the mitochondria under favorable conditions. We speculate that within the organelle, these repair proteins along with PfMtDNA and PfTopoIII might assemble in a multi-protein complex (recombinase complex) for facilitating the repair and/or replication of *P. falciparum* mtDNA.

The mitochondrial genome (mtDNA) experiences DNA damage to a greater extent than the nuclear genome (nDNA) due to the absence of histone proteins which provide chromosomal DNA specialized chromatin packing, thus protecting it from DNA damage. Furthermore, the proximity of mtDNA to the oxidative phosphorylation site constantly exposes it to oxidative stress making it vulnerable to DNA damage. In a living human cell, the estimated rate of point mutations in the mitochondrial genome is 6 x 10⁻⁸ per base pair per year which is 100 fold higher than the nuclear somatic point mutation rate (Marcelino and Thilly 1999). Initially, it was believed that DNA repair machinery to preserve the mitochondrial genome was either nonexistent or highly inefficient. The most prevailing theory concerning mitochondrial genome stability was that the mtDNA molecule with excessive mutations would be degraded and subsequently replaced with a newly generated undamaged copy of the genome. Such notions were conceived based on a preliminary study showing that UV-induced pyrimidine dimers were not repaired in the mitochondrial genome (Clayton et al. 1974). However, subsequent studies confirmed that various kinds of mtDNA abrasions are efficiently repaired in the mitochondria. The existence of several key enzymes involved in the BER pathway of DNA repair in the mitochondria of model organisms established BER as the predominant repair pathway for safeguarding mtDNA. However, in addition to BER, Rad51 and its paralogs which are the active components of HR were also found to be functional in the mitochondria of yeast and human cells. MMEJ is considered to play a central role in the maintenance of mammalian mitochondrial genome integrity (Tadi et al. 2016).

So far, in *P. falciparum*, two AP-endonucleases, namely, PfApn and PfApe1 have shown mitochondrial localization (Srivastava et al. 2021; Tiwari et al. 2020; Verma et al. 2021), indicating the presence of the BER pathway in the parasite mitochondria. Despite the discovery of A-NHEJ in *Plasmodium*, the role of MMEJ in the mitochondrial DSB repair is unknown.

Nevertheless, we find that the lack of a functional HR mechanism completely suppresses the DSB repair in mtDNA. Hence, not only does the study establish that the HR pathway is functional in the parasite mitochondria, but it also suggests that it is likely to be the preferred DSB repair mechanism and cannot be substituted by other DSB repair mechanisms. In humans, Rad51 and its paralogue XRCC3 are involved in mtDNA replication (Mishra et al. 2018). PfRad51 and PfBlm have been found to be associated with mtDNA to a higher extent at schizont stages of the parasite, which may indicate their possible role in mtDNA replication since the replication of mtDNA takes place during this stage of parasite development. However, the enrichment of repair proteins observed at mtDNA during schizont could also be the result of a higher rate of DSB formation due to replication errors during this stage. It has long been speculated that the atypical *Plasmodium* mtDNA replication involves recombination intermediates but further studies are required to establish this fact (Preiser et al. 1996).

Although *P falciparum* has functional BER and HR mechanisms in its mitochondria to look after its genome stability, however, it is still highly prone to mutational alterations. For the nuclear genome, HR serves as the most faithful DSB repair mechanism to safeguard the genome. To date, it is unclear why mtDNA has a greater tendency to accumulate mutations as compared to nuclear DNA. A possible reason could be the lack of other efficient repair machinery such as mismatch repair (MMR) in *Plasmodium* mitochondria, but further investigations are required to support this possibility. However, our findings show that the repair proteins PfRad51 and PfBlm interact with the mitochondrial DNA polymerase PfmtDNAP presenting an alternative explanation for such a phenomenon. Another reason for the vulnerability of mtDNA to mutations could be that the PfmtDNAP enzyme may be lacking proof-reading activity resulting in the wrong nucleotide insertion during genome replication and repair to a higher extent than

usual. The detailed biochemical characterization of this enzyme might shed light on many aspects of mitochondrial genome stability.

In human cells, mitochondria-specific DNA helicase known as Twinkle plays a central role by promoting the binding of Rad51 and its paralogues to the damaged mtDNA (Mishra et al. 2018). Another DNA helicase of the RecQ family, namely, RecQ4 has been implicated in mammalian mtDNA maintenance (Croteau et al. 2012; Ding and Liu 2015). The PfTwinkle helicase has also been identified and it was found to be located exclusively in the apicoplast organelle, but not in the parasite mitochondria (Seow et al. 2005). In our study, we found that in *P. falciparum*, the RecQ helicase PfBlm is involved in the maintenance of the mtDNA. However, whether additional helicases are involved in this process remains elusive at this point.

All the proteins investigated in this study except PfmtDNAP are devoid of conserved mitochondrial targeting signal sequence. Nonetheless, mitochondrial localization of PfRad51, PfBlm, and PfTopoIII has been established. Further studies are required to identify the mode of mitochondrial import of such proteins. A similar event of mitochondrial translocation of proteins lacking a mitochondrial targeting sequence has been reported in other systems, though the mechanism of transport is not clear. Moreover, the nuclear import of proteins like Rad51 which lacks nuclear localization signal (NLS) sequence is likely to be dependent on other carrier proteins namely BRCA1 and BRCA2, which contain a functional NLS sequence. In the current state of knowledge, it is unclear whether mitochondrial membranes possess multiple import machinery or not for aiding the translocation of proteins carrying or lacking mitochondrial localization signals. The mitochondrial transport of proteins without mitochondria targeting sequence may be aided by the carrier proteins with the appropriate signal sequence as is seen during the nuclear import of proteins lacking the NLS (Jeyasekharan et al. 2013). Our study revealed that stress factors such as DNA damage lead to the mitochondrial translocation of

proteins with varying molecular sizes (PfRad51, 38 kDa and PfBlm, 80 kDa). This finding could serve as a starting point for future investigations to uncover parasite mitochondrial import mechanisms.

In human cells, stress-induced phosphorylation of Rad51 at tyrosine 315 (Y315) residue promotes its nuclear localization, and mutation at this position results in increased cytosolic retention of Rad51. However, in our study, we found unaltered nuclear or mitochondrial localization of double mutant of Pfrad51 at 144 and 319 serine residues which were bioinformatically predicted to undergo phosphorylation. A possible explanation for this could be that the phosphorylation of these residues does not play a role in Rad51 subcellular localization and rather regulates other activities of this recombinase protein. Moreover, it is unclear whether or not this parasite protein undergoes phosphorylation, and even if such a modification happens, which functional aspect/s of this protein is under the control of this phosphorylation event is currently not known.

Although *Plasmodium* mitochondrion is not the powerhouse of the cell, nonetheless it is an essential organelle. Its ETC is an indispensable process, primarily for the pyrimidine biosynthesis pathway, and probably for other metabolic pathways as well (Painter et al. 2007). Thus, the ETC as a whole and more specifically the mtDNA encoded PfCytB emerged as a lucrative drug target. While increased resistance to Atovaquone somehow dampened the prospect of PfCytB as a drug target, the low frequency of resistance to ELQ-300 is encouraging (Stickles et al. 2016). Thus there is a renewed interest in targeting *Plasmodium* mitochondria. Hence, it is not unreasonable to propose that targeting the DSB repair mechanism of the *Plasmodium* mitochondria is likely to have deleterious consequences for the maintenance of the mitochondrial genome of this parasite, which may eventually impact the mitochondrial biology and the survival of the parasites. Since only the maternal mitochondrion is present in the zygote

that cannot be complemented by the paternal copy, we speculate that any aberration of the mtDNA due to the inhibition of the DSB repair pathway is likely to have a profound effect on the parasites during the mosquito stages, including the transmission biology. Such a hypothesis needs to be tested in the future.

In conclusion, the present study has documented the possibility of repairing DSBs in *Plasmodium* mtDNA which was initially believed to undergo degradation and be replaced by undamaged mtDNA (Clayton et al. 1974). Their increased occupancy on mtDNA at the later ABSs indicates the role of HR during these metabolically active and DNA-prone stages of development. This study established the direct and more importantly predominant role of homology-directed repair in *P. falciparum* mitochondrial DSB repair. Moreover, genotoxic stress has stimulated translocation of HR components to both nucleus and mitochondria that indicates their essential function in mitochondria similar to their nuclear role. Their association with PfMtDNA polymerase directs the possibility of the formation of a multi-protein complex that aids in mtDNA repair and/or replication. Overall, our study has suggested that the inhibition of the *Plasmodium* HR pathway will render the indispensable mitochondrial genome more vulnerable to genotoxic stress and would offer a novel strategy for curbing malaria.



- Aamann, M. D., et al. (2010), 'Cockayne syndrome group B protein promotes mitochondrial DNA stability by supporting the DNA repair association with the mitochondrial membrane', *Faseb j*, 24 (7), 2334-46.
- Ahmad, M., et al. (2012), 'Plasmodium falciparum UvrD helicase translocates in 3' to 5' direction, colocalizes with MLH and modulates its activity through physical interaction', *PLoS One*, 7 (11), e49385.
- Badugu, S. B., et al. (2015), 'Identification of Plasmodium falciparum DNA Repair Protein Mre11 with an Evolutionarily Conserved Nuclease Function', *PLoS One*, 10 (5), e0125358.
- Barr, C. M., Neiman, M., and Taylor, D. R. (2005), 'Inheritance and recombination of mitochondrial genomes in plants, fungi and animals', *New Phytol*, 168 (1), 39-50.
- Bansod, S., et al. (2020), 'Elucidation of an essential function of the unique charged domain of Plasmodium topoisomerase III', *Biochem J*.
- Baruch, D. I., et al. (1995), 'Cloning the P. falciparum gene encoding PfEMP1, a malarial variant antigen and adherence receptor on the surface of parasitized human erythrocytes', *Cell*, 82 (1), 77-87.
- Bhattacharyya, M. K. and Kumar, N. (2003), 'Identification and molecular characterisation of DNA damaging agent induced expression of Plasmodium falciparum recombination protein PfRad51', *Int J Parasitol*, 33 (12), 1385-92.
- Bhattacharyya, M. K., et al. (2005), 'Characterization of kinetics of DNA strand-exchange and ATP hydrolysis activities of recombinant PfRad51, a Plasmodium falciparum recombinase', *Mol Biochem Parasitol*, 139 (1), 33-9.
- Bozdech, Z., Mok, S., and Gupta, A. P. (2013), 'DNA microarray-based genome-wide analyses of Plasmodium parasites', *Methods Mol Biol*, 923, 189-211.

- Brunyanszki, A., et al. (2016), 'Mitochondrial poly(ADP-ribose) polymerase: The Wizard of Oz at work', *Free Radic Biol Med*, 100, 257-70.
- Buguliskis, J. S., et al. (2007), 'Expression and biochemical characterization of Plasmodium falciparum DNA ligase I', *Mol Biochem Parasitol*, 155 (2), 128-37.
- Casta, L. J., et al. (2008), 'Expression and biochemical characterization of the Plasmodium falciparum DNA repair enzyme, flap endonuclease-1 (PfFEN-1)', *Mol Biochem Parasitol*, 157 (1), 1-12.
- Chalapareddy, S., et al. (2014), 'Radicicol confers mid-schizont arrest by inhibiting mitochondrial replication in Plasmodium falciparum', *Antimicrob Agents Chemother*, 58 (8), 4341-52.
- Chan, J. A., Fowkes, F. J., and Beeson, J. G. (2014), 'Surface antigens of Plasmodium falciparum-infected erythrocytes as immune targets and malaria vaccine candidates', *Cell Mol Life Sci*, 71 (19), 3633-57.
- Chavalitshewinkoon-Petmitr, P., et al. (2000), 'Partial purification and characterization of mitochondrial DNA polymerase from Plasmodium falciparum', *Parasitol Int*, 49 (4), 279-88.
- Claessens, A., et al. (2018), 'RecQ helicases in the malaria parasite Plasmodium falciparum affect genome stability, gene expression patterns and DNA replication dynamics', *PLoS Genet*, 14 (7), e1007490.
- Clayton, D. A., Doda, J. N., and Friedberg, E. C. (1974), 'The absence of a pyrimidine dimer repair mechanism in mammalian mitochondria', *Proc Natl Acad Sci U S A*, 71 (7), 2777-81.
- Croteau, D. L., et al. (2012), 'RECQL4 localizes to mitochondria and preserves mitochondrial DNA integrity', *Aging Cell*, 11 (3), 456-66.

- Deshmukh, A. S., et al. (2012), 'The role of N-terminus of Plasmodium falciparum ORC1 in telomeric localization and var gene silencing', *Nucleic Acids Res*, 40 (12), 5313-31.
- Ding, L. and Liu, Y. (2015), 'Borrowing nuclear DNA helicases to protect mitochondrial DNA', Int J Mol Sci, 16 (5), 10870-87.
- Dmitrieva, N. I., Malide, D., and Burg, M. B. (2011), 'Mre11 is expressed in mammalian mitochondria where it binds to mitochondrial DNA', *Am J Physiol Regul Integr Comp Physiol*, 301 (3), R632-40.
- Dondorp, A. M., et al. (2009), 'Artemisinin resistance in Plasmodium falciparum malaria', *N Engl J Med*, 361 (5), 455-67.
- Frankenberg-Schwager, M. and Frankenberg, D. (1990), 'DNA double-strand breaks: their repair and relationship to cell killing in yeast', *Int J Radiat Biol*, 58 (4), 569-75.
- Gardner, M. J., et al. (2002), 'Genome sequence of the human malaria parasite Plasmodium falciparum', *Nature*, 419 (6906), 498-511.
- Graziewicz, M. A., Longley, M. J., and Copeland, W. C. (2006), 'DNA polymerase gamma in mitochondrial DNA replication and repair', *Chem Rev*, 106 (2), 383-405.
- Gopalakrishnan, A. M. and Kumar, N. (2013), 'Opposing roles for two molecular forms of replication protein A in Rad51-Rad54-mediated DNA recombination in Plasmodium falciparum', *mBio*, 4 (3), e00252-13.
- Hikosaka, K., et al. (2011), 'Highly conserved gene arrangement of the mitochondrial genomes of 23 Plasmodium species', *Parasitol Int*, 60 (2), 175-80.
- Kamenisch, Y., et al. (2010), 'Proteins of nucleotide and base excision repair pathways interact in mitochondria to protect from loss of subcutaneous fat, a hallmark of aging', *J Exp Med*, 207 (2), 379-90.

- Jeyasekharan, A. D., et al. (2013), 'A cancer-associated BRCA2 mutation reveals masked nuclear export signals controlling localization', *Nat Struct Mol Biol*, 20 (10), 1191-8.
- Kehr, S., et al. (2010), 'Compartmentation of redox metabolism in malaria parasites', *PLoS Pathog*, 6 (12), e1001242.
- Kirkman, L. A., Lawrence, E. A., and Deitsch, K. W. (2014), 'Malaria parasites utilize both homologous recombination and alternative end joining pathways to maintain genome integrity', *Nucleic Acids Res*, 42 (1), 370-9.
- Krungkrai, J. (2004), 'The multiple roles of the mitochondrion of the malarial parasite', *Parasitology*, 129 (Pt 5), 511-24.
- Ledesma, A., de Lacoba, M. G., and Rial, E. (2002), 'The mitochondrial uncoupling proteins', *Genome Biol*, 3 (12), Reviews3015.
- Liu, J., et al. (2015), 'XPD localizes in mitochondria and protects the mitochondrial genome from oxidative DNA damage', *Nucleic Acids Res*, 43 (11), 5476-88.
- Marcelino, L. A. and Thilly, W. G. (1999), 'Mitochondrial mutagenesis in human cells and tissues', *Mutat Res*, 434 (3), 177-203.
- Mishra, A., et al. (2018), 'RAD51C/XRCC3 Facilitates Mitochondrial DNA Replication and Maintains Integrity of the Mitochondrial Genome', *Mol Cell Biol*, 38 (3).
- Milena Popova, Sébastien Henry and Fabrice Fleury (2011), 'Posttranslational Modifications of Rad51 Protein and Its Direct Partners: Role and Effect on Homologous Recombination

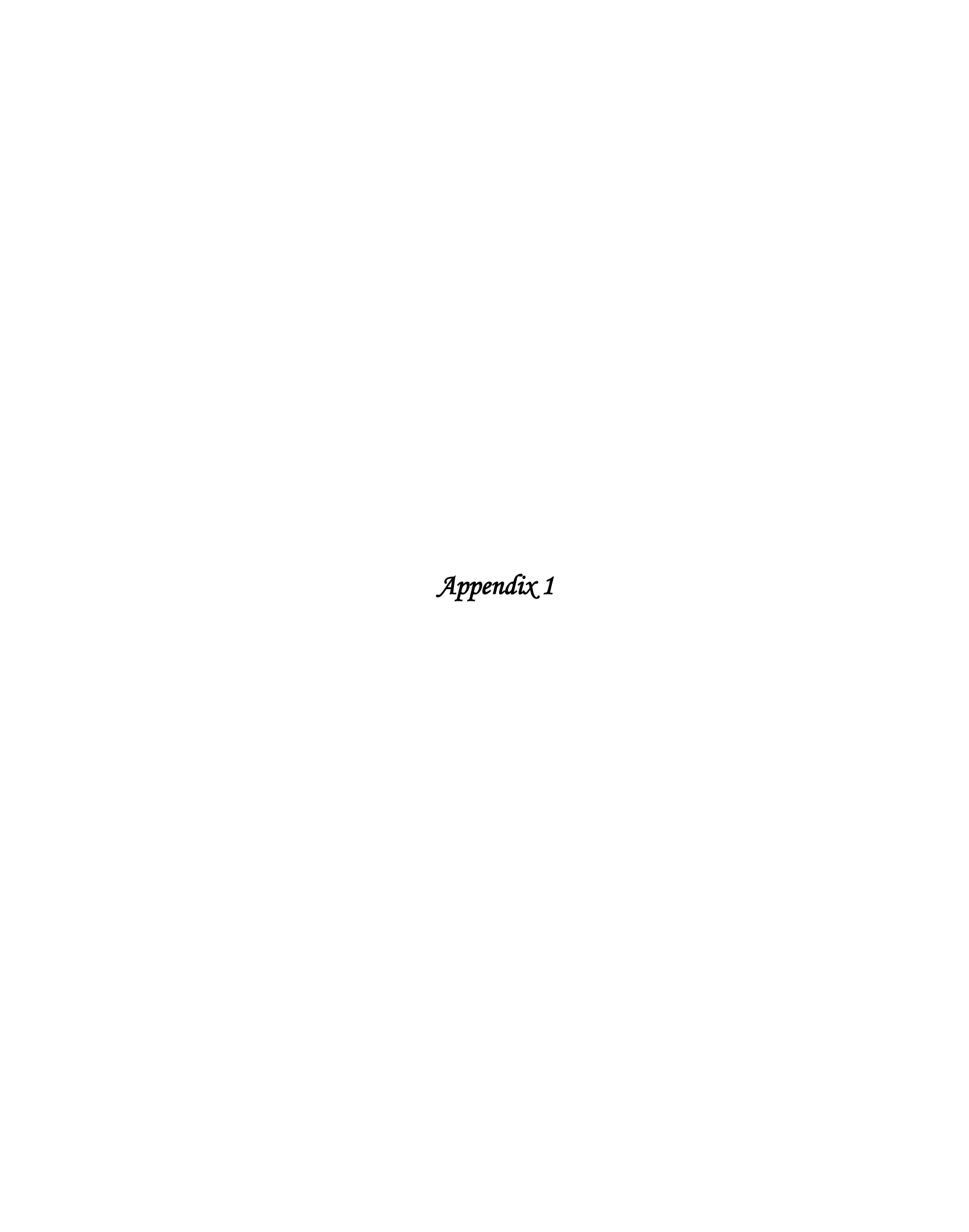
 Mediated DNA Repair', *IntechOpen*.
- Okamoto, N., et al. (2009), 'Apicoplast and mitochondrion in gametocytogenesis of Plasmodium falciparum', *Eukaryot Cell*, 8 (1), 128-32.
- Painter, H. J., et al. (2007), 'Specific role of mitochondrial electron transport in blood-stage Plasmodium falciparum', *Nature*, 446 (7131), 88-91.

- Pavlov, Y. I., Shcherbakova, P. V., and Rogozin, I. B. (2006), 'Roles of DNA polymerases in replication, repair, and recombination in eukaryotes', *Int Rev Cytol*, 255, 41-132.
- Payne, D. (1987), 'Spread of chloroquine resistance in Plasmodium falciparum', *Parasitol Today*, 3 (8), 241-6.
- Preiser, P. R., et al. (1996), 'Recombination associated with replication of malarial mitochondrial DNA', *Embo j.* 15 (3), 684-93.
- Reesey, Emily C. (2017), 'Characterization of the Mitochondrial DNA Polymerase in Plasmodium falciparum', Master of Science Dissertation (Drexel University College of Medicine).
- Roy, N., et al. (2014), 'Dominant negative mutant of Plasmodium Rad51 causes reduced parasite burden in host by abrogating DNA double-strand break repair', *Mol Microbiol*, 94 (2), 353-66.
- Sage, J. M. and Knight, K. L. (2013), 'Human Rad51 promotes mitochondrial DNA synthesis under conditions of increased replication stress', *Mitochondrion*, 13 (4), 350-6.
- Sage, J. M., Gildemeister, O. S., and Knight, K. L. (2010), 'Discovery of a novel function for human Rad51: maintenance of the mitochondrial genome', *J Biol Chem*, 285 (25), 18984-90.
- Seow, F., et al. (2005), 'The plastidic DNA replication enzyme complex of Plasmodium falciparum', *Mol Biochem Parasitol*, 141 (2), 145-53.
- Scherf, A., et al. (1998), 'Antigenic variation in malaria: in situ switching, relaxed and mutually exclusive transcription of var genes during intra-erythrocytic development in Plasmodium falciparum', *Embo j*, 17 (18), 5418-26.
- Shedge, V., et al. (2007), 'Plant mitochondrial recombination surveillance requires unusual RecA and MutS homologs', *Plant Cell*, 19 (4), 1251-64.

- Slupianek, A., et al. (2011), 'Targeting RAD51 phosphotyrosine-315 to prevent unfaithful recombination repair in BCR-ABL1 leukemia', *Blood*, 118 (4), 1062-8.
- Smith, J. D., et al. (1995), 'Switches in expression of Plasmodium falciparum var genes correlate with changes in antigenic and cytoadherent phenotypes of infected erythrocytes', *Cell*, 82 (1), 101-10.
- Srivastava, P. N., Narwal, S. K., and Mishra, S. (2021), 'Mitochondrial apurinic/apyrimidinic endonuclease Apn1 is not critical for the completion of the Plasmodium berghei life cycle', *DNA Repair (Amst)*, 101, 103078.
- Stickles, A. M., et al. (2016), 'Atovaquone and ELQ-300 Combination Therapy as a Novel Dual-Site Cytochrome bc1 Inhibition Strategy for Malaria', *Antimicrob Agents Chemother*, 60 (8), 4853-9.
- Suthram, N., et al. (2020), 'Elucidation of DNA Repair Function of PfBlm and Potentiation of Artemisinin Action by a Small-Molecule Inhibitor of RecQ Helicase', *mSphere*, 5 (6).
- Tadi, S. K., et al. (2016), 'Microhomology-mediated end joining is the principal mediator of double-strand break repair during mitochondrial DNA lesions', *Mol Biol Cell*, 27 (2), 223-35.
- Tarique, M., et al. (2012), 'Plasmodium falciparum MLH is schizont stage specific endonuclease', *Mol Biochem Parasitol*, 181 (2), 153-61.
- Tiwari, A., et al. (2020), 'Plasmodium falciparum Apn1 homolog is a mitochondrial base excision repair protein with restricted enzymatic functions', *Febs j*, 287 (3), 589-606.
- Uyemura, S. A., et al. (2004), 'Oxidative phosphorylation and rotenone-insensitive malate- and NADH-quinone oxidoreductases in Plasmodium yoelii yoelii mitochondria in situ', J *Biol Chem*, 279 (1), 385-93.

- Vaidya, A. B. and Mather, M. W. (2005), 'A post-genomic view of the mitochondrion in malaria parasites', *Curr Top Microbiol Immunol*, 295, 233-50.
- Verma, N., et al. (2021), 'Plasmodium Ape1 is a multifunctional enzyme in mitochondrial base excision repair and is required for efficient transition from liver to blood stage infection', *DNA Repair (Amst)*, 101, 103098.
- Vydyam, P., et al. (2019), 'A small-molecule inhibitor of the DNA recombinase Rad51 from Plasmodium falciparum synergizes with the antimalarial drugs artemisinin and chloroquine', *J Biol Chem*, 294 (20), 8171-83.
- WHO 'Malaria', < https://www.who.int/news-room/fact-sheets/detail/malaria>, accessed 15

 April 2021.



A1.1 Stage-specific expression level of endogenous PfBlm and PfRad51 proteins:

Tightly synchronized *P. falciparum* culture with high parasitemia was used to prepare the whole-cell extract. Followed by the western blotting technique to assess the levels of PfRad51 and PfBlm at indicated ASBs. PfActin served as the loading control. Consistent with previous findings we found that the expression of PfBlm was seen predominantly in the schizonts stages of parasite culture while low expression was observed in rings and trophozoites (Suthram et al. 2020). The expression of PfRad51 was observed primarily observed in the mid- and late-schizont staged parasite culture extracts whereas in ring and trophozoite their levels were non-detectable (Figure A1).

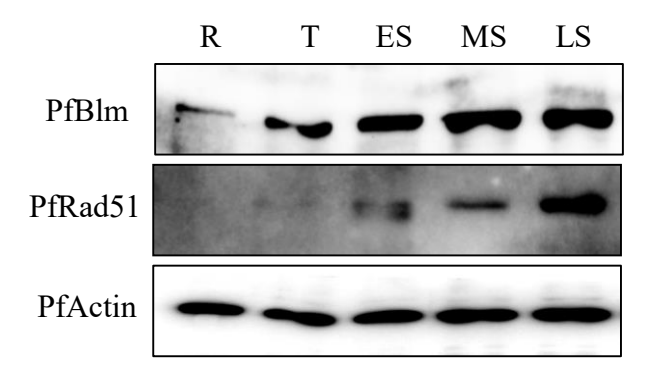


Figure A1: Stage-specific expression level of endogenous PfBlm and PfRad51 proteins:

Western blot representing stage-specific expression level of PfBlm and PfRad51 proteins. Pf Actin was used as a loading control. Synchronized ring (R), trophozoite (T), early-schizont (ES), mid schizont (MS), and late schizont (LS) parasites were used for protein extraction.

A1.2 Cloning of *PfRAD51* gene into *Plasmodium* expression vector pARL [pARL*PfRAD51*]:

ORF of *PfRAD51* gene without the stop codon was cloned into *P falciparum* episomal plasmid pARL containing ampicillin and WR99210/ pyrimethamine resistance marker (Deshmukh et al 2012). The ORF was amplified using OMKB598 and OMKB621. *KpnI* was incorporated in the forward primer and *AvrII* was incorporated in the reverse primer. The cloned gene expression was under the control of Pf*CRT* promoter. The cloning was confirmed by double digestion with *KpnI* and *AvrII* and the release of *PfRAD51* was analyzed on agarose gel (Figure. A2).

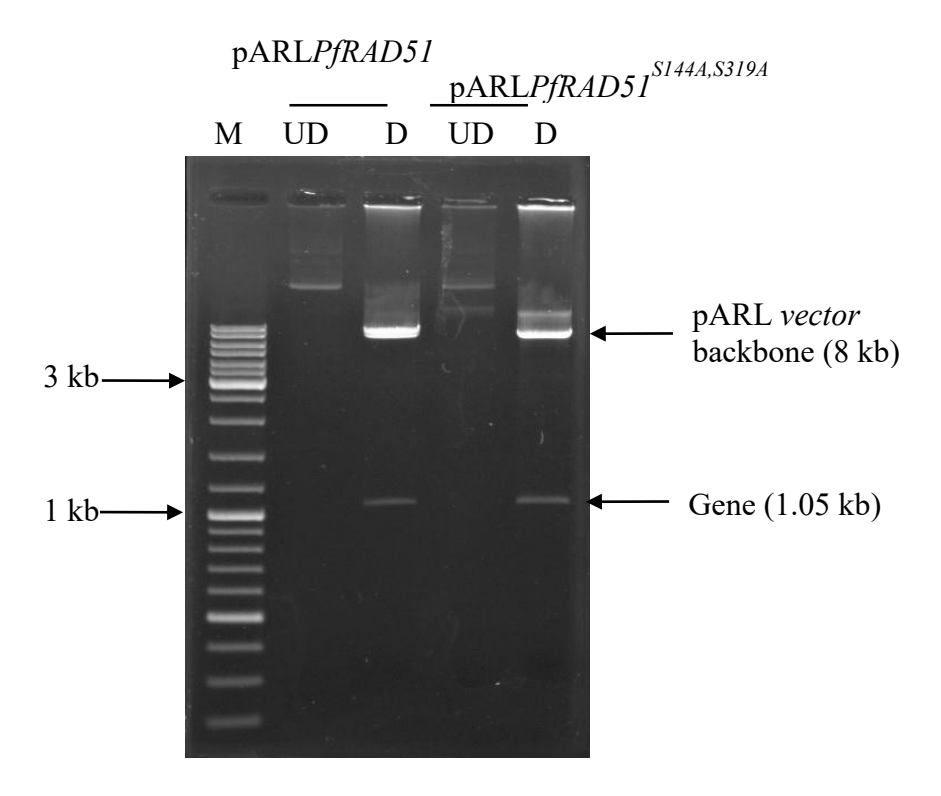


Figure A2: Cloning of *PfRAD51* gene into *Plasmodium* expression vector pARL [pARL*PfRAD51*]: Agarose gel represents the *KnpI* and *AvrII* double digestion of pARL*PfRAD51* and pARL*PfRAD51*^{S144A, S319A} plasmid. Here, M, UD, and D stand for DNA

marker, undigested control plasmid, and digested test. Arrow marks show the digestion product in the form of vector backbone and released gene along with their respective sizes in kb.

A1.3 Ectopic expression of the dominant-negative mutant of PfRad51^{K143R}: Splice overlap technique was used to create this point mutation in the *PfRAD51* gene product followed by cloning into *Plasmodium* expression vector PfCENv3 (generated by Vydyam P.). The overexpression of mutant p-PfRad51 in the transgenic parasite line was monitored using western blotting (Figure A3). The parasite cultures with high parasitemia, majorly schizonts were used to prepare whole-cell protein (WCP). The level of PfRad51 protein was analyzed in transgenic strain and compared to the laboratory strain 3D7 level of this protein. Endogenously expressing another nuclear-encoded repair protein that is PfBlm along with PfActin were used as the loading controls. We found a higher level of PfRad51 protein in the transgenic than 3D7 WCP (Figure A3). The intrinsic, as well as episomal PfRad51, had the same protein size (38 kDa), Thus elevated levels of PfRad51 protein in transgenic indicates expression of the mutant form of this protein.

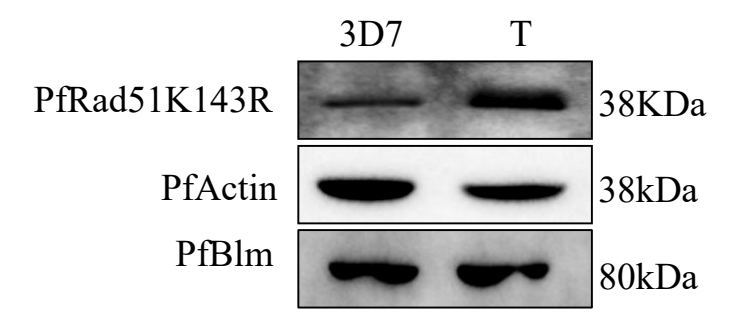


Figure A3: Ectopic expression of a dominant-negative mutant of PfRad51^{K143R}: The western blot representing over-expression of $PfRad51^{K143R}$ mutant allele from an episomal plasmid PfCENv3 in the transfected parasite strain. PfActin and PfBlm were used as a loading

control. Schizont staged 3D7 and transfected (T) parasites were used to extract whole-cell proteins. The right panel displays the size of the protein WRT protein ladder.

A1.4 Cloning of *PfRAD51* gene harboring mutation/s into bacterial expression vector:

The splice overlap technique was used to create the point mutation/s at Ser144 and/or Ser319 to Ala residue in the *PfRAD51* gene product followed by cloning into bacterial expression vector pET28a/ pGEX-6p-2. The wild-type *PfRAD51* gene was already cloned in pET101D by Bhattacharyya MK (Bhattacharyya et al. 2005). For the amplification of the PfRAD51 gene ORF, OMKB19 and OMKB17 primers were used. *BamHI* was incorporated in the forward primer and *SalI* was incorporated in the reverse primer. The cloning was confirmed by double digestion with *BamHI* and *SalI* and the release of *PfRAD51* was analyzed on agarose gel (Figure A4).

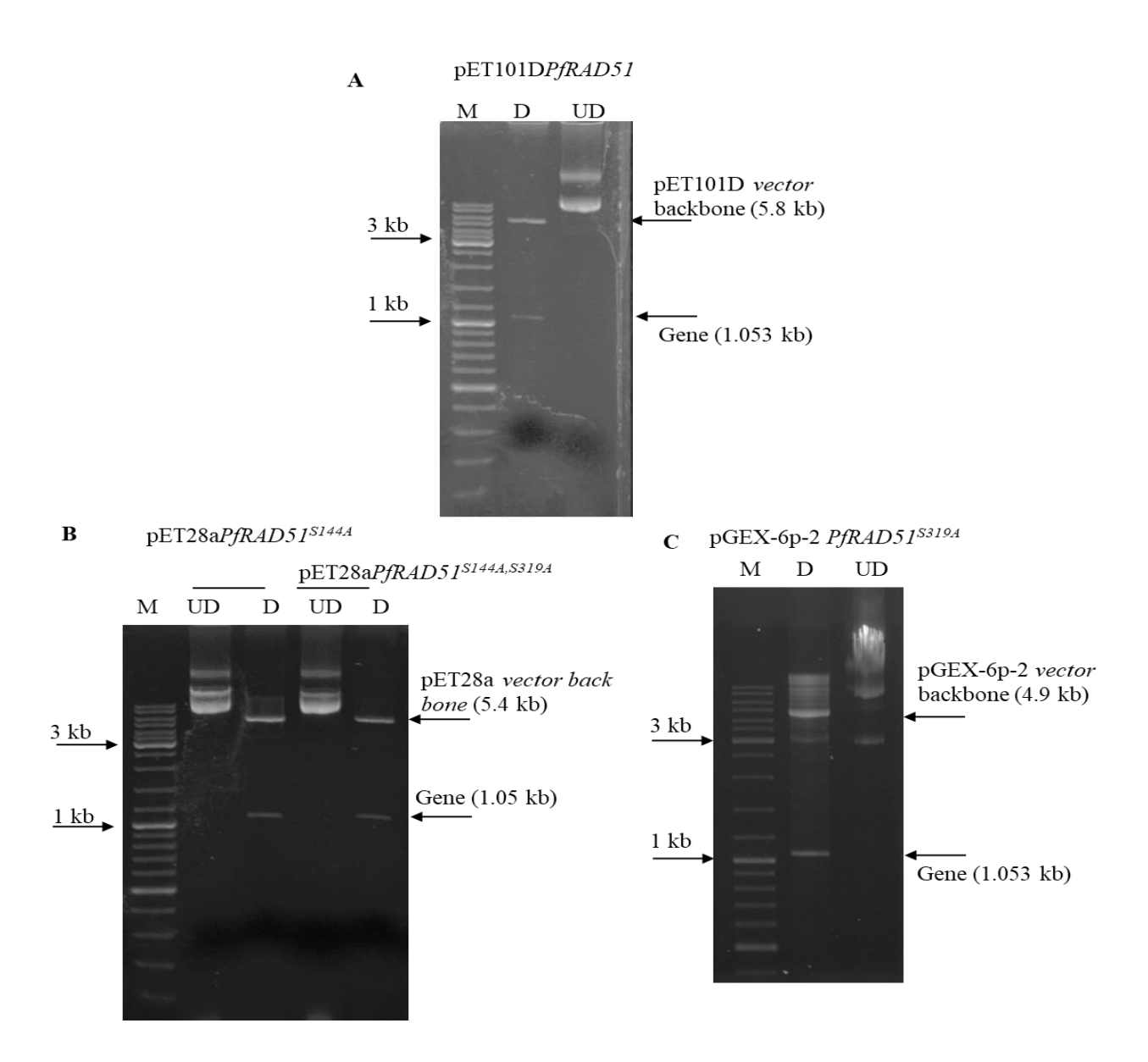


Figure A4: Cloning of *PfRAD51* gene harboring mutation/s into bacterial expression vector: Agarose gels represent the *BamHI* and *SalI* double digestion. (A) Agarose gel represents the clone confirmation by double digestion of pET101D*PfRAD51* (Wild type), (B) gel displays the clone confirmation of pET28a*PfRAD51*^{S144A} and pET28a*PfRAD51*^{S144A}, S319A, and (C) gel displays the clone confirmation of pGEX-6p-2*PfRAD5* S319A. Here, M, UD, and D stand for DNA marker, undigested control plasmid, and digested test, respectively. Arrow marks show the 120 | Page

digestion products in the form of vector backbone and released gene along with their respective sizes in kb.

A1. 5 Expression of recombinant PfRad51 and its mutants:

Confirmed plasmid constructs containing wild-type or mutant forms of PfRAD51 genes were transformed into Rosetta bacterial strain except for pGEX-6p-2PfRAD51S319 its expression was seen only in BL21 bacterial strain. The expression level of recombinant proteins was checked on SDS-PAGE followed by the coomassie staining and destaining method. We found that all recombinant proteins were showing maximum expression at 37°C with 4 hours of incubation (Figure A5).

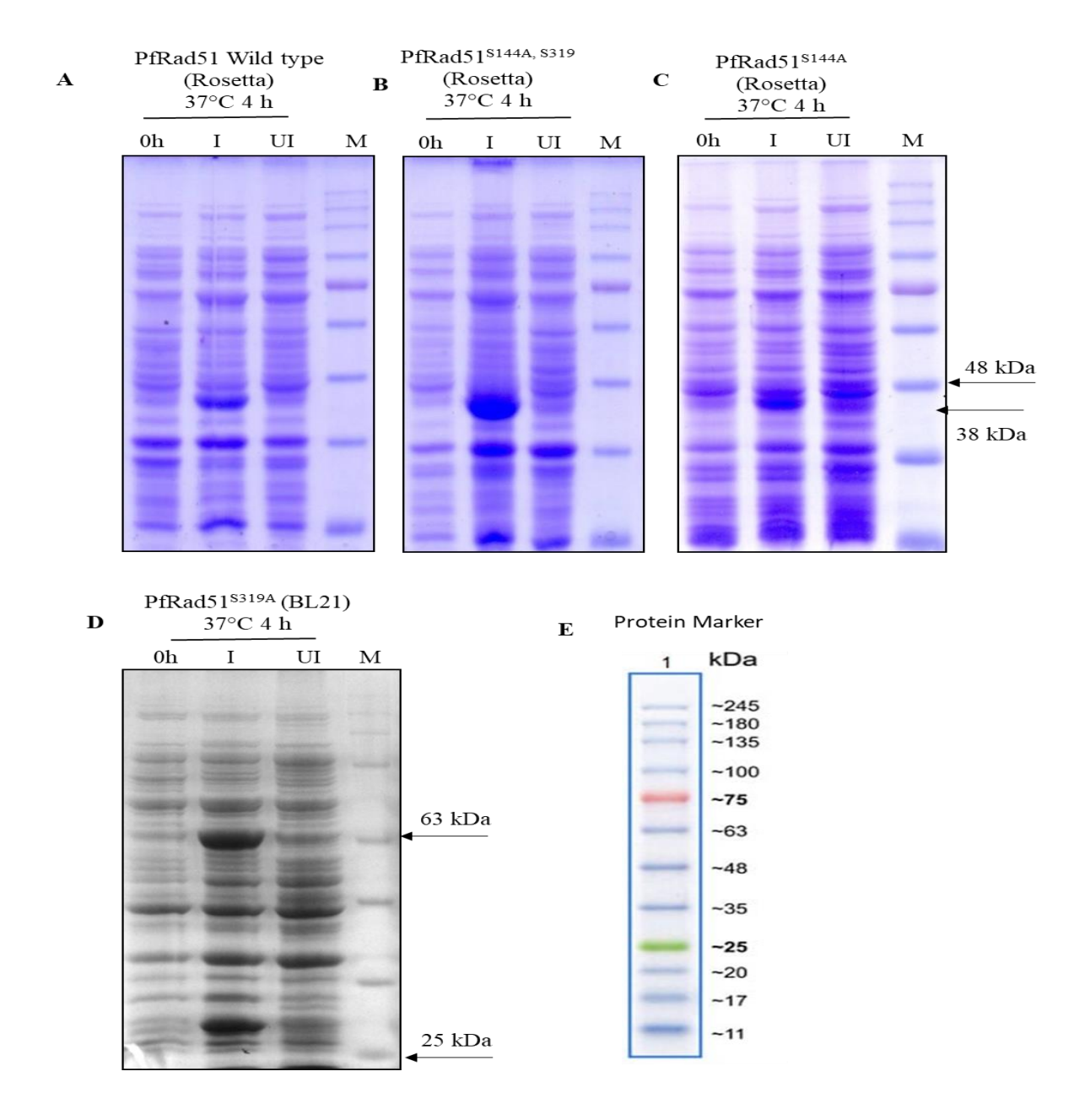


Figure A5: Expression of recombinant PfRad51 and its mutants: SDS-PAGE represents the proteins in the bacterial lysate in the 0-hour post IPTG induction (0h), 0.1 mM IPTG induction at 37 °C for 4 hours (I) and without IPTC induction at 37 °C for 4 hours (UI) samples. (A) SDS-

PAGE shows the induction of wild-type PfRad51 in the Rosetta strain from the pET101D plasmid. (B) SDS-PAGE shows the induction of double mutant of PfRad51 (PfRad51^{S144A, S319A}) protein in the Rosetta strain from the pET28a plasmid. (C) SDS-PAGE shows the induction of single mutant of PfRad51 protein (PfRad51^{S144A}) in the Rosetta strain from the pET28a plasmid. (D) SDS-PAGE shows the induction of single mutant of PfRad51 protein (PfRad51^{S319A}) in the BL21 strain from the pGEX-6p-2 plasmid. (E) The picture depicts the banding pattern of the protein ladder used in this study with their sizes in kDa. Arrow marks depict the size of desired protein along with the relevant marker protein bands.

A1. 6 Purification of recombinant PfRad51 and its mutants:

The recombinant proteins were purified either with the use of Ni-NTA purification or the GST purification method. First, the solubility of the proteins was checked by lysing the cells in an appropriate buffer followed by SDS-PAGE. The soluble proteins were purified and fractions collected. The resultant fractions were separated on SDS-PAGE for monitoring the presence of recombinant proteins in the samples as shown in Figure A6. The elution fractions with the highest amount of recombinant protein were pooled down and subjected to dialysis.

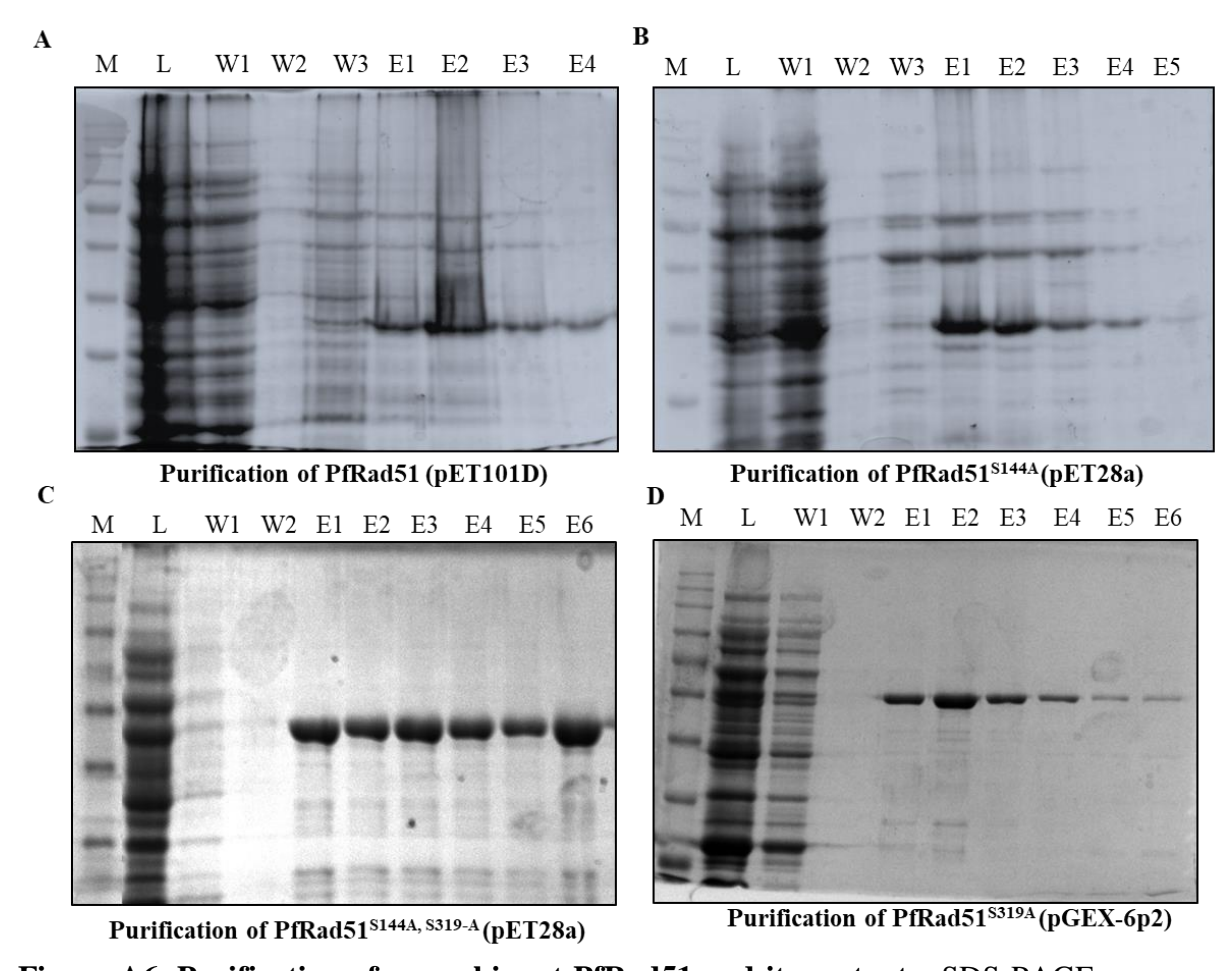


Figure A6. Purification of recombinant PfRad51 and its mutants: SDS-PAGEs represent the protein profile in loading flow-through (L), washes (W1-6), and elutions (E1-6) fractions collected while purifying wild-type and mutants of PfRad51 proteins. The extreme left lane contains the protein marker. (A) PAGE represents the proteins in the fractions collected while purifying wild-type PfRad51 (B) PAGE represents the proteins in the fractions collected while purifying single mutant of PfRad51^{S144A}. (C) PAGE represents the proteins in the fractions collected while purifying double mutant of PfRad51^{S144A}, S319. C) PAGE represents the proteins in the fractions collected while purifying single mutant of PfRad51^{S319}.

A1. 7 In vitro phosphorylation of PfRad51 and its mutants:

The mid schizont staged parasite culture with high parasitemia was treated with 0.05% MMS for 6 hours to provoke DNA damaging stress response, the simultaneously, equal volume culture was grown as control under favorable conditions. The cell-free extract harboring endogenous kinases was prepared from the control and MMS treated parasite cultures. The incorporation of radiolabeled phosphate upon phosphorylation of PfRad51 and its mutant was analyzed on the blot using a typhoon radioactive scanner. We did not find a distinguished signal at the desired size, however, a non-specific signal was observed on the autoradiogram around the size of PfRad51 (38kDa) (Figure A7). This nonspecific band was seen in the no recombinant protein negative control also. Thus, this data was inconclusive and we were unable to determine the phosphorylation of PfRad51 and its mutant.

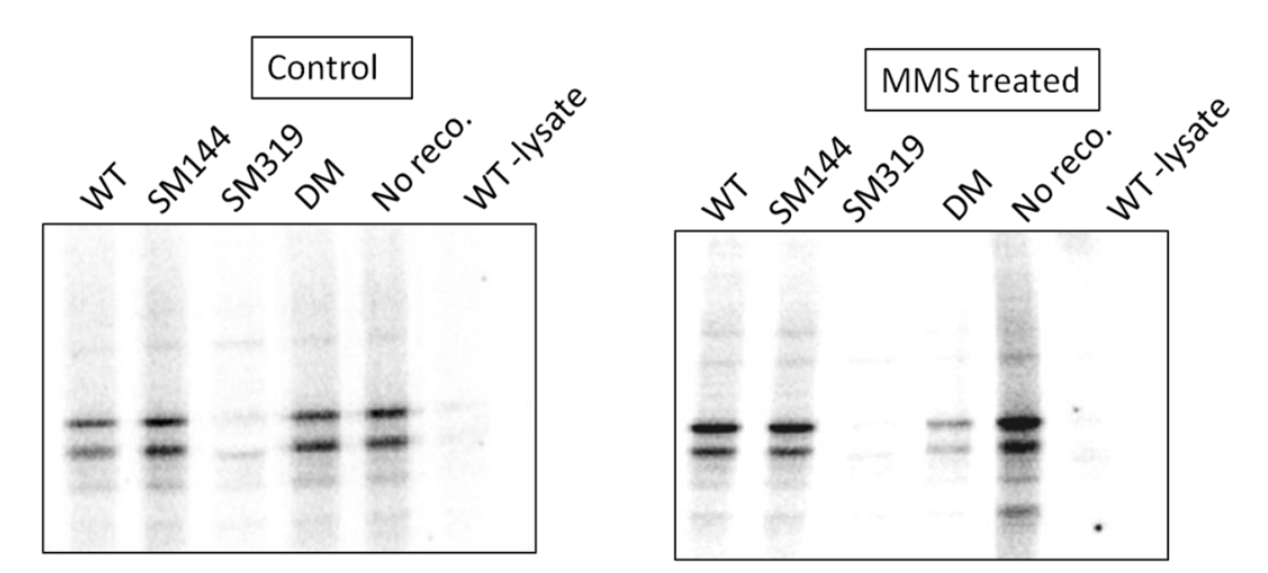


Figure A7. *In vitro* phosphorylation of PfRad51 and its mutants: Autoradiograms represent the presence of radioactive protein/s in the reaction samples containing whole-cell extract (kinases) either from control (left autoradiogram) or MMS treated (right autoradiogram) *P. falciparum* culture along with either wild type PfRad51 (WT), PfRad51^{S144A} single mutant at

144 amino acid residue (SM144), PfRad51^{S319A} single mutant at 319 amino acid residue (SM319), or PfRad51^{S144A, S319A} double mutant at 144, 319 amino acid residues (DM). Reactions without recombinant protein but with lysate (No reco: No recombination protein control) and without lysate only wild-type PfRad51 (WT –lysate: No lysate but with WT PfRad51) were supposed to serve as the negative controls.

A1.8 Cloning of *PfMTDNAP* gene into *Plasmodium* expression vector pARL [pARL *PfMTDNAP*]:

ORF of *PfMTDNAP* gene without the stop codon was cloned into *P. falciparum* episomal plasmid pARL containing ampicillin and WR99210/ pyrimethamine resistance marker (Deshmukh et al 2012). The ORF was amplified using OMKB745 and OMKB756 primer pair. *KpnI* was incorporated in forward primer and *AvrII* was incorporated in reverse primer. The expression cloned gene was under the control of Pf*CRT* promoter. The cloning was confirmed by double digestion with *KpnI* and *AvrII* and the release of *PfRAD51* was analyzed on agarose gel (Figure A8).

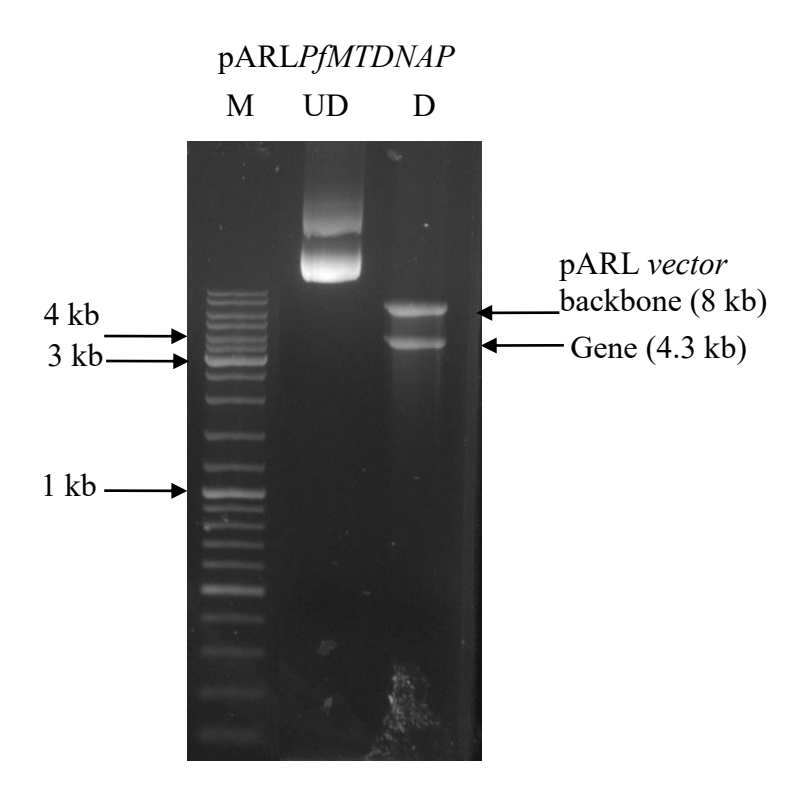


Figure A 8. Cloning of *PfRAD51* gene into *Plasmodium* expression vector pARL [pARL*PfMTDNAP*]: Agarose gel represents the *KnpI* and *AvrII* double digestion of pARL*PfMTDNAP* plasmid. Here, M, UD, and D stand for DNA marker, undigested control plasmid, and digested test, respectively. Arrow marks show the digestion products in the form of vector backbone and released gene along with their respective sizes in kb.

Appendix 2 <u>SYNOPSIS</u> Malaria continues to be one of the deadliest infectious diseases of mankind in the modern era. Half of the world's population is at risk of malaria; children and pregnant women are severely affected by this pathogen (WHO 2021). *Plasmodium falciparum*, one out of the five species known to infect human beings, accounts for the highest mortality rate by causing cerebral malaria. The global burden of malaria infection has been reduced in the last decade by the use of artemisinin-based combination therapies (ACT). However, the complete eradication of this life-threatening disease is still unachievable owing to the increasing cases of anti-malarial drug resistance and the absence of an effective vaccine (Wongsrichanalai and Sibley 2013). Thus, the current scenario is urging for expanding our understanding of parasite biology in order to identify novel antimalarial drug targets.

In *Plasmodium*, the mitochondrial biology is unconventional in several aspects. Firstly, although the genome codes for the tricarboxylic acid (TCA) cycle enzymes, the TCA cycle is not cyclic, and does not result in full oxidation of glucose to yield ATP in the blood stage of the parasites (Vaidya and Mather 2009). Secondly, the protein translation machinery seems to be unusual with the highly fragmented mitochondrial ribosomal RNA genes (Feagin et al. 1992; Feagin et al. 2012; Suplick et al. 1990). Thirdly, the main purpose of the electron transport chain (ETC) appears to serve the pyrimidine biosynthesis (Painter et al. 2007). Owing to these unusual features and its indispensable nature, the *Plasmodium* mitochondrion continues to be an attractive drug target. However, until now only the *Plasmodium* ETC has been investigated extensively as a drug target (Goodman et al. 2017; Nixon et al. 2013). We urge that other aspects of the mitochondrial biology of this parasite, including genome maintenance, deserve thorough exploration for the identification of novel drug targets.

Each malaria parasite contains a single mitochondrion with multiple genomes (approximately 30-100 copies) (Vaidya and Mather 2005). The mitochondrial genome of *Plasmodium* is the 128 | P a g e

smallest genome reported till date that harbors only three protein-coding genes. Several such linear unit mitochondrial genomes are arranged in tandem arrays forming concatemers of highly branched structures (Preiser et al. 1996). The mitochondrial DNA (mtDNA) replication is believed to take place either via the rolling-circle mode or by involving recombination intermediates (Preiser et al. 1996). Among the DNA repair mechanisms, only the base excision repair (BER) mechanism is characterized in *Plasmodium* mitochondria (Srivastava et al. 2021; Tiwari et al. 2020; Verma et al. 2021). In model organisms, factors involved in the mismatch repair (MMR), and nucleotide excision repair (NER) have been identified in the mitochondrial extracts (Bohr and Anson 1999). The role of Rad51 mediated homology-directed repair (HDR), and micro-homology mediated end-joining (MMEJ or alt-EJ) have also been implicated in the repair of DNA double-strand breaks (DSBs) of human mtDNA (Boesch et al. 2011; Mishra et al. 2018; Sage et al. 2010; Sage and Knight 2013; Tadi et al. 2016). In this study, we have addressed whether HDR is operational in the mitochondria of *P. falciparum*, and characterized the factors involved in it.

For the repair of the *Plasmodium* nuclear genome, both the homologous recombination (HR) pathway and the alt-EJ mechanism have been implicated (Bhattacharyya and Kumar 2003; Kirkman et al. 2014). While the factors involved in alt-EJ remain elusive, several factors of the HR pathway have been identified. The central player of HR, PfRad51 possesses the canonical ATP hydrolysis, and strand-exchange activities (Bhattacharyya et al. 2005). Small molecule inhibitors that block the ATPase activity and the homodimerization of PfRad51, displayed a profound effect on the DSB repair of the nuclear genome (Vydyam et al. 2019). In *P. berghei*, functional loss of Rad51 resulted in the complete abrogation of DSB repair, implying that the HR pathway is the predominant DSB repair mechanism (Roy et al. 2014). The DNA damage sensor PfalMre11 nuclease has also been identified and characterized (Badugu et al. 2015). The

important role of one of the RecQ helicases, PfBlm, in Plasmodium DNA repair has recently been appreciated (Suthram et al. 2020). A chemical inhibitor of PfBlm blocked DSB repair in this parasite and thereby rendered parasites hyper-sensitive to the DNA-damaging agents. Such DNA-damage sensitivity can be reversed by the overexpression of PfBlm (Suthram et al. 2020). PfBlm was found to interact with PfRad51, PfalMre11, and PfTopoIII (Bansod et al. 2020; Suthram et al. 2020), implying the existence of a 'recombinosome' complex in the parasite. PfTopoIII, a protein located in both nucleus and mitochondria, has been found to provide a growth advantage to the hydroxyurea (HU)-arrested parasites (Bansod et al. 2020).

In this work, we have addressed two major questions. First, we asked whether *Plasmodium* HR machinery is involved in mitochondrial DNA double-strand break (DSB) repair. Second, we wanted to test whether the *Plasmodium* recombinosome engages themselves with mitochondrial DNA polymerase.

We first investigated the organelle localization of three key components of HR, namely PfalMre11, PfRad51, and PfBlm which has been biochemically characterized in *P. falciparum*, and more importantly reported to have essential functions in this parasite under DNA damaging conditions (Badugu et al. 2015; Bhattacharyya et al. 2005; Roy et al. 2014; Suthram et al. 2020). Our subcellular fractionation data suggested that PfRad51 and PfBlm proteins were present in both nuclear as well as mitochondrial enriched organelle fractions. Contrary to this, PfalMre11 has shown nuclear exclusive localization. Second, we have tested the mitochondrial localization of PfRad51 and PfBlm using thermolysin protection assay and indirect immunofluorescence assay. Both of these experiments verified the mitochondrial existence of the nuclear-encoded repair proteins that are PfRad51 and PfBlm.

Since the function of these proteins is directly dependent on their ability to bind to DNA, therefore, we next investigated the association of PfRad51 and PfBlm with the mitochondrial genome (mtDNA) using mtDNA-IP. Our anti-PfRad51 and -PfBlm mtDNA IP data established the interaction between these repair proteins and mtDNA. Interestingly such association was observed throughout the 6 kb mtDNA. With the basic reasoning that the parasite genome experiences variable degrees of DNA damaging stress during asexual developmental stages, we next investigated stage-specific occupancy of these HR proteins to mtDNA. We noted a gradual increase in the occupancy of both PfBlm, and PfRad51 proteins at all loci with gradual maturation of parasite asexual stage. The mature stages are not only active in DNA replication but are also expected to experience a higher propensity for DNA damage due to the increased metabolic activity. Thus, our finding of stage-specific occupancy of both PfRad51 and PfBlm on the mtDNA may point to the involvement of these two nuclear-encoded proteins in mtDNA replication and/or repair.

Next, to establish their direct role in the parasite genome repair, we have developed a PCR-based methodology by which the repair kinetics of UV induced random DBS in the genome (mtDNA/ nDNA) can be monitored within the *P. falciparum*. Firstly, we have compared the repair kinetics of the damaged mitochondrial DNA and the nuclear DNA. It was observed that similar to the nuclear DNA most of the damages of the mtDNA were repaired by 24 hours post UV treatment. Next, we investigated the effect of B02 or ML216 (the inhibitors of PfRad51 and PfBlm, respectively) on the kinetics of mtDNA damage repair. We found that blocking the function of these proteins had abolished the repair of mtDNA DSB. This was similar to the abrogation these drugs have caused on nuclear genome DSB repair. However, treatment with Atovaquone, a Cyt bc1 complex inhibitor did not affect DNA repair, since the damaged DNA was repaired by 24 hours post UV irradiation similar to the mock-treated parasites. Hence these

findings indicated that PfBlm and PfRad51 have a role in mitochondrial genome repair apart from their conventional function in nuclear genome stability. Further, this finding was validated by an alternative approach wherein we have overexpressed PfRad51 or PfBlm in the wild-type parasites and investigated for any improvement in the kinetics of DSB repair in the mitochondrial genome. Significantly faster repair kinetics of both mtDNA and nDNA were observed in the two transgenic parasite lines overexpressing PfBlm or PfRad51 proteins. The overexpression of helicase dead mutant of PfBlm^{K83R} protein did not improve the repair kinetics as expected since earlier it was reported that overexpression of this mutant could not confer any survival advantage to the MMS treated parasites as opposed to the parasites overexpressing PfBlm. Whereas the repair kinetics was severely compromised in the parasite line overexpressing dominant-negative mutant of PfRad51^{K143R}. This finding was consistent with the previous report that documented that the expression of this mutant PfRad51 had a dominantnegative effect on the function of wild-type PbRad51 in repairing MMS-induced DNA damage. Next, we investigated the effect of DNA damaging stress on organelle localization and mtDNA association of HR proteins. Our findings suggest that in response to mtDNA damage stress, PfRad51 and PfBlm translocate more to the mitochondria and are recruited at the damaged sites in mtDNA during the first 12-24 hours, a duration that coincides with the time required for the completion of the mtDNA repair. However, once the damage is repaired, these proteins are dislodged from the DNA.

For the successful completion of HR pathway the invaded strand needs to be extended by a coordinated action of DNA polymerase, recombinase, and helicase. Therefore, we sought to investigate whether PfRad51 and PfBlm are also engaged with the mitochondrial DNA polymerase. The *Plasmodium* gene PF3D7_0625300 harboring a type A polymerase domain is predicted to be a mitochondrial DNA polymerase (mtDNAP) in *P. falciparum* owing to a very 132 | Page

high score by the software predicting mitochondrial localization (Mitoport-II score = 96%). Therefore, we sought to investigate the cellular localization of the putative PfMtDNAP. To this end, we created a parasite line harboring GFP tagged PfMtDNAP. We investigated the organelle(s) localization of this protein using the cellular fractionation method and found the organelle exclusive localization of PfMtDNAP. This finding was further validated by protease protection assay. Indeed the putative PfMtDNAP was found to be exclusively localized in the organelle. Additionally, the immunofluorescence assay also confirmed the mitochondrial localization of this protein. Being a DNA-dependent DNA polymerase, PfMtDNAP must associate itself with the mitochondrial genome. Therefore, we inspected the recruitment of this protein on mtDNA using anti-GFP mtChIP. In agreement with our hypothesis, Pf MtDNAP was found to be associated with mtDNA. Taken together, it appears that PF3D7_0625300 encodes for DNA polymerase that is likely to be targeted to the parasite mitochondria. Next, we investigated whether PfRad51 and PfBlm interact with the putative PfMtDNAP to carry out homology-directed repair of the damaged mtDNA. Yeast two-hybrid assay was employed for protein-protein interaction studies. We found weak interaction between repair proteins and PfMtDNAP. We further investigated the interaction between PfRad51 and PfTopoIII, as PfTopoIII was reported to be localized in *P. falciparum* mitochondria (28). A strong interaction was observed between PfRad51 and PfTopoIII. Earlier, both PfTopoIII and PfRad51 were found to interact with PfBlm (Bansod et al. 2020; Suthram et al. 2020). Thus, it is likely that PfMtDNAP, PfRad51, PfBlm, and PfTopoIII could be parts of a multi-protein complex. Our localization studies reiterate the possibility that such a complex may exist within the mitochondria.

Overall our data provided evidence for the role of nuclear-encoded repair proteins in mitochondrial genome stability. While DNA damaging stress conditions were found to stimulate

133 | Page

their mitochondrial localization and mitochondrial genome association, the completion of repair triggered their disassociation from repaired mtDNA. Additionally, the findings of this study indicated that homology directed repair is the predominant mechanism for fixing the mtDNA DBS since any perturbation of this pathway leads to the abolishment of repair of such catastrophic lesions. We have provided strong evidence supporting the previous assumption that the putative DNA polymerase I encoded by nuclear gene Pf3D7_0625300 is the mitochondrial DNA polymerase. Importantly it has the ability to bind to mtDNA and engages itself with other repair and replication proteins that are found to reside within *Plasmodium* mitochondria.

- Badugu, S. B., et al. (2015), 'Identification of Plasmodium falciparum DNA Repair Protein Mre11 with an Evolutionarily Conserved Nuclease Function', *PLoS One*, 10 (5), e0125358.
- Bansod, S., et al. (2020), 'Elucidation of an essential function of the unique charged domain of Plasmodium topoisomerase III', *Biochem J*.
- Bhattacharyya, M. K. and Kumar, N. (2003), 'Identification and molecular characterisation of DNA damaging agent induced expression of Plasmodium falciparum recombination protein PfRad51', *Int J Parasitol*, 33 (12), 1385-92.
- Bhattacharyya, M. K., et al. (2005), 'Characterization of kinetics of DNA strand-exchange and ATP hydrolysis activities of recombinant PfRad51, a Plasmodium falciparum recombinase', *Mol Biochem Parasitol*, 139 (1), 33-9.

- Boesch, P., et al. (2011), 'DNA repair in organelles: Pathways, organization, regulation, relevance in disease and aging', *Biochim Biophys Acta*, 1813 (1), 186-200.
- Bohr, V. A. and Anson, R. M. (1999), 'Mitochondrial DNA repair pathways', *J Bioenerg Biomembr*, 31 (4), 391-8.
- Feagin, J. E., et al. (1992), 'Homologies between the contiguous and fragmented rRNAs of the two Plasmodium falciparum extrachromosomal DNAs are limited to core sequences', *Nucleic Acids Res*, 20 (4), 879-87.
- Feagin, J. E., et al. (2012), 'The fragmented mitochondrial ribosomal RNAs of Plasmodium falciparum', PLoS One, 7 (6), e38320.
- Goodman, C. D., Buchanan, H. D., and McFadden, G. I. (2017), 'Is the Mitochondrion a Good Malaria Drug Target?', *Trends Parasitol*, 33 (3), 185-93.
- Kirkman, L. A., Lawrence, E. A., and Deitsch, K. W. (2014), 'Malaria parasites utilize both homologous recombination and alternative end joining pathways to maintain genome integrity', *Nucleic Acids Res*, 42 (1), 370-9.
- Mishra, A., et al. (2018), 'RAD51C/XRCC3 Facilitates Mitochondrial DNA Replication and Maintains Integrity of the Mitochondrial Genome', *Mol Cell Biol*, 38 (3).
- Nixon, G. L., et al. (2013), 'Targeting the mitochondrial electron transport chain of Plasmodium falciparum: new strategies towards the development of improved antimalarials for the elimination era', *Future Med Chem*, 5 (13), 1573-91.
- Painter, H. J., et al. (2007), 'Specific role of mitochondrial electron transport in blood-stage Plasmodium falciparum', *Nature*, 446 (7131), 88-91.
- Preiser, P. R., et al. (1996), 'Recombination associated with replication of malarial mitochondrial DNA', *Embo j,* 15 (3), 684-93.
- Roy, N., et al. (2014), 'Dominant negative mutant of Plasmodium Rad51 causes reduced parasite burden in host by abrogating DNA double-strand break repair', *Mol Microbiol*, 94 (2), 353-66.
- Sage, J. M. and Knight, K. L. (2013), 'Human Rad51 promotes mitochondrial DNA synthesis under conditions of increased replication stress', *Mitochondrion*, 13 (4), 350-6.
- Sage, J. M., Gildemeister, O. S., and Knight, K. L. (2010), 'Discovery of a novel function for human Rad51: maintenance of the mitochondrial genome', *J Biol Chem*, 285 (25), 18984-90.
- Srivastava, P. N., Narwal, S. K., and Mishra, S. (2021), 'Mitochondrial apurinic/apyrimidinic endonuclease Apn1 is not critical for the completion of the Plasmodium berghei life cycle', *DNA Repair (Amst)*, 101, 103078.

- Suplick, K., Morrisey, J., and Vaidya, A. B. (1990), 'Complex transcription from the extrachromosomal DNA encoding mitochondrial functions of Plasmodium yoelii', *Mol Cell Biol*, 10 (12), 6381-8.
- Suthram, N., et al. (2020), 'Elucidation of DNA Repair Function of PfBlm and Potentiation of Artemisinin Action by a Small-Molecule Inhibitor of RecQ Helicase', *mSphere*, 5 (6).
- Tadi, S. K., et al. (2016), 'Microhomology-mediated end joining is the principal mediator of doublestrand break repair during mitochondrial DNA lesions', *Mol Biol Cell*, 27 (2), 223-35.
- Tiwari, A., et al. (2020), 'Plasmodium falciparum Apn1 homolog is a mitochondrial base excision repair protein with restricted enzymatic functions', *Febs j*, 287 (3), 589-606.
- Vaidya, A. B. and Mather, M. W. (2005), 'A post-genomic view of the mitochondrion in malaria parasites', *Curr Top Microbiol Immunol*, 295, 233-50.
- --- (2009), 'Mitochondrial evolution and functions in malaria parasites', *Annu Rev Microbiol*, 63, 249-67.
- Verma, N., et al. (2021), 'Plasmodium Ape1 is a multifunctional enzyme in mitochondrial base excision repair and is required for efficient transition from liver to blood stage infection', *DNA Repair* (Amst), 101, 103098.
- Vydyam, P., et al. (2019), 'A small-molecule inhibitor of the DNA recombinase Rad51 from Plasmodium falciparum synergizes with the antimalarial drugs artemisinin and chloroquine', *J Biol Chem*, 294 (20), 8171-83.
- WHO 'Malaria', <https://www.who.int/news-room/fact-sheets/detail/malaria>, accessed 15 April 2021.
- Wongsrichanalai, C. and Sibley, C. H. (2013), 'Fighting drug-resistant Plasmodium falciparum: the challenge of artemisinin resistance', *Clin Microbiol Infect*, 19 (10), 908-16.

Elucidating the function of nuclear-encoded repair proteins in Plasmodium mitochondrial genome repair.

by Payal Iha

Central University P.O.

Submission date: 22-Feb-2022 10:22AM (UTC+0530)

Submission ID: 1768098429

File name: Payal_Jha_Thesis.pdf (3.11M)

Word count: 24524

Character count: 131204

Elucidating the function of nuclear-encoded repair proteins in Plasmodium mitochondrial genome repair.

ORIGINA	I ITV	DEDC	דסר

17% SIMILARITY INDEX

15%
INTERNET SOURCES

13% PUBLICATIONS

%STUDENT PAPERS

PRIMARY SOURCES

Payal Jha, Abhilasha Gahlawat, Sunanda Bhattacharyya, Sandeep Dey, Kota Arun Kumar, Mrinal Kanti Bhattacharyya. "Bloom Helicase Along with Recombinase Rad51 Repairs the Mitochondrial Genome of the Malaria Parasite", mSphere, 2021

5%

Publication

www.ncbi.nlm.nih.gov

3%

Submitted to University of Hyderabad, Hyderabad

3%

Student Paper

Submitted to Royal Veterinary College
Student Paper

1 %

Lee, A. H., L. S. Symington, and D. A. Fidock.
"DNA Repair Mechanisms and Their Biological
Roles in the Malaria Parasite Plasmodium
falciparum", Microbiology and Molecular
Biology Reviews, 2014.

<1%

Publication

6	hdl.handle.net Internet Source	<1%
7	Submitted to Institute of Technology Carlow Student Paper	<1 %
8	Submitted to University of Birmingham Student Paper	<1 %
9	Achanta, Sita Swati, Shalu M. Varunan, Sunanda Bhattacharyya, and Mrinal Kanti Bhattacharyya. "Characterization of Rad51 from Apicomplexan Parasite Toxoplasma gondii: An Implication for Inefficient Gene Targeting", PLoS ONE, 2012.	<1%
10	Submitted to National University of Ireland, Galway Student Paper	<1%
11	ebin.pub Internet Source	<1%
12	etheses.bham.ac.uk Internet Source	<1%
13	eprints.keele.ac.uk Internet Source	<1%
14	theses.gla.ac.uk Internet Source	<1%

archiv.ub.uni-heidelberg.de
Internet Source

		<1%
16	livrepository.liverpool.ac.uk Internet Source	<1%
17	patents.justia.com Internet Source	<1%
18	estudogeral.sib.uc.pt Internet Source	<1%
19	tel.archives-ouvertes.fr Internet Source	<1%
20	edepositireland.ie Internet Source	<1 %
21	www.pubmedcentral.nih.gov Internet Source	<1 %
22	dora.dmu.ac.uk Internet Source	<1 %
23	www.frontiersin.org Internet Source	<1%
24	Submitted to Heriot-Watt University Student Paper	<1%
25	Sheau-Shya Ju, Long-Liu Lin, Hungchien Roger Chien, Wen-Hwei Hsu. "Substitution of the critical methionine residues in Trigonopsis variabilisD-amino acid oxidase with leucine	<1%

enhances its resistance to hydrogen peroxide", FEMS Microbiology Letters, 2000

Publication

26	escholarship.umassmed.edu Internet Source	<1%
27	link.springer.com Internet Source	<1%
28	Roy, Nabamita, Sunanda Bhattacharyya, Swati Chakrabarty, Shyamasree Laskar, Somepalli Mastan Babu, and Mrinal Kanti Bhattacharyya. "Dominant negative mutant of P lasmodium Rad51 causes reduced parasite burden in host by abrogating DNA doublestrand break repair: HR is the major DNA repair mechanism in Plasmodium", Molecular Microbiology, 2014.	<1%
29	Submitted to University of Leeds Student Paper	<1%
30	Brandon R. Lowe, Rajesh K. Yadav, Ryan A. Henry, Patrick Schreiner et al. "Surprising Phenotypic Diversity of Cancer-associated mutations of Gly 34 in the Histone H3 tail", Cold Spring Harbor Laboratory, 2020 Publication	<1%
	Submitted to University of Ulster	1

Submitted to University of Ulster Student Paper

<1%

32	Usir.Salford.Ac.Uk Internet Source	<1%
33	www.jbc.org Internet Source	<1%
34	diagnostics1.com Internet Source	<1%
35	pure.rug.nl Internet Source	<1%
36	citeseerx.ist.psu.edu Internet Source	<1%
37	os.zhdk.cloud.switch.ch Internet Source	<1%
38	www.omicsonline.org Internet Source	<1%
39	discovery.ucl.ac.uk Internet Source	<1%
40	epdf.pub Internet Source	<1%
41	researchspace.auckland.ac.nz Internet Source	<1%
42	repository.ntu.edu.sg Internet Source	<1%
43	Erin K. Zess, Yasin F. Dagdas, Esme Peers, Abbas Maqbool, Mark J. Banfield, Tolga O.	<1%

Bozkurt, Sophien Kamoun. "Regressive evolution of an effector following a host jump in the Irish Potato Famine Pathogen Lineage", Cold Spring Harbor Laboratory, 2021

Publication

44	krishikosh.egranth.ac.in Internet Source	<1 %
45	publications.aston.ac.uk Internet Source	<1%
46	www.biorxiv.org Internet Source	<1%

Exclude quotes

On

Exclude matches

< 14 words

Exclude bibliography On

This is to certify that the primary source I represents Ms. Payal That's own publication from her theirs work, and the primary source 3 contains the method Section of sourcal theirs from our lab. Certain phrases under the method section cannot be modified and need to be written as is. Hence elemination these two sources the similarity is only 9%.

Dr. MRINAL KANTI BHATTACHARYYA PhD

1 mb hall.

PROFESSOR
DEPARTMENT OF BIOCHEMISTRY
SCHOOL OF LIFE SCIENCES
UNIVERSITY OF HYDERABAD
HYDERABAD-500046, INDIA.

UNIVERSITY OF HYDERABAD SCHOOL OF LIFE SCIENCES DEPARTMENT OF BIOCHEMISTRY

PROFORMA FOR SUBMISSION OF THESIS/DISSERTATION

	I ROPORMATOR 3	OBMISSION OF THESIS/BISSERTATION
1	Name of the Candidate	: Payal Tha
2.	Roll No.	: 15LBPHOI
3.	Year of Registration	: 2015
4.	Topic	Elucidating the function of nuclear-encoded supoir proteins in Plasmodium Mitochardia genome suspecis. Prof. Mainal Kanti Bhattacharyya University of Hyderabad. granted:
5.	Supervisor(s) and affiliations	Prof. Minal Kanti Bhattacharyya Huderabad.
6.	Whether extension/re-registration (Specify below)	granted:
7.	Date of submission	: 23 02 2022
8.	Last class attended on (M.Phil/Pre	e-Ph.D): Pre-Pup scrimer 22 rd Sept. 2021.
9.	Whether tuition fee for the current	period Paid: Receipt No. & Dt: No dues done
10	Whather thesis submission for pai	d. Pereint No. & Dt. 220207113459959

11. Whether hostel dues cleared : Receipt No & Dt: Nodues done

12. Whether a summary of the dissertation enclosed: $\gamma e \leq$

Supervisor(s) PROFESSOR
Signature MENT OF BLOCHEMISTRY

Signature TMENT OF BIOCHEMISTRY
SCHOOL OF LIFE SCIENCES
UNIVERSITY OF HYDERABAD
HYDERABAD-500046, INDIA.
Signature of the

Dean, of the School

Signature of the Head of the

Signature of the Head of the Department.

Dept. of Biochemistry SCHOOL OF LIFE SCIENCES UNIVERSITY OF HYDERABAD HYDERABAD-500 046.

Forwarded pp : 24/2/2022

School of Life Sciences University of Hyderabad Hyderabad-500 046.